

## **NOTE TO USERS**

**This reproduction is the best copy available.**

UMI<sup>®</sup>



**PUNCHING SHEAR FAILURE OF FOUNDATIONS ON STRONG  
SAND OVERLYING DEEP WEAK DEPOSIT**

**ZEINA PAULS**

A thesis  
in  
The Department  
of  
Building, Civil and Environmental Engineering

Presented in Partial Fulfillment of the Requirements  
For the Degree of Master of Applied Science (Civil Engineering) at  
Concordia University  
Montreal, Quebec, Canada

April 2009

© Zeina Pauls, 2009



Library and Archives  
Canada

Published Heritage  
Branch

395 Wellington Street  
Ottawa ON K1A 0N4  
Canada

Bibliothèque et  
Archives Canada

Direction du  
Patrimoine de l'édition

395, rue Wellington  
Ottawa ON K1A 0N4  
Canada

*Your file* *Votre référence*  
ISBN: 978-0-494-63269-7  
*Our file* *Notre référence*  
ISBN: 978-0-494-63269-7

**NOTICE:**

The author has granted a non-exclusive license allowing Library and Archives Canada to reproduce, publish, archive, preserve, conserve, communicate to the public by telecommunication or on the Internet, loan, distribute and sell theses worldwide, for commercial or non-commercial purposes, in microform, paper, electronic and/or any other formats.

The author retains copyright ownership and moral rights in this thesis. Neither the thesis nor substantial extracts from it may be printed or otherwise reproduced without the author's permission.

---

In compliance with the Canadian Privacy Act some supporting forms may have been removed from this thesis.

While these forms may be included in the document page count, their removal does not represent any loss of content from the thesis.

**AVIS:**

L'auteur a accordé une licence non exclusive permettant à la Bibliothèque et Archives Canada de reproduire, publier, archiver, sauvegarder, conserver, transmettre au public par télécommunication ou par l'Internet, prêter, distribuer et vendre des thèses partout dans le monde, à des fins commerciales ou autres, sur support microforme, papier, électronique et/ou autres formats.

L'auteur conserve la propriété du droit d'auteur et des droits moraux qui protègent cette thèse. Ni la thèse ni des extraits substantiels de celle-ci ne doivent être imprimés ou autrement reproduits sans son autorisation.

---

Conformément à la loi canadienne sur la protection de la vie privée, quelques formulaires secondaires ont été enlevés de cette thèse.

Bien que ces formulaires aient inclus dans la pagination, il n'y aura aucun contenu manquant.

  
**Canada**

# **ABSTRACT**

## **PUNCHING SHEAR FAILURE OF FOUNDATIONS ON STRONG SAND OVERLYING DEEP WEAK DEPOSIT**

The ultimate bearing capacity of shallow foundations under axial vertical loads on dense sand overlying deep loose deposit has been investigated. In the literature, several theories can be found using simplified failure mechanisms in conjunction with the punching shear failure. Accordingly, assumptions were used to simplify the evaluation of the level of mobilization of the shear strength on the punching column. This is mainly due to the complexity of modeling the earth pressure distribution on the punching column.

In this study a numerical model was developed to investigate the case of continuous footing on dense sand overlying loose sand. The model utilizes the powerful software "PLAXIS" version 8.6, which is capable to model such complex interaction in two-dimensional stress analysis. The model was validated with the prototype test results of Meyerhof and Hanna (1978) and Hanna (1981- a). The results of this investigation showed that the shear strength mobilized on the punching column depends on the relative strength of the two layers, the width of the footing and the thickness and angle of shearing resistance of the upper layer. Design procedure and design charts have been presented to assist foundation engineers to predict the bearing capacity of footing on dense sand overlying deep loose deposit.

## **ACKNOWLEDGMENTS**

I would like to express my thanks and gratitude to my supervisor, Dr. Adel Hanna; I am eternally indebted for the help, advice, guidance and the patience throughout my studies. Thank you, for all the precious academic and life advices.

The support and help I received from my parents and family is priceless, thank you, for believing in me. My friends and colleges thank you for the continuous encouragement, help and support. Last but not least, to the candles of my life my two little kids, Cathrin and Brunell, thank you for helping make this dream come true.

## TABLE OF CONTENTS

LIST OF FIGURES	viii
LIST OF TABELS	xii
LIST OF SYMBOLS	xiv
<b>CHAPTER 1</b>	
INTRODUCTION	1
<b>CHAPTER 2</b>	
LITRUATURE REVIEW	
2.1 GENERAL	3
2.2 REVIEW OF THE PREVIOUS WORK	3
2.2.1 THIEORITICAL AND EXPERIMENTAL INVESTIGATIONS	3
2.2.2 KINEMATICAL AND NUMERICAL INVESTIGATIONS	13
2.3 DISCUSSIONS	18
2.4 OBJECTIVES	19
<b>CHAPTER 3</b>	
NUMERICAL MODEL	
3.1 GENERAL	20

<b>3.2 NUMERICAL MODEL</b>	<b>21</b>
<b>3.3 CONSTITUTIVE LAW</b>	<b>22</b>
<b>3.4 BOUNDARY CONDITIONS</b>	<b>23</b>
<b>3.5 ELEMENT'S TYPE</b>	<b>25</b>
<b>3.6 DETERMINATION OF MOBILIZED ANGLE OF SHEARING RESISTANCE <math>\delta</math> NUMERICALLY</b>	<b>26</b>
<b>3.7 GENERATION OF MESH</b>	<b>28</b>
<b>3.8 MODEL VALIDATION</b>	<b>31</b>
<b>3.8.1 BEARING CAPACITY MODEL VALIDATION</b>	<b>32</b>
<b>3.8.2 VALIDATION OF THE CUSTOMIZED MODEL FOR <math>\delta</math></b>	<b>38</b>
<b>CHAPTER 4</b>	
<b>RESULTS AND DATA ANALYSIS</b>	<b>40</b>
<b>4.1 GENERAL</b>	<b>40</b>
<b>4.2 TEST RESULTS</b>	<b>40</b>
<b>4.3 DATA ANALYSIS</b>	<b>48</b>
<b>4.4 PARAMETRIC STUDY</b>	<b>49</b>
<b>4.4.1 EFFECT OF THE RATIO H/B</b>	<b>49</b>

4.4.2 EFFECT OF THE RELATIVE STRENGTH OF THE LAYERS ( $\phi_1/\phi_2$ )	49
4.4.3 EFFECT OF THE STRENGTH OF THE UPPER LAYER	50
4.4.4 EFFECT OF THE STRENGTH OF THE LOWER LAYER	51
4.5 DETERMINATION OF THE SHEAR STRENGTH MOBILIZED ON THE PUNCHING COLUMN	52
4.6 RESULTS AND ANALYSIS	55
4.7 RELATIVE STRENGTH OF BOTH LAYERS	70
4.8 DESIGN CHARTS	71
4.9 SUGESTED DESIGN PROSEDURE	77
4.10 DESIGN EXAMPLE	78
CHAPTER 5	
CONCLUTIONS AND RECOMMENDATIONS	80
5.1 CONCLUSION	80
5.2 RECOMMENDATIONS	81
REFERENCES	82

## LIST OF FIGURES

2-1	Graphical description of strip footings in layered sub-soil by Button (1953).	4
2-2	Results of Meyerhof and Browns' discussion for the Button's analysis.	5
2-3	Failure mechanism for footings on layered soil(left side) and homogenous sand (right side) after Meyerhof (1974).	6
2-4	Design charts for determination of $N'_y, N'_q$ after Hanna (1981)	8
2-5	Failure mechanism in layered cohesionless soils ,after Hanna (1981)	10
2-6	Inclined failure surface as proposed by Carlos Abou Farah (2004)	12
2-7	Triangular element used in the upper bound limit analysis presented by Sloan (1989)	14
2-8	Florkiewicz's assumption of layered sub-soils	14
3-1	Strip footing on layered soils	20
3-2	Numerical model and redefined mesh.	22
3-3	Plastic points distribution on the deformed mesh.	24
3-4	Deformed mesh scaled up to five times of homogeneous dense sand of (42B X 36B) model size, with prescribed displacement of 1m in the.	24
3-5	Elements type showing the allocation of nodes and stress- points.	25
3-6	Punching shear column.	27
3-7	Distribution of stress points in interface elements and their connection with the soil elements.	28

<b>3-8</b>	Cross section showing the position of the interfaces and the geometry lines.	29
<b>3-9</b>	Cross section in the generated mesh , with finer mesh around punching column.	29
<b>3-10</b>	Comparison between the results of the present study with Hanna 1981 results; for $\varphi_1 = 43^\circ$ and, $\varphi_2 = 30^\circ$	35
<b>3-11</b>	Comparison between the results of the present study with Hanna 1981 results; for $\varphi_1 = 43^\circ$ and, $\varphi_2 = 35^\circ$	36
<b>3-12</b>	Comparison between the results of the present study with Hanna 1981 results; for $\varphi_1 = 47^\circ$ and, $\varphi_2 = 35^\circ$	37
<b>3-13</b>	Comparison between the results of the present study with Hanna (1978) results.	38
<b>4-1</b>	Variation of the bearing capacity for different H/B ratios for $\varphi_1 = 43^\circ$ and, $\varphi_2 = 30^\circ$	42
<b>4-2</b>	Variation of the bearing capacity for different H/B ratios for $\varphi_1 = 43^\circ$ and, $\varphi_2 = 35^\circ$	43
<b>4-3</b>	Variation of the bearing capacity for different H/B ratios for $\varphi_1 = 43^\circ$ and, $\varphi_2 = 40^\circ$	44
<b>4-4</b>	Variation of the bearing capacity for different H/B ratios for $\varphi_1 = 43^\circ$ and, $\varphi_2 = 42^\circ$	45
<b>4-5</b>	Variation of the bearing capacity for different H/B ratios for $\varphi_1 = 47^\circ$ and, $\varphi_2 = 35^\circ$	46
<b>4-6</b>	Variation of the bearing capacity for different H/B ratios for $\varphi_1 = 47^\circ$ and, $\varphi_2 = 40^\circ$	47
<b>4-7</b>	Load-displacement curve.	48
<b>4-8</b>	Different stiffness ratios of the two layers, for $\varphi_1 = 47, 43,$ & $\varphi_2 = 35$ & $40$	50
<b>4-9</b>	Effect of the strength of the lower layer for different stiffness ratios of the two layers. for $\varphi_1 = 43$	51

<b>4-10</b>	Effect of the strength of the lower layer for different stiffness ratios of the two layers. for $\varphi_1 = 47$	52
<b>4-11</b>	Variation of $(\delta/\varphi_1)$ with the height of the punching column for $q_2/q_1 = 0.1$	65
<b>4-12</b>	Variation of $(\delta/\varphi_1)$ with the height of the punching column for $q_2/q_1 = 0.22$	66
<b>4-13</b>	Variation of $(\delta/\varphi_1)$ with the height of the punching column for $q_2/q_1 = 0.54$	66
<b>4-14</b>	Variation of $(\delta/\varphi_1)$ with the height of the punching column for $q_2/q_1 = 0.08$	67
<b>4-15</b>	Variation of $(\delta/\varphi_1)$ with the height of the punching column for $q_2/q_1 = 0.24$	67
<b>4-16</b>	Variation of $(\delta/\varphi_1)$ with the height of the punching column for $q_2/q_1 = 0.04$	68
<b>4-17</b>	Variation of $(\delta/\varphi_1)$ with the height of the punching column for $q_2/q_1 = 0.15$	68
<b>4-18</b>	Variation of $(\delta/\varphi_1)$ with the height of the punching column for $q_2/q_1 = 0.37$	69
<b>4-19</b>	Variation of $(\delta/\varphi_1)$ for different $q_2/q_1$ ratios and $H/B = 1$	70
<b>4-20</b>	Variation of $(\delta/\varphi_1)$ for different $q_2/q_1$ ratios and $H/B = 3$	71
<b>4-21</b>	$\delta/\varphi_1$ for different $H/B$ ratios and $(q_2/q_1 = 0.54)$	72
<b>4-22</b>	$\delta/\varphi_1$ for different $H/B$ ratios and $(q_2/q_1 = 0.37)$	73
<b>4-23</b>	$\delta/\varphi_1$ for different $H/B$ ratios and $(q_2/q_1 = 0.24)$	73
<b>4-24</b>	$\delta/\varphi_1$ for different $H/B$ ratios and $(q_2/q_1 = 0.22)$	74

<b>4-25</b>	$\delta/\varphi_1$ for different H/B ratios and ( $q_2/q_1= 0.15$ )	74
<b>4-26</b>	$\delta/\varphi_1$ for different H/B ratios and ( $q_2/q_1= 0.1$ )	75
<b>4-27</b>	$\delta/\varphi_1$ for different H/B ratios and ( $q_2/q_1= 0.08$ )	75
<b>4-28</b>	$\delta/\varphi_1$ for different H/B ratios and ( $q_2/q_1= 0.05$ )	76
<b>4-29</b>	$\delta/\varphi_1$ for different H/B ratios and ( $q_2/q_1= 0.04$ )	76

## LIST OF TABLES

<b>3-1</b>	Soil properties used in this investigation	31
<b>3-2</b>	Input data for the validation purpose	33
<b>3-3</b>	$\varphi_1 = 43^\circ, \varphi_2 = 30^\circ, C_u = 1 \text{ KN/m}^2$	35
<b>3-3.1</b>	$\varphi_1 = 43^\circ, \varphi_2 = 35^\circ, C_u = 1 \text{ KN/m}^2$	36
<b>3-4</b>	$\varphi_1 = 47^\circ, \varphi_2 = 35^\circ, C_u = 1 \text{ KN/m}^2$	37
<b>4-1</b>	Input data for the numerical model	41
<b>4-2</b>	$\varphi_1 = 43^\circ, \varphi_2 = 30^\circ, C_u = 1 \text{ KN/m}^2$	42
<b>4-3</b>	$\varphi_1 = 43^\circ, \varphi_2 = 35^\circ, C_u = 1 \text{ KN/m}^2$	43
<b>4-4</b>	$\varphi_1 = 43^\circ, \varphi_2 = 40^\circ, C_u = 1 \text{ KN/m}^2$	44
<b>4-5</b>	$\varphi_1 = 43^\circ, \varphi_2 = 42^\circ, C_u = 1 \text{ KN/m}^2$	45
<b>4-6</b>	$\varphi_1 = 47^\circ, \varphi_2 = 35^\circ, C_u = 1 \text{ KN/m}^2$	46
<b>4-7</b>	$\varphi_1 = 47^\circ, \varphi_2 = 40^\circ, C_u = 1 \text{ KN/m}^2$	47
<b>4-8</b>	Properties for the assumed soils for the generation of $\delta$ results model	53
<b>4-9</b>	Bearing capacity of homogenous sand layers $q_1$ & $q_2$ , and the ratio $q_2/q_1$	54
<b>4-10</b>	Calculated $\delta$ angle for five selective points for the case of ( $q_2/q_1 = 0.08$ ) and different H/B ratios.	56
<b>4-11</b>	Calculated $\delta$ angle for five selective points for the case of ( $q_2/q_1 = 0.22$ ) and different H/B ratios.	57

<b>4-12</b>	Calculated $\delta$ angle for five selective points for the case of ( $q_2/q_1 = 0.54$ ) and different H/B ratios.	58
<b>4-13</b>	Calculated $\delta$ angle for five selective points for the case of ( $q_2/q_1 = 0.04$ ) and different H/B ratios.	59
<b>4-14</b>	Calculated $\delta$ angle for five selective points for the case of ( $q_2/q_1 = 0.1$ ) and different H/B ratios.	60
<b>4-15</b>	Calculated $\delta$ angle for five selective points for the case of ( $q_2/q_1 = 0.24$ ) and different H/B ratios.	61
<b>4-16</b>	Calculated $\delta$ angle for five selective points for the case of ( $q_2/q_1 = 0.05$ ) and different H/B ratios.	62
<b>4-17</b>	Calculated $\delta$ angle for five selective points for the case of ( $q_2/q_1 = 0.15$ ) and different H/B ratios.	63
<b>4-18</b>	Calculated $\delta$ angle for five selective points for the case of ( $q_2/q_1 = 0.37$ ) and different H/B ratios.	64

## LIST OF SYMBOLS

$B$	width of the footing
$C$	undrained shear strength "Cohesion" ( $KN/m^2$ )
$E$	Young's modulus ( $KN/m^2$ )
$H$	thickness of the upper soil layer below the footing's base.
$K_0$	coefficient of initial earth pressure, and ( $K_0 = 1 - \sin \phi$ )
$N_c, N_q, N_\gamma$	bearing capacity factors corresponding to plane-strain angle of shearing $\phi$ .
$q_u$	ultimate bearing capacity.
$q_b$	ultimate bearing capacity of strip footing on a very thick bed of the lower layer.
$q_t$	the ultimate bearing capacity of strip footing on a very thick bed of the upper layer.
$\nu$	Poisson's ratio.
$\psi$	dilatancy angle in degrees, and ( $\psi = \phi - 30$ ).
$\phi_1, \phi_2$	angles internal friction of the first and second soil layers respectively, measured in degrees.
$\gamma_1, \gamma_2$	unit weight of the upper and lower soils respectively.
$\alpha$	angle between the vertical and assumed actual failure surface.
$\delta$	mobilized angle of shearing resistance on the plane of failure.
$\sigma$	principal stress.
$\epsilon$	strain.

$\tau$  shear stress

$\varphi_1 / \varphi_2$  strong over loose sand layer referred to by the value of their angles of internal friction.

## CHAPTER ONE

### INTRODUCTION

Foundation design consists of two distinct parts: the ultimate bearing capacity of the soil under the foundation, and the allowable settlement that the footing can undergo without causing any damage to the superstructure. The ultimate bearing capacity is defined as the load that the soil under the foundation can support before massive shear failure.

Research on the ultimate bearing capacity can be carried out using either analytical solutions or experimental investigations. The former could be studied through theory of plasticity or finite element analysis, while the latter is achieved through conducting prototype, model and full-scale tests. A satisfactory solution is found only when theoretical results agree with those obtained experimentally.

In the literature, most of the reports found are dealing with the bearing capacity theories for foundations on homogeneous soils. Soil properties were assumed to remain constant during loading. However, in cases where the underlying soil is made of layers of different properties, these theories will not accurately predict the bearing capacity of these footings.

Layered soil profiles are often encountered whether naturally deposited or artificially made. In recent years, approximate solutions for the bearing capacity

of shallow foundations on layered soil have been presented. Theories were developed for footings on a strong layer overlying a weak layer, and vice versa.

For the case of strong layer overlying a weak deposit, the theories developed were based on the assumption that, at the ultimate load a soil mass in the upper sand layer, will fail in a roughly truncated pyramid in shape, pushed into the lower soil layer. The calculation of the mobilized shear on the punching column is difficult at best, and accordingly several simplified assumption were made, which further leads to inaccurate predictions.

The objective of this thesis is to develop a numerical model to simulate the case of footings on a dense sand layer overlying deep deposit of loose sand, which is regarded as a typical case often encountered in the field. The model is capable to evaluate the level of shear mobilization on the punching column and accordingly will lead to accurate prediction of the bearing capacity of these footings. After model validation, the model will be used to generate data for a wide range of parameters, based on which a design theory will be developed. The results of this thesis will be presented in the form of design procedure for practicing use.

## CHAPTER TWO

### LITERATURE REVIEW

#### 2.1 GENERAL

During the last four decades, several reports can be found in the literature dealing with foundations resting on layered soils. Theories were developed based on the results of laboratory model testing and numerical modeling. In this chapter a brief review of the historical development of the subject matter followed by discussions.

One of the early proposed solutions for bearing capacity in layered soils was that of Button (1953), yet the semi-empirical and experimental data of Meyerhof and Hanna since (1978) remained unchallenged yet.

#### 2.2 REVIEW OF PREVIOUS WORK

##### 2.2.1 THEORITICAL AND EXPEREMENTAL INVESTIGATIONS

Button (1953) was the first to study the bearing capacity of strip foundations resting on two layers of clay soils. He assumed that the failure surface is cylindrical in shape and starts from the edge of the footings, fig. (2-1). Then he used a bearing capacity factor ( $N_c$ ) that depended on the upper layer and the ratio of the lower layer cohesion over the upper layer cohesion ( $C_2/C_1$ ). Yet he introduced series of simplified assumptions, which have significantly reduced the level of accuracy of the results.

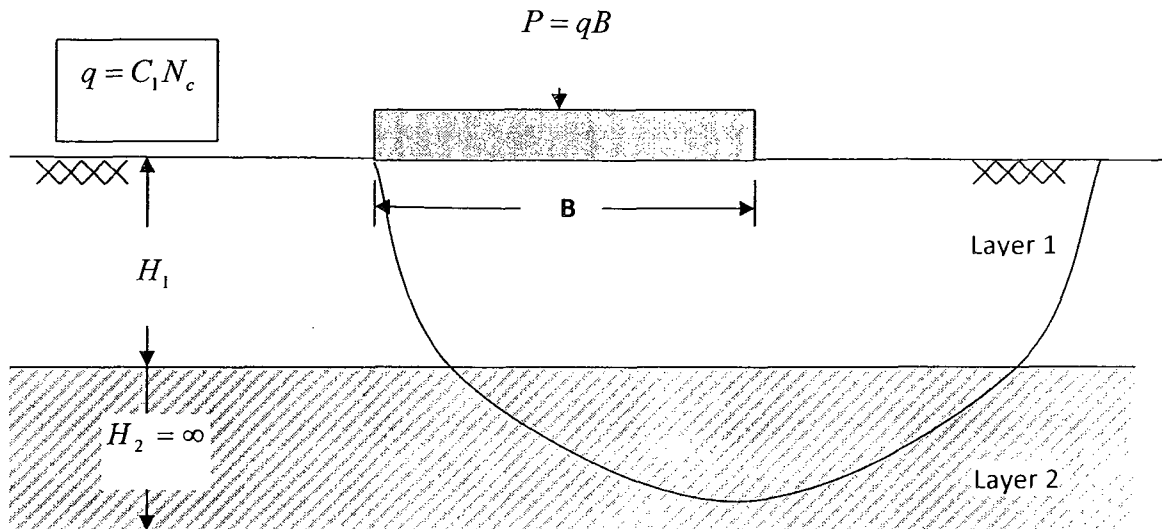


Fig. (2-1), Graphical description of strip footings in layered subsoil by Button (1953)

In 1967 Reddy and Srinivasan (1967) combined the work of Button (1953) and the graphic suggestion of Casagrande and Carrillo (1954) for the variation of shear strength with depth to study the effect of non-homogeneous and anisotropy on bearing capacity of layers of clay soils. They presented their results in graphical form that can be used directly to calculate the bearing capacity for a variety of (K) values. They concluded that the bearing capacity for anisotropic medium could increase by 15% or decrease by 30% of that for isotropic medium for the range of K values = 0.75 – 2.0.

Where:

K is the coefficient of anisotropy, which is equal to vertical shear strength over horizontal shear strength.

The experimental results of Brown and Meyerhof (1969) have disputed the assumption of cylindrical failure surface for layered soils, fig. (2-2).

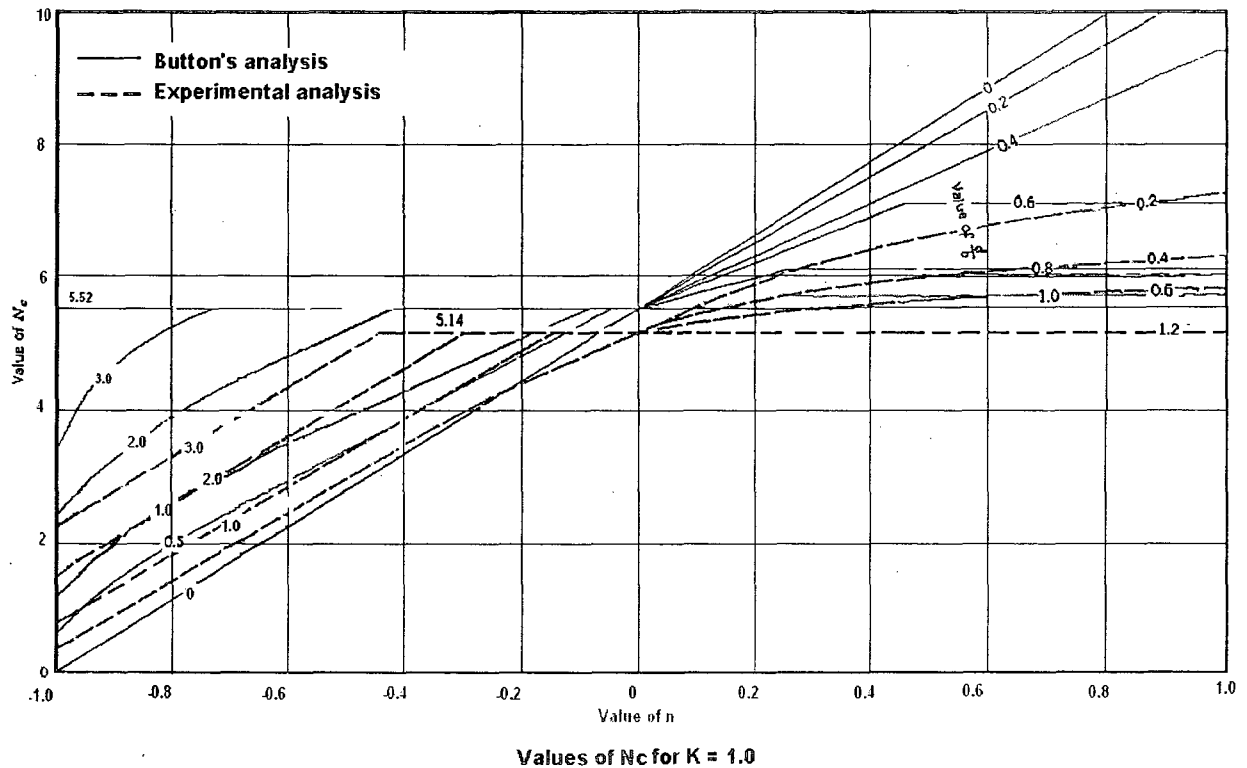


Fig. (2-2), Results of Meyerhof and Brown's discussion for the Button's analysis

Brown and Meyerhof (1969) presented a design charts to estimate the modified bearing capacity factor ( $N_c$ ) for a given shear strength ratio ( $c_2/c_1$ ) of two clay layers based on experimental work. These charts were used to evaluate the bearing capacity of layered clay for both strip and circular footings.

Meyerhof (1974) investigated the cases of shallow foundations on a thin layer of sand over deep deposit of clay for the combination of dense sand overlying soft clay and loose sand overlying stiff clay (Figure 2-3).

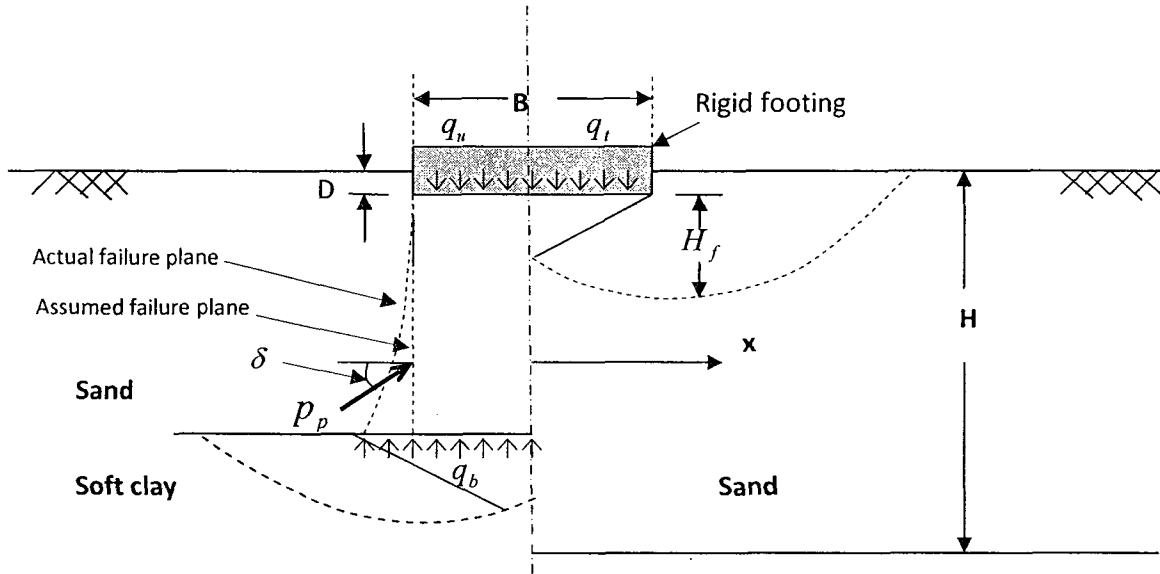


Fig. (2-3); Failure mechanism for footings on layered soil (left side) and homogenous sand (right side) after Meyerhof (1974)

Meyerhof concluded that the failure mode for strong layer overlying weak deposit occurred in punching shear and he considered the lowest of:

$$q_u = 1.2CN_c + 2\gamma H^2(1 + 2D/H)K_s \frac{\tan \phi}{B} + \gamma D \quad (2-1)$$

$$q_u = q_t = 0.3\gamma BN_\gamma + \gamma DN_q \quad (2-2)$$

Where,

$N_c$  = bearing capacity factor,

$\gamma$  = unit weight of sand and,

$K_s$  = coefficient of punching shearing resistance which is effected by the value of  $\phi$  and the ratio H/B

While for the case of loose layer overlying dense deposit the failure took place by squeezing the upper layer soil laterally, and the ultimate bearing capacity was given as:

$$q_u = 0.5\gamma b N'_\gamma + \gamma D N'_q \quad (2-3)$$

Where's,  $N'_\gamma, N'_q$  are modified factors that are depend on the angle of shearing resistance  $\phi, H/B$  ratio, and the degree of roughness of the base.

In an attempt to simplify the design procedure for the case of loose sand overlying deep strong deposit, Hanna (1982) presented design charts that assist designers to determine the modified bearing capacity factors  $N'_\gamma, N'_q$ , fig. (2-4).

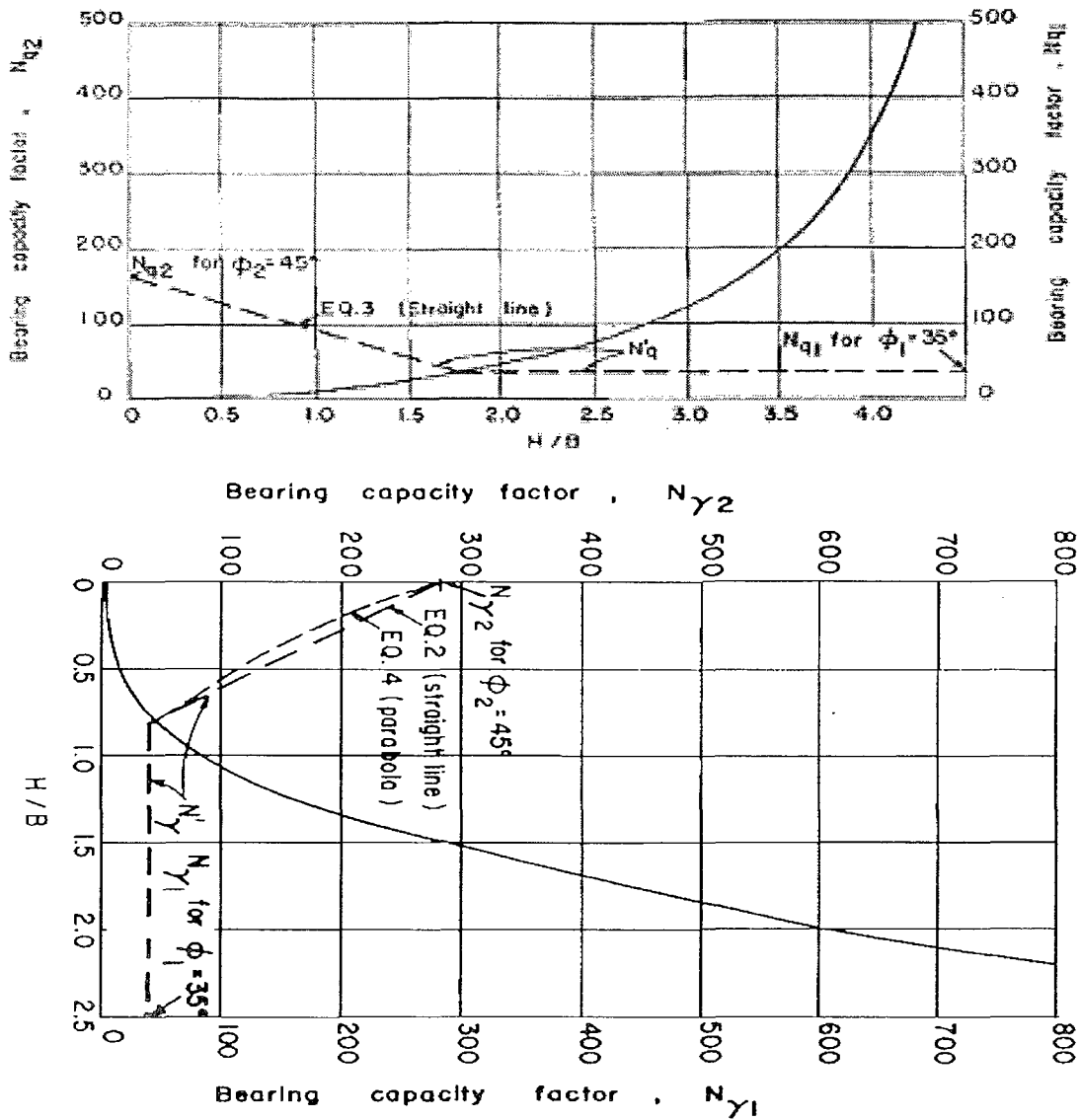


Fig. (2-4); Design charts for determination of  $N'_\gamma, N'_q$  After Hanna (1981)

Hanna and Meyerhof (1979) presented a rational theory for the case of strip footing resting on three layers, having the two upper layers stronger and thinner layers overlying deep deposit of weaker soil. Extending the punching theory developed by the authors; they presented a design theory for practicing use.

Das and Puri (1989) presented the results of a laboratory model test for the ultimate bearing capacity of shallow strip foundation on stiff clay overlying weak clay. By comparing the experimental results with those available in the literature, they concluded that the theory of Meyerhof and Hanna (1979) provides the best results.

In 1980 Hanna and Meyerhof extended their work by presenting design charts that can be used directly in predicting the bearing capacity of strip or circular footings resting on dense sand layer over soft clay deposit.

Hanna (1981- a) investigated theoretically the case of footings on dense sand overlying loose cohesionless deposit, as shown in Figure (2-5). He presented a design theory to estimate the coefficient of punching shear resistance ( $K_s$ ) for given values of ( $\phi_1$  and  $\phi_2$ ), to be used to calculate the bearing capacity for strip or circular footings as follow:

$$q_u = q_b + \gamma_1 H^2 \left( 1 + \frac{2D}{H} \right) K_s \frac{\tan \phi_1}{B} - \gamma_1 H \leq q_t \quad (\text{For strip footings}) \quad (2-4)$$

$$q_u = q_b + \gamma_1 H^2 \left( 1 + \frac{2D}{H} \right) S_s K_s \frac{\tan \phi_1}{B} - \gamma_1 H \leq q_t \quad (\text{For circular footings}) \quad (2-5)$$

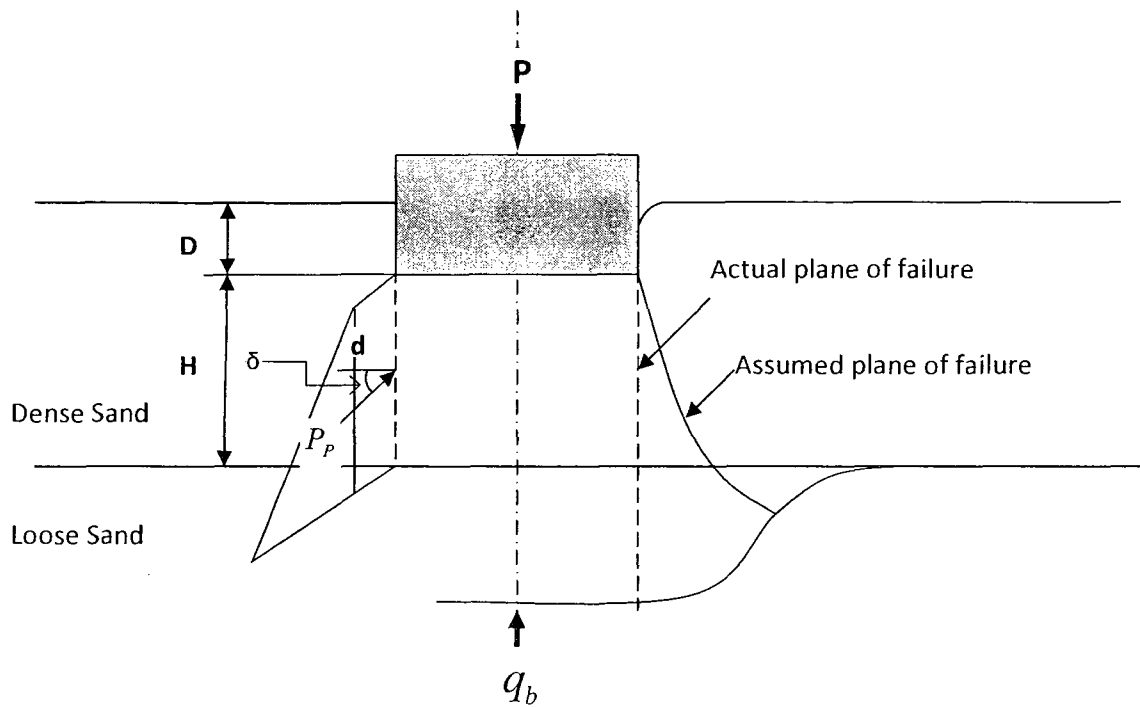


Fig. (2-5); Failure mechanism in layered cohesionless soils, after Hanna (1981)

Satyanarayana and Garg (1980) proposed an empirical equations that considers the average value for both  $C$ , and  $\phi$ , and the concept of the equivalent significant depth ( $D_e$ ) to calculate the ultimate bearing capacity.

$$C_a = \frac{C_1 Z_1 + C_2 Z_2}{Z_1 + Z_2} \quad (2-6)$$

$$\phi_a = \tan^{-1} \left( \frac{\phi_1 Z_1 + \phi_2 Z_2}{Z_1 + Z_2} \right) \quad (2-7)$$

$$D_e = Z_1 + (2B - Z_1) \left( \frac{C_1 + \tan \phi_1}{C_2 + \tan \phi_2} \right) \quad (2-8)$$

Hanna (1981- b), argued the validity of the theory and presented compiling evidences to support that this assumption will lead to discrepancies ranging from 70- 85% between the experiments results and the empirical ones. Also he noted that the depth of the upper layer at which the lower layer has no more influence on the bearing capacity depends on the relative strength of both layers as well as on the footings type.

In 1987 Hanna compared the results that were obtained from a small scale model strip footing on homogeneous and layered sand, with those obtained theoretically using finite element technique that had been developed by Duncan and Chang for non-linear stress-strain relationship, where good agreement was noted.

Oda and Win (1990) carried out 12 laboratory tests to study the effect of sandwiched thin soil layer on the bearing capacity of strip footings. They concluded that the effect of the thin layer extends to 5 times the footing width and that the plastic flow occurs in the lateral direction, causes reduction in the bearing capacity of the footing. These finding agree with the work of Hanna and Meyerhof (1978), but defied that of Terzaghi (1943) which claims that the effect of the clay layer diminishes at a depth of at least 1.5 times the footing's width (B).

Kenny and Andrawes (1996) based on a laboratory tests results; for the case of sand overlying soft clay, agreed with the solution proposed by Meyerhof (1974). Nevertheless, they suggested that local shear failure of the clay layer should be



driven as a function of layers properties, the depth/width ratio and the angle of failure planes with the vertical.

$$q_u = q_b - \gamma_1 H + \frac{\gamma_1 KP \sin \delta}{\tan \alpha} \left[ DF + \frac{2H \tan \alpha - BF}{2 \tan \alpha} \right] \quad (2-10)$$

### 2.2.2 KINEMATICAL AND NUMERICAL INVESTIGATIONS

Georgiadis and Michalopoulos (1984) introduced a numerical method to estimate the bearing capacity of footing on layered soils of any soil/loading conditions. They developed a computer program that determines the minimum factor of safety for different combinations of the depth of failure surface and the lengths  $L_1$  and  $L_2$ . Comparing the result from this method with the existing finite elements method gave good agreements for two layers of clay soils, but when comparing with the several semi-empirical methods for the case of two sand layers the results scattered.

Sloan (1989) presented a finite element and linear programming method, which he used along with the upper bound theorem, to assess the stability of undrained soils, and assuming Tresca's yield criteria with a perfectly plastic soil model. He used a three-noded triangle with six nodal velocities, fig. (2-7).

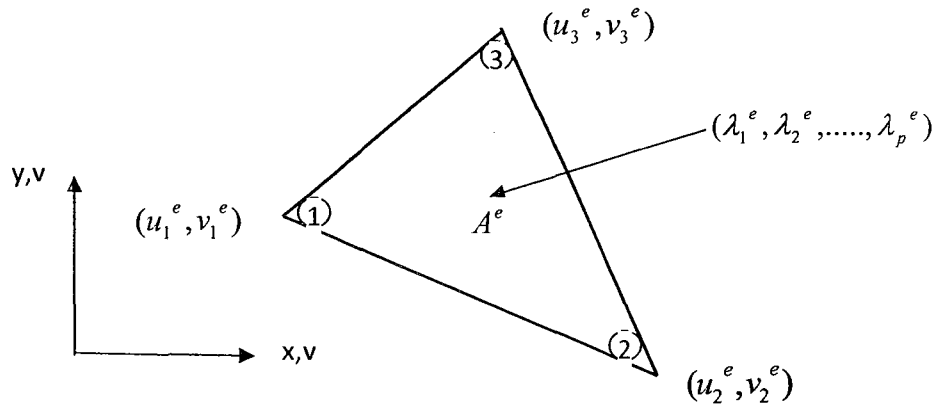


Fig. (2-7); Triangle element used in the upper bound limit analysis presented by Sloan (1989)

Florkiewicz (1989), has dealt with the problem from a different angle, assuming the interface surface between the two layers as non-horizontal, he tried to find the upper bound load limit numerically, by modeling a kinematically admissible failure surface, that consists of rigid-motion blocks then minimizing the limit load ( $P_k$ ) with respect to the  $\alpha_i$  &  $\beta_i$  angles.

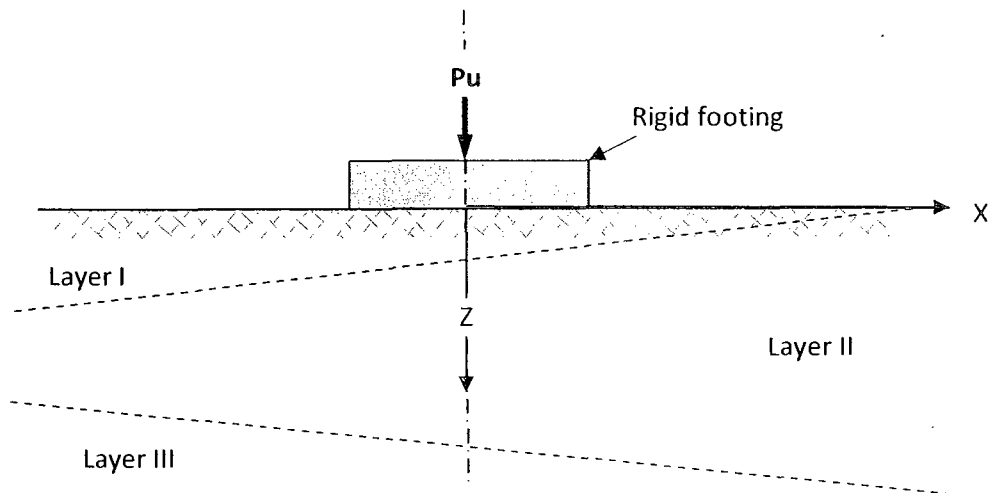


Fig. (2-8); Florkiewicz's assumption of layered sub-soils

Then he compared his results with the previous experimental work of Hanna & Meyerhof (1978) for two clay layers and with Hanna (1981- a) for two sand layers. In both cases his theory yielded upper bound solutions, though in all of the experimental the interfaces of the soils' layers were horizontal.

Tamura (1989), in his work he combined both Drucker-Prager and Mohr-Coulomb plasticity models with and without the association of flow rule in order to formulate a finite element method that can determine the bearing capacity for a medium with discontinuities. The most important factors that can affect this kind of problems are the location and the distribution of the discontinuities among the soil mass.

Michalowski and Shi (1995) have equated the rate of the external forces work to the rate of internal energy dissipation; an upper bound to the true limit load was found. Two failure mechanisms were considered for the case of strong sand over weak clay, as they yielded the minimum bearing capacities.

Sloan and Kleeman (1995) presented a procedure for computing the rigorous upper bounds under plain-strain strip footing as the exact collapse load. Using finite element and linear programming, based on linear three-noded triangular element, but without the need to arrange them in a specific pattern or specifying shear signs. This formulation is quite general for all type of materials, drained or undrained and less time consuming by permitting velocity discontinuities at all edges shared by adjacent triangles finding the directions of shearing automatically.

Frydmen and Burd (1997), have used both FLAC and OXFEM numerical methods to carry out a detailed parametric study on bearing capacity of sand layer over-laying clay, which helped specifying the system mechanism and producing dimensionless design charts for the bearing capacity.

Sloan, Merifield and Yu (1999) have tried to bracket the true collapse load from both the lower bound and upper bound, by applying the limit analysis numerically to evaluate the untrained bearing capacity of a rigid surface footing on two layers of clay. The results showed an accuracy of about 12% with the exact collapse load. They presented them in the form of modified bearing capacity factors  $N_c^*$ . Nevertheless, they reported that the effect of the thickness of the upper stronger layer on the bearing capacity continued until 1.5 – 2 times the footing's width.

Wang and Carter (2001) considered the large deformation analysis in strip and circular footing resting on two layers of clay. They reported that in the cases where the second layer is very soft and where punching through the top layer is a possibility the small displacement assumption is not a function any more, and the large deformation analysis should take a role. By modifying the algorithm of the ALE (Arbitrary Lagrangian-Eulerian) approach that was previously introduced by Hu and Randolph to consider the two-layered soils, and using the AFENA finite element package of Carter and Balaam. They concluded:

1. The load-displacement curves predicted for the large deformation analysis differs significantly from those for the small deformation analysis.

2. The large deformation effect is more significant for circular footing on tow-layered soils than for strip footing.
3. Soil-self weight has a big effect on the bearing capacity of footings in layered cohesive soils analyzed for large deformation. Therefore, the addition of the soil-self weight ( $\gamma_s$ ) to the bearing resisting yields a more accurate estimation of the bearing capacity.

Combining the newly presented techniques, of upper and lower bounds limit analysis of Lyamin and Sloan (2001-2002), to bracket the true solution, and the classical approach of the bearing capacity of two layers of clays, Lyamin, Shiau and Sloan (2003) proposed a method to obtain the rigorous plasticity solutions for the bearing capacity of sand over clay layered soils. Assuming that the soil layers obey an associated flow rule, their results ranged within  $\pm 10\%$ .

## 2.3 DISCUSSIONS

Despite of all the previous work that had been done to solve the problem of layered soils, yet there is no rational solution can be found in the literature.

One of the most widely used solution in foundation engineering to determine the bearing capacity in layered soils is the semi-empirical approach of Meyerhof (1974) and Hanna and Meyerhof (1978) which is also known as punching shear models. Examining those theories experimentally or numerically has proven its accuracy so far. Even the results that didn't agree with it, like the results of Das and Puri (1989) or Madhira & Sharma (1991) was in the range of  $\pm 10-30\%$  with theory.

Other researchers such as Radoslaw, Michalowiski and Shi, and Florkiwicz, approached the solution kinematically with a more rigorous approach by assuming power dissipation at the interfaces of the geometrically optimized rigid blocks. Despite the agreement of those approaches with the previous experimental or theoretical solutions they are limited to the specific assumptions that they were used to develop their models.

## **2.4 OBJECTIVES**

The objective of this thesis is to develop a numerical model to simulate the case of strip footing on a dense sand layer overlying weak deposit. The model should be capable to address the shortcoming of the previously reported theories by providing accurate and realistic evaluation of the level of shear mobilization on the punching failure plans. The results of this study will be presented in the form of design procedure for practicing use.

## CHAPTER THREE

### NUMERICAL MODEL

#### 3.1 GENERAL:

In this Chapter the case of bearing capacity of rigid plane-strain shallow strip footing placed on the surface of a uniform dense sand layer with limited thickness overlying a deep, homogeneous bed of loose sand was examined (Figure 3-1). A numerical model is developed to simulate this case using finite element technique and the computer program "PLAXIS" version 8.6. The model is capable to measure the mobilized shear strength on the punching failing column. "PLAXIS" was developed in 1987 in the Technical University of Delft (Holland) to evaluate river embankments. Nowadays, it becomes one of the most reliable software to analyze complicated geotechnical problems.

The numerical results produced in this thesis were validated using the

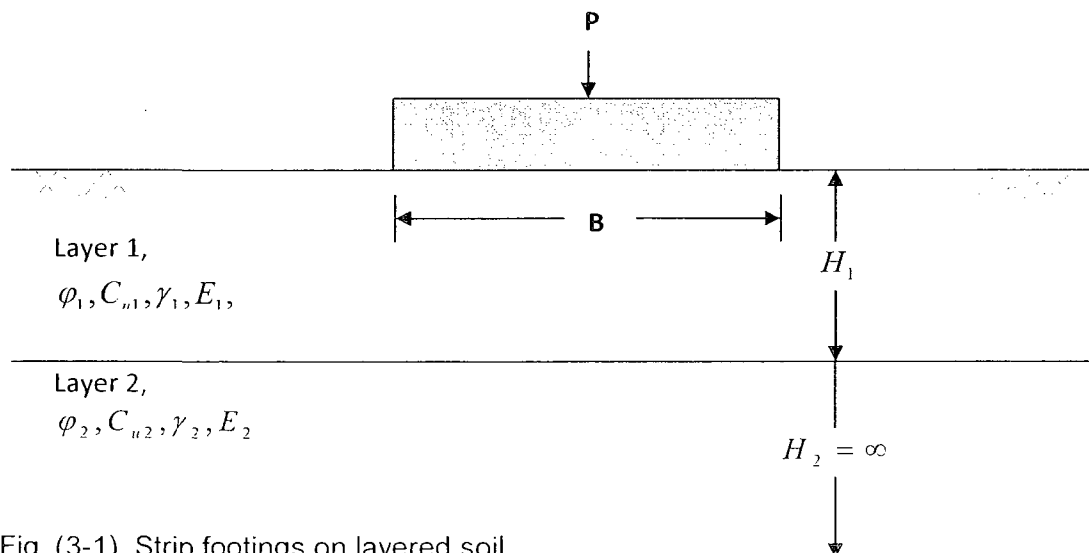


Fig. (3-1), Strip footings on layered soil

experimental data of Meyerhof and Hanna (1978) and the theory of punching failure mechanism in layered soils proposed by Hanna (1981- a).

### **3.2 NUMERICAL MODEL**

Two-dimensional finite element model will be developed to simulate the problem stated. The dimensions of the model were chosen conservatively to prevent any boundary condition. An assumption is made so that for each layer the soil properties and stiffness are constant within the depth of the layer.

A finite element mesh was generated using a finite number of triangular elements with 15-node each. This will provide a fourth order interpolation for displacements and a numerical integration that involves twelve stress points. The meshes were medium in size with fine elements in the zones where deformation is expected. Figure (3-2) represents a sample of the numerical model as defined in the program.

The program operates by prescribing values for the vertical displacement, applied incrementally on the nodes at the base of the footing. The bearing capacity was obtained from values of the pressure that developed below the footing due to the increase of the footing displacements. The evaluation of the results of the numerical model is made with those obtained by the Semi-empirical formula of Hanna (1981- a). In this investigation, the ultimate bearing capacity of a foundation was defined as the maximum load (the peak load) that the soil can withstand at failure; i.e. the pressure which causes shear failure.

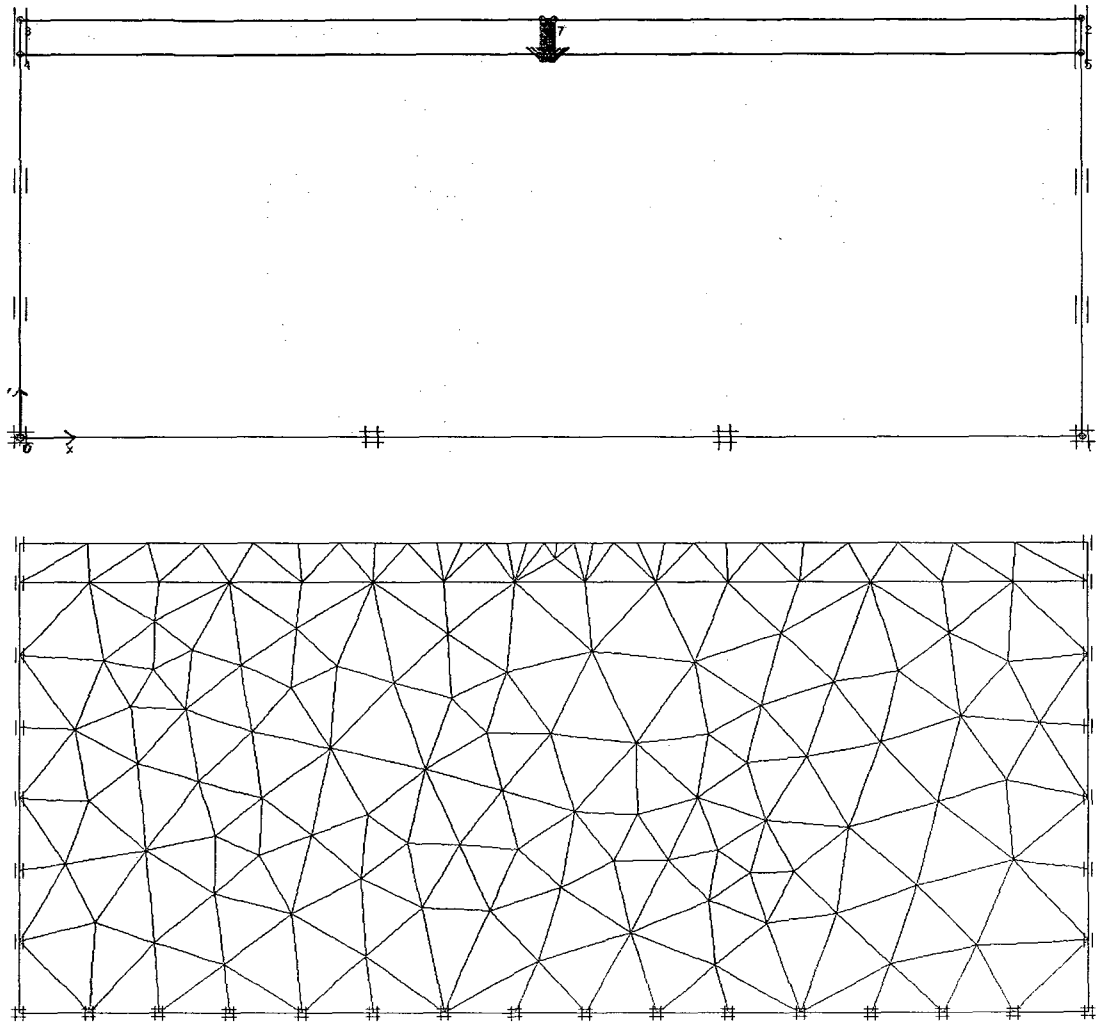


Fig.(3-2) Numerical model and redefined mesh

### 3.3. CONSTITUTIVE LAW

The elastic perfectly- plastic non-linear behavior of the soil is simulated using the Mohr-Coulomb failure criteria model, which requires five input parameters that are commonly available; these are: Young's modulus,  $E$ , Poisson's ratio  $\nu$ , cohesion  $C$ , friction angle  $\varphi$ , and dilatancy angle  $\psi$ .

In this investigation, the elastic modulus of the soil,  $E$  and the Poisson's ratio are used to calculate the stiffness module as follows:

$$G = \frac{E}{2(1+\nu)} \quad (3-1)$$

$$K = \frac{E}{3(1-2\nu)} \quad (3-2)$$

Furthermore: the angle of dilatancy is obtained from:

$$\psi = (\varphi - 30)^\circ \quad (3-3)$$

A minimum value of the cohesion  $C$  is assumed equal to unity for cohesionless soil as stipulated by "PLAXIS".

### 3.4 BOUNDARY CONDITIONS

To insure that the entire plastic zone is contained in the meshes and that the boundaries are sufficiently distant from the footings; fig. (3-3); the meshes were initiated on a model dimensions that are  $(42 \times B)$  in the X-direction from the center line of the footings and  $(36 \times B)$  in the Y-direction measured from the base of the footing. Figure (3-4) presents a typical mesh used in this investigation.

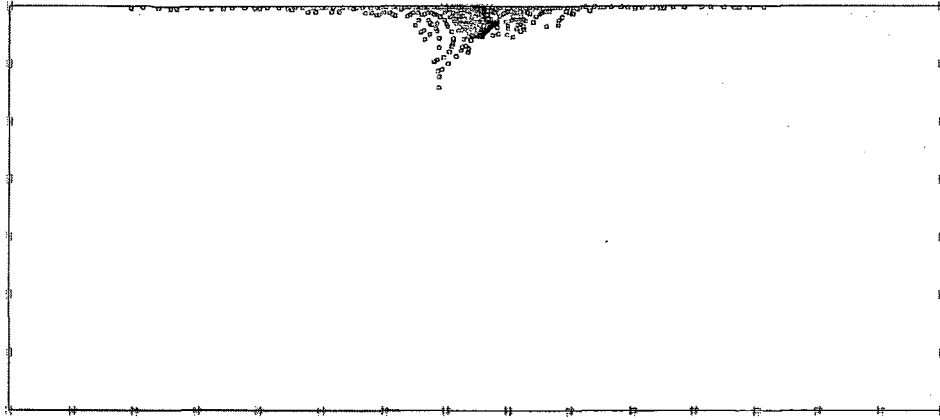


Fig. (3-3); Plastic points distribution on the deformed mesh.

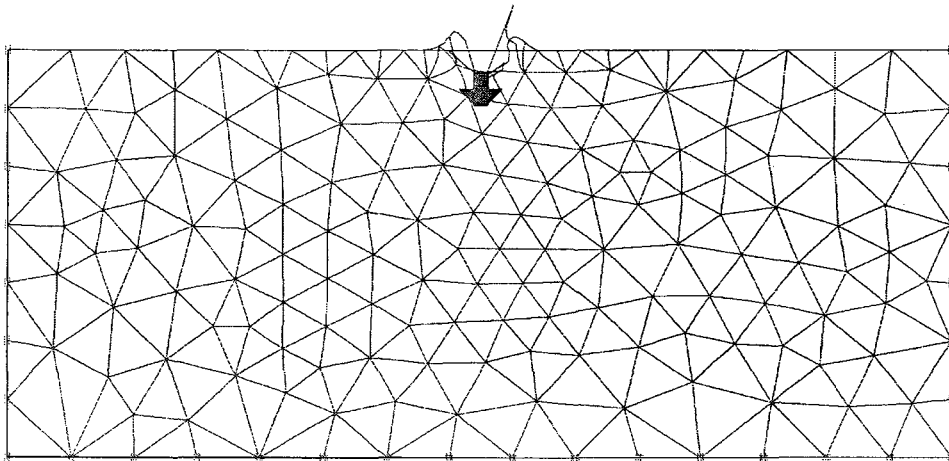


Fig. (3-4); Deformed mesh scaled up to five times of homogeneous dense sand of (42B X 36B) model size, with prescribed displacement of 1m in the Y-direction with fixed boundaries in the X-direction.

To eliminate the boundary effect during loading of the footing, the stresses at the boundaries were compared with the classic values of the horizontal and vertical earth pressures as follow:

$$\sigma_{hor.} = K_o \gamma_{sat} Z \quad (3-4)$$

$$\sigma_{ver.} = \gamma_{sat} Z \quad (3-5)$$

Where:  $\sigma_{hor.}$  and  $\sigma_{ver.}$  are the horizontal and vertical stresses at rest, respectively.

### 3.5. ELEMENTS TYPE

During the mesh generation, the clusters are divided into triangular elements. The powerful 15-node element is chosen to provide accurate calculations of the stresses and failure loads, as it's composed of much finer and much more flexible meshes than those composed of 6-node elements. Preselected nodes will be used to generate the load-displacement curve. In addition to the nodes each element contains 12 individual stress points which can be preselected to generate the stress paths or the stress-strain diagrams. Figure (3-5) shows the element's nodes and stress points.

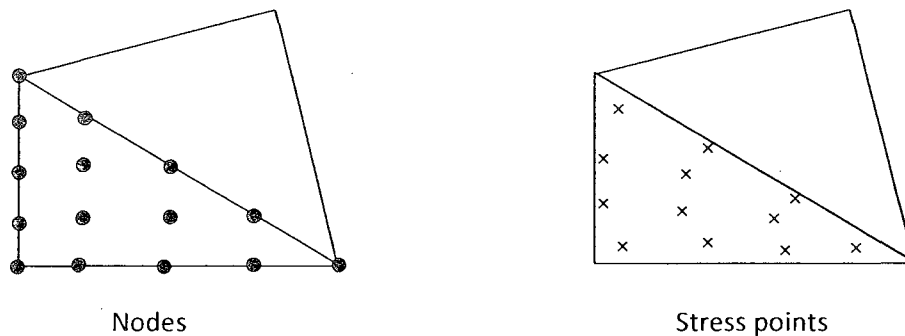


Fig. (3-5), Elements type showing the allocation of nodes and stress- points

### 3.6 DETERMINATION OF THE MOBILIZED ANGLE OF SHEARING RESISTANCE $\delta$ NUMERICALLY

Hanna (1978) considered three important points to determine the theoretical value of the angle of shearing resistance, ( $\delta$ ), mobilized on the assumed planes of failure, which are:

1.  $\delta < \phi_1$ , if the analysis made on the vertical assumed planes of failure, and it will reach a maximum value of  $\delta = \phi_1$ , when the assumed planes becomes the actual curved planes of failure.
2. Since the upper sand layer is stronger than the lower one, the strain in the upper layer at failure is much smaller than that of the lower layer, which leads to the fact that the occurrence of failure strains in both layers simultaneously is impossible. Thus, the mobilized angle of shearing resistance of the upper layer is less than the peak value, this can be reflected on the value of  $\delta$  and  $K_p$ .
3. the vertical displacement of the upper sand punching column increases as the strength of the lower sand layer decreases, in other words, the mobilized passive earth pressure on the assumed vertical failure planes decreases with a decrease of the lower sand layer strength. In order to overcome the mathematical difficulties verifying any of the above arguments he used the dimensionless expression of ( $\delta/\phi_1$ ).

In this investigation, the following procedure was considered to calculate the angle of shearing resistance ( $\delta$ ) mobilized on the plane of failure using the "PLAXIS" program.

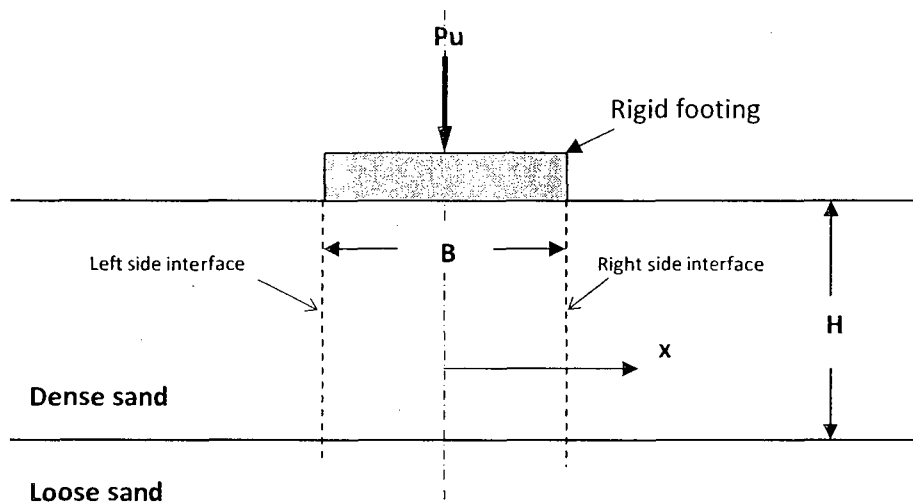


Fig. (3-6); Punching shear column.

Two vertical interfaces are introduced in the numerical model from the outer sides of both edges of the footing and along the upper layer, to give an indication of the model behavior and the stresses and strains distributions on these critical areas, fig.(3-6). Each interface is assigned a virtual thickness to it, which is an imaginary dimension used to define the material properties of the interface. The virtual thickness is calculated by multiplying the virtual thickness factor by the average element size which is determined according to the global coarseness setting. Since the normal stresses used in our case are considerably large, then the virtual thickness factor of the element was taken as the minimum value of

(0.05mm). In the 15-node soil elements the interface elements are connected to the soil elements with five pairs of nodes, and the coordinates of each node pair are identical; which means that the interface element has no thickness. Figure (3-7) shows the 15-nodes soil element used in this study and its connection with the

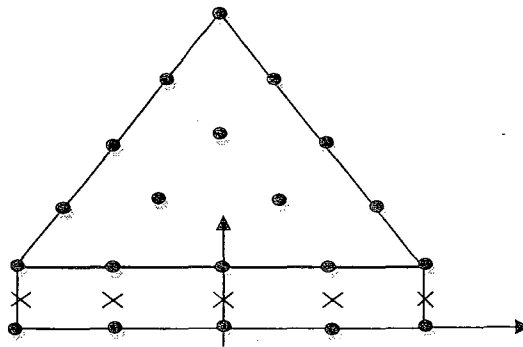


Fig. (3-7); Distribution of stress points in interface elements, and their connection with the soil elements.

introduced interface element. Interface elements are generally modeled by means of bilinear Mohr-Coulomb model, this means that these elements will pick the corresponding cluster material data set  $(C, \varphi, \psi, E, \nu)$  for the Mohr-Coulomb model.

### 3.7 GENERATION OF MESH

To generate a finer mesh around the area of interest in the numerical model, extra geometry lines were introduced at certain distances from the interfaces, figure (3-7). these lines will not affect the calculations of the total stresses and

strains in the soil but it will help assigning finer meshes in these areas to give smoother stresses or strains distribution curves. Local element size factor reaches 0.1 around the previously mentioned geometry lines. The global coarseness of the mesh was fine, then additional refinement is done under the footing and at the two layers interface, to control uniformly distribution of the finite elements mesh at these areas, but without elongating the calculations time significantly.

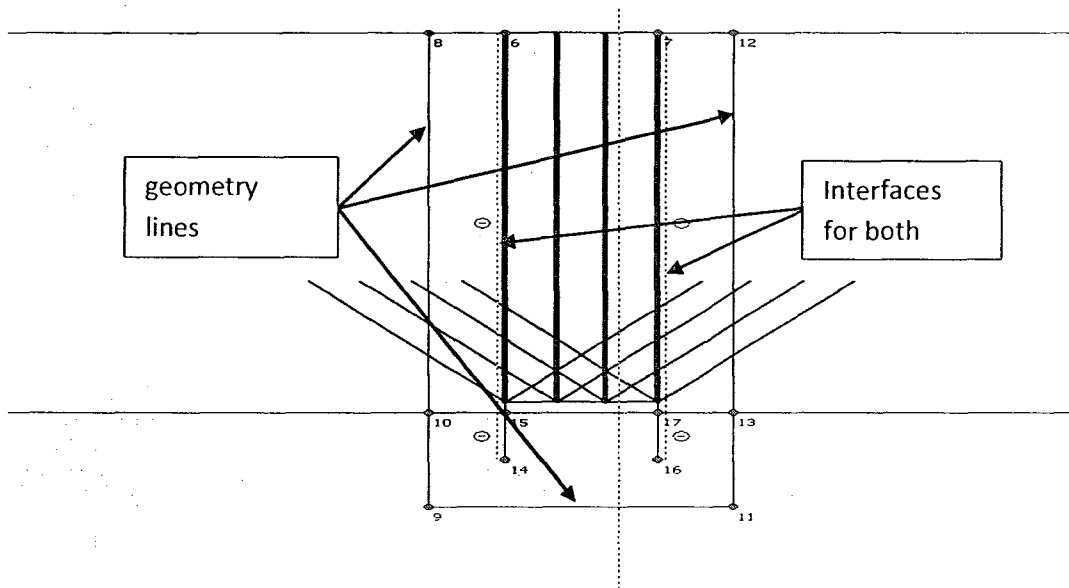


Fig. (3-8); cross-section showing the position of the Interfaces and the geometry

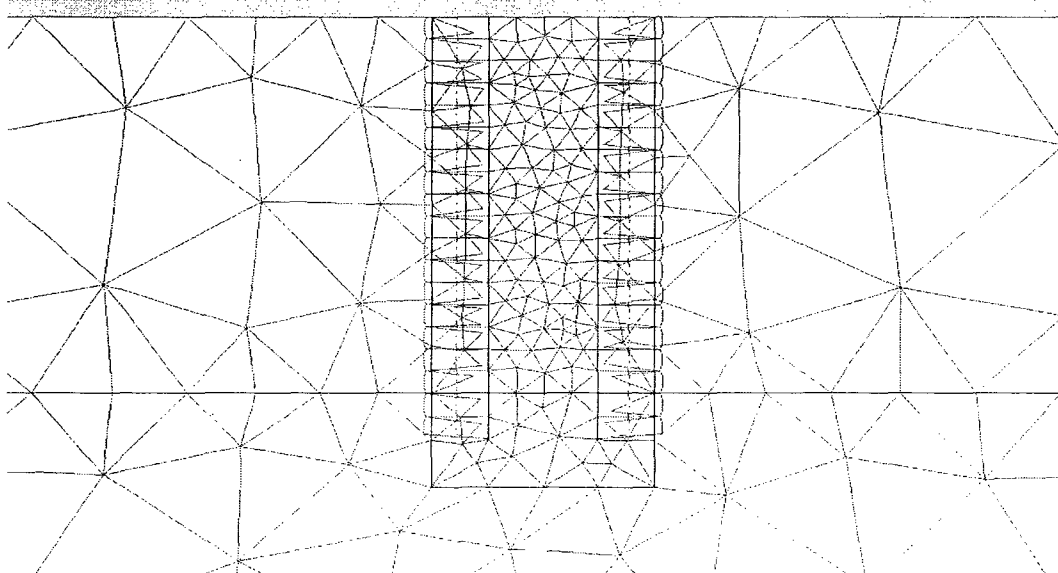


Fig. (3-9); cross-section in the generated mesh with finer mesh around the punching

Figure (3-9), shows a cross section in the generated fine mesh with the finer elements around the punching column.

From the menu of "PLAXIS", a plastic analysis was chosen with an updated mesh option, as it gave better results without any significant extension in the computation period. This option considers the calculation for a large deformation effect as it automatically updates the stiffness matrix at the beginning of any load increment. Then a prescribed displacement of 0.5m was assigned to the soil under the footings.

The interfaces were activated at the beginning of the calculation stage, and then at the end of the calculation program, tables were automatically generated for all the information regarding each point's coordinates, stresses, strains and other data. The mobilized angle of shearing resistance  $\delta$  is calculated for every point in these tables using the relation of the normal and shearing stresses along the plans of failure:

Figure (3-9) shows the deformed mesh at the end of the calculations and the contour lines of the total displacement for the same model.

$$\tau = \sigma \tan \delta \quad (3-6)$$

This gives:

$$\delta = \tan^{-1} \frac{\tau}{\sigma} \quad (3-7)$$

### 3.8 MODEL VALIDATION

The validation of the model was done on two parts, first for the bearing capacity model which were validated with Hanna (1981- a). The second is for the customized model for the  $\delta$  calculations, and this is modified with the prototype results of Meyerhof and Hanna (1978).

The input of the material data for the model was assigned after intense study of the available experimental ranges. Table (3.1) presents a wide range of these

Table (3-1); Soil properties used in this investigation

Soil Type	Friction Angle ( $\phi$ )	$E_s$ ( $KN/m^2$ ) * $10^3$	$\gamma_{dry}$ ( $KN/m^3$ )	$\gamma_{sat}$ ( $KN/m^3$ )	$C_u$ Cohesion ( $KN/m^2$ )	$\nu$ Poisson's ratio
Very soft clay		2 - 15	8	15 - 17	12	0.1 - 0.2
soft clay		5 - 25	8	16 - 19	18.2 - 30.2	0.15 - 0.3
medium clay		15 - 50	16	17 - 20	36 - 54.1	0.35 - 0.4
stiff clay,		50 - 100	18	19 - 22	59.9 - 95.8	0.4 - 0.45
dense sand	35 - 43	48 - 81	19 - 22	17 - 23		0.3 - 0.45
dense sand and	28 - 50	96 - 190	18	14 - 24		0.15 - 0.35
silt sand loose to	28 - 38	7 - 21	14 - 20	14 - 22		0.2 - 0.4
loose sand	27 - 32	10 - 24	13 - 18	14 - 18		0.2 - 0.4

properties which are of practical interest and will be used as guiding data for the model.

### 3.8.1 BEARING CAPACITY MODEL VALIDATION

In the generation of data, two sets of properties were assigned for the upper layers separately ( $\varphi_1 = 43^\circ$ , and  $\varphi_1 = 47^\circ$ ) for which, the lower layers  $\varphi_2$  will be ranging from ( $30^\circ$  to  $42^\circ$ ). But for the validation purpose only three set of layered soil system will be used. Hanna's (1981) semi-empirical equations (3-11, 3-12, & 3-13) were used to calculate the ultimate bearing capacity for the same parameters, as those of the present study.

$$q_b = 0.5\gamma_2 BN_{\gamma_2} + \gamma_1(H + D)N_{q_2} \quad (3-8)$$

$$q_t = 0.5\gamma_1 BN_{\gamma_1} + \gamma_1 DN_{q_1} \quad (3-9)$$

In which  $N_{\gamma_1}, N_{q_1}$  and  $N_{\gamma_2}, N_{q_2}$ , are the bearing capacity factors that are corresponding to the shearing resistance angles  $\varphi_1, \varphi_2$  of the upper and lower layers of sand respectively. There values were obtained from the charts presented by Meyerhof (1974).

$$q_u = q_b + 2\gamma_1 H^2 \left(1 + \frac{2D}{H}\right) K_s \frac{\tan \varphi_1}{B} - \gamma_1 H \leq q_t \quad (3-10)$$

Were the value of  $K_s$  obtained from the design chart proposed in the same study from the intersecting of the values of  $\varphi_1, \varphi_2$ .

The cases that were considered in the numerical study assume a shallow foundation at the ground level ( $D= 0$ ) so the above equations were adjusted to that case as shown below:

$$q_b = 0.5\gamma_2BN_{\gamma_2} + \gamma_1HN_{q_2} \quad (3-11)$$

$$q_t = 0.5\gamma_1BN_{\gamma_1} \quad (3-12)$$

And;

$$q_u = q_b + 2\gamma_1H^2K_s \frac{\tan \phi_1}{B} - \gamma_1H \leq q_t \quad (3-13)$$

For the numerical model, the load settlement curves are obtained for each set of soil properties, and first layer height. Then the bearing capacity is the value of the load at the maximum curvature point of each curve.

The properties of the soil layers for the validation models are shown in table (3-2) below.

Table (3-2); Input data for the validation purpose.

Soil Type	$\phi$	$E_s$	$\gamma_{dry}$	$\gamma_{sat.}$	$C_u$	$\nu$	$\psi$
V.D.sand& gravel	47	100	20	23	1	0.38	17
v.d. sand	43	80	19.5	22	1	0.38	13
L. sand	35	48	17	19	1	0.35	5
v.L. sand	30	11	13	16	1	0.3	0

Tables (3-3 to 3-5) represent the bearing capacity values for each H/B ratio, obtained from the present and the previous investigations. A graphical presentation is provided in figures (3- 10) to (3-12).

The results of both investigations are in good agreement especially for higher ratios of H/B. it is noticeable that at smaller values of the presiding ratio, and for stronger lower layers, there was a small different between the compared values, which can be due to the sensitivity of the finite element analysis in such small heights of the upper layer.

Table 3.3:  $\varphi_1 = 43^\circ, \varphi_2 = 30^\circ, C_u = 1 \text{ KN/m}^2$

$H/B$	$q_u$ Hanna1981 ( $\text{KN/m}^2$ )	$q_u$ present study ( $\text{KN/m}^2$ )	displacement @ failure for present study (m)
0.5	356	328.02	0.088
1.0	614.3	618.67	0.191
1.5	931.6	942.3	0.305
2.0	1308.1	1302.9	0.47
2.5	1743.6	1741.0	0.666
3.0	1818.8	1811.4	0.638
3.5	1818.8	1815.6	0.644
5.0	1818.8	1825.4	0.384
7.0	1818.8	1874	0.28
10.0	1818.8	1911.9	0.204
15.0	1818.8	1936.5	0.144

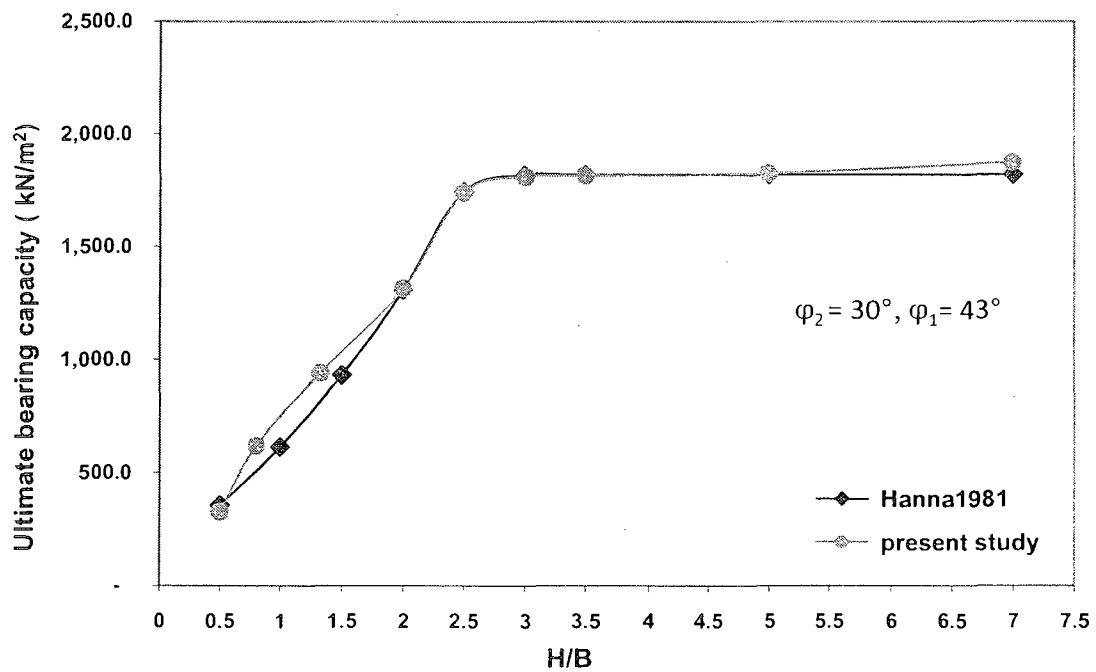


Fig. (3-10); Comparison between the results of the present study and Hanna 1981 results; for  $\varphi_1 = 43^\circ$  and,  $\varphi_2 = 30^\circ$

Table 3.4:  $\varphi_1 = 43^\circ, \varphi_2 = 35^\circ, C_u = 1 \text{ KN/m}^2$

$H/B$	$q_u$ Hanna1981 ( $\text{KN/m}^2$ )	$q_u$ present study ( $\text{KN/m}^2$ )	displacement @ failure for present study(m)
0.5	759.5	322.88	0.015
1.0	1183.5	1172.5	0.089
1.5	1680.2	1574.5	0.128
2.0	1818.4	1737.5	0.146
2.5	1818.4	1796.6	0.142
3.0	1818.4	1808.5	0.142
3.5	1818.4	1812.4	0.156
5.0	1818.4	1816.4	0.12
7.0	1818.4	1809.5	0.114
10.0	1818.4	1808.6	0.101
15.0	1818.4	1818.4	0.09

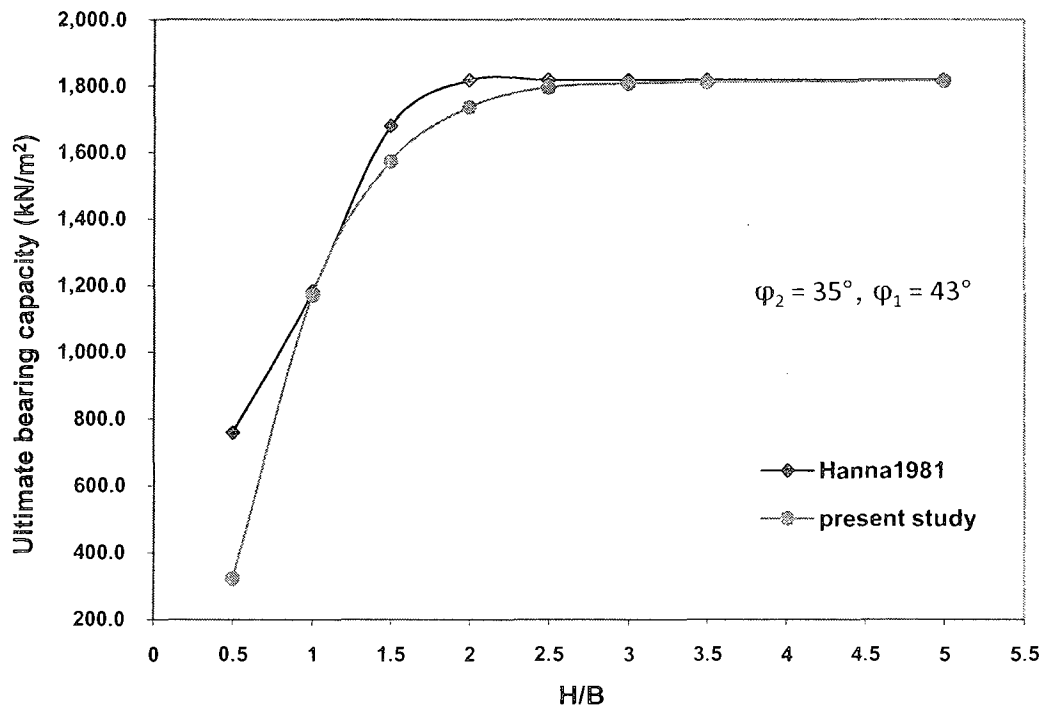


Fig. (3-11); Comparison between the results of the present study and Hanna 1981 results; for  $\varphi_1 = 43^\circ$  and  $\varphi_2 = 35^\circ$

Table 3.5:  $\varphi_1 = 47^\circ, \varphi_2 = 35^\circ C_u = 1 \text{ KN/m}^2$

$H/B$	$q_u$ Hanna1981 ( $\text{KN/m}^2$ )	$q_u$ present study ( $\text{KN/m}^2$ )	displacement @ failure for present study(m)
0.5	782.7	380.02	0.18
1.0	1260.1	1232.02	0.095
1.5	1840.4	1830.3	0.141
2.0	2523.6	2519.2	0.207
2.5	3309.7	3279.6	0.29
3.0	4036.7	3994.7	0.378
3.5	4036.7	4074.0	0.359
5.0	4036.7	4082.6	0.298
7.0	4036.7	4056.1	0.286
10.0	4036.7	4041.2	0.258
15.0	4036.7	4065.9	0.179

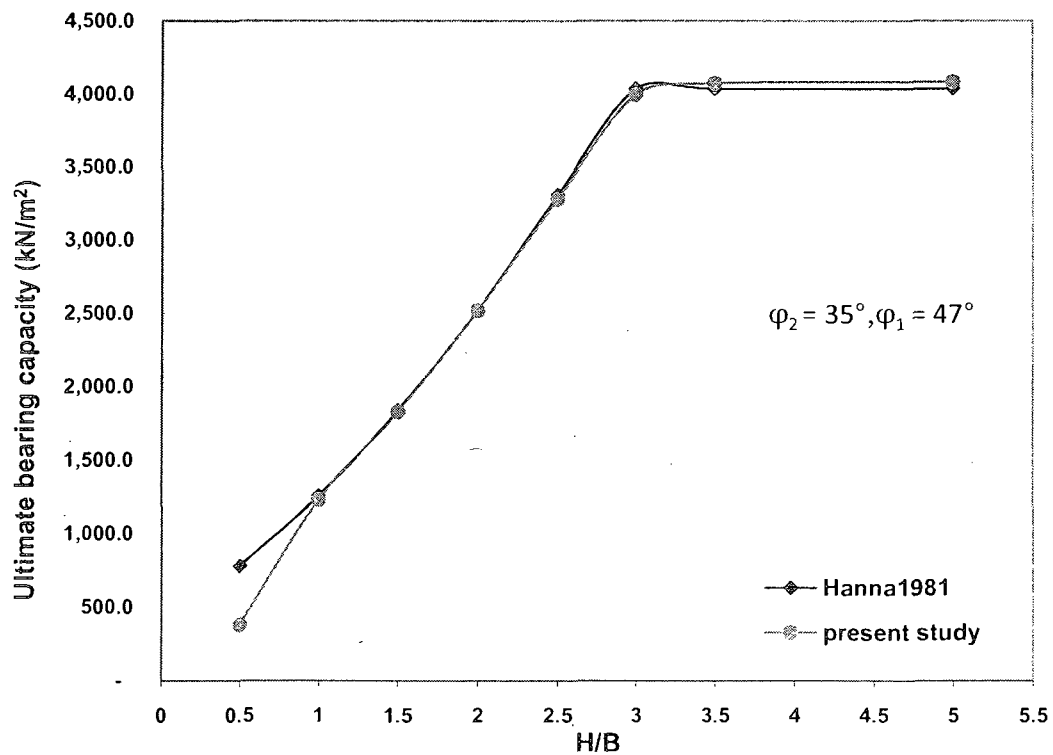


Fig. (3-12); Comparison between the results of the present study and Hanna 1981 results; for  $\varphi_1 = 47^\circ$  and  $\varphi_2 = 35^\circ$

### 3.8.2 VALIDATION OF THE CUSTOMIZED MODEL FOR $\delta$

The previous model was then modified to include the possibility to calculate the mobilized angle of shearing resistance on the plane of failure, which is validated herein with the experimental results of Hanna (1978). To do so a model was made with the same soil properties ( $q_2/q_1, H/B, \varphi_1$  and  $\varphi_2$ )

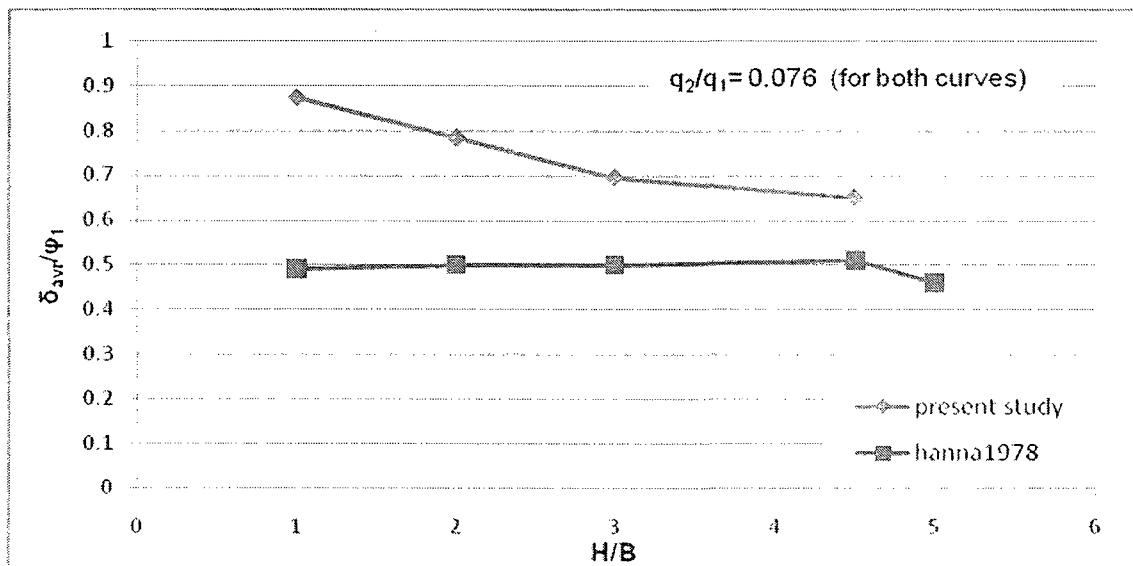


Fig. (3-13); Comparison between the results of the present study and Hanna (1978) results.

as those used in Hanna (1978) study. Then the average value of  $\delta_{avr}$  was calculated for the new study from the equivalent normal and shear stresses at the vertical interfaces sections, which are calculated automatically in the program by integrating the stress components along the cross-section. Then by applying equation (3-7) the average value of  $\delta$  is found. The ratio of  $\delta_{avr}/\varphi_1$  against the

H/B ratio was plotted for both the present and the previous studies and the results are shown in figure (3-13).

From these figures, it can be noted that good agreement for higher H/B ratio. The effect of the H/B ratio on the ratio of the the average angle of mobilized shearing resistance to the angle of internal shearing resistance of the upper layer ( $\delta_{avr}/\phi_1$ ) has been ignored in the previous study and that might have caused the disagreement of both curves for smaller H/B ratios.

## CHAPTER FOUR

### RESULTS AND DATA ANALYSIS

#### 4.1 GENERAL

In this chapter the numerical model developed herein, presented and validated with the data available in the literature in Chapter 3, will be used to generate results for a wide range of parameters. Design theory and design procedure will be presented.

#### 4.2 TEST RESULTS

The test results obtained in the present investigation for the case of strong sand overlying weak sand are summarized in Tables 4.2 to 4.7 and presented in graphical form in figures 4-1 to 4-6. It can be noted from these Tables and Figures that the bearing capacity of the footing increases due to an increase of the ratio H/B up to a limit at which the bearing capacity will become equal to the ultimate bearing capacity of the footing on homogeneous upper layer sand.

Two sets of properties were assigned for the upper layers separately ( $\varphi = 43^\circ$ , and  $\varphi = 47^\circ$ ) for which, the lower layers  $\varphi$  will be ranging from ( $30^\circ$  to  $42^\circ$ ). The thickness of the upper layer, will be changing for the same set of the two layers' system from a ratio of H/B= 0.5 to 10. This is necessary to

establish the effect of the upper layer thickness on the bearing capacity of the footing.

The input properties needed for each soil type were introduced in table (3-1) earlier, and summarized in table (4-1) below.

Table (4-1): Input data for the numerical model

Soil Type	$\phi$	$E_s$	$\gamma_{dry}$	$\gamma_{sat.}$	$C_u$	$\nu$	$\psi$
V.D.sand& gravel	47	100	20	23	1	0.38	17
v.d. sand	43	80	19.5	22	1	0.38	13
D. sand	42	7.5	19	21	1	0.36	12
d. sand	40	65.1	18	20	1	0.35	10
L. sand	35	48	17	19	1	0.35	5
v.L. sand	30	11	13	16	1	0.3	0

Table 4.2:  $\phi_1 = 43^\circ$   $\phi_2 = 30^\circ$ ,  $C_u = 1 \text{ KN/m}^2$

$H/B$	$q_u$ Hanna1981 ( $\text{KN/m}^2$ )	$q_u$ present study ( $\text{KN/m}^2$ )	displacement @ failure for present study (m)
0.5	356	328.02	0.088
1.0	614.3	618.67	0.191
1.5	931.6	942.3	0.305
2.0	1308.1	1302.9	0.47
2.5	1743.6	1741.0	0.666
3.0	1818.8	1811.4	0.638
3.5	1818.8	1815.6	0.644
5.0	1818.8	1825.4	0.384
7.0	1818.8	1874	0.28
10.0	1818.8	1911.9	0.204
15.0	1818.8	1936.5	0.144

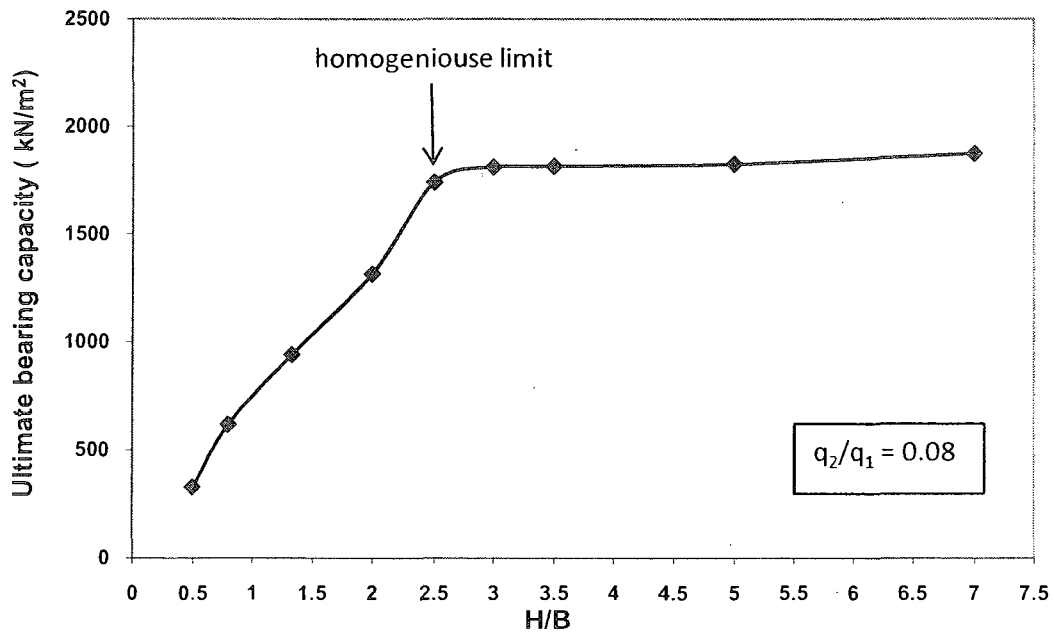


Fig. (4-1) Variation of the bearing capacity with H/B for the present study for  $\phi_1 = 43^\circ$  and  $\phi_2 = 30^\circ$

Table 4.3:  $\phi_1 = 43^\circ$   $\phi_2 = 35^\circ$ ,  $C_u = 1 \text{ KN/m}^2$

$H/B$	$q_u$ Hanna <sup>1981</sup> ( $\text{KN/m}^2$ )	$q_u$ present study ( $\text{KN/m}^2$ )	displacement @ failure for present study(m)
0.5	759.5	322.88	0.015
1.0	1183.5	1172.5	0.089
1.5	1680.2	1574.5	0.128
2.0	1818.4	1737.5	0.146
2.5	1818.4	1796.6	0.142
3.0	1818.4	1808.5	0.142
3.5	1818.4	1812.4	0.156
5.0	1818.4	1816.4	0.12
7.0	1818.4	1809.5	0.114
10.0	1818.4	1808.6	0.101
15.0	1818.4	1818.4	0.09

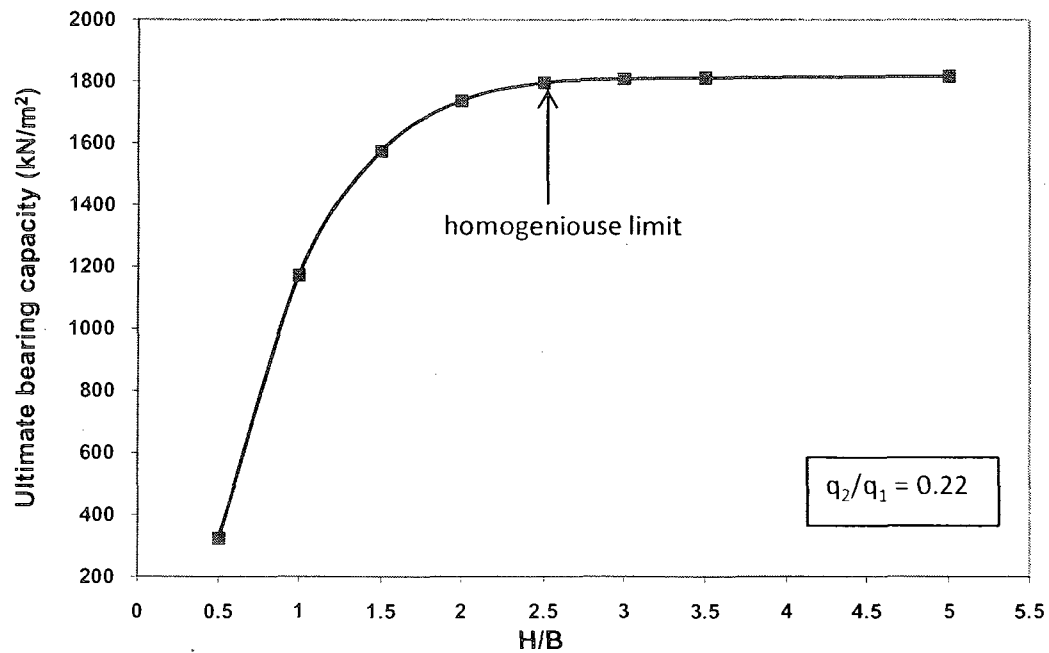


Fig. (4-2) Variation of the bearing capacity with H/B for the present study for  $\phi_1 = 43^\circ$  and  $\phi_2 = 35^\circ$

Table 4.4:  $\varphi_1 = 43^\circ$   $\varphi_2 = 40^\circ$   $C_u = 1 \text{ KN/m}^2$

$H/B$	$q_u$ Hanna1981 ( $\text{KN/m}^2$ )	$q_u$ present study ( $\text{KN/m}^2$ )	displacement @ failure for present study (m)
0.5	1660	350.57	0.012
1.0	1818.4	1280.3	0.059
1.5	1818.4	1643.3	0.082
2.0	1818.4	1787.4	0.095
2.5	1818.4	1829.3	0.097
3.0	1818.4	1832.8	0.100
3.5	1818.4	1838.1	0.111
5.0	1818.4	1831.2	0.107
7.0	1818.4	1843.4	0.092
10.0	1818.4	1850.9	0.104
15.0	1818.4	1848.0	0.095

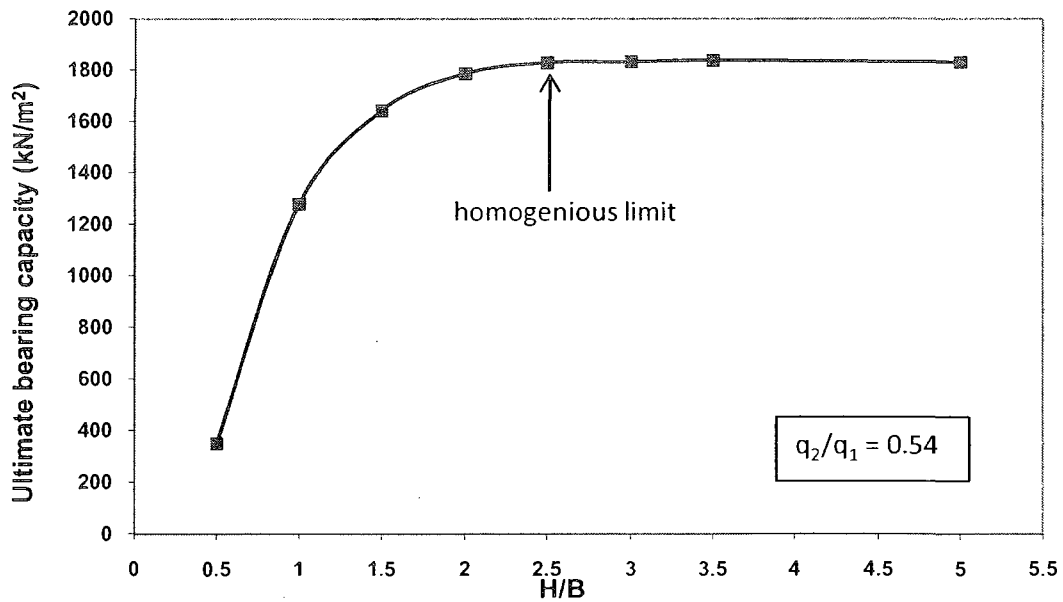


Fig. (4-3) Variation of the bearing capacity with H/B for the present study for  $\varphi_1 = 43^\circ$  and,  $\varphi_2 = 40^\circ$

Table 4.5:  $\phi_1 = 43^\circ$   $\phi_2 = 42^\circ$   $C_u = 1 \text{ KN/m}^2$

$H/B$	$q_u$ Hanna1981 ( $\text{KN/m}^2$ )	$q_u$ present study ( $\text{KN/m}^2$ )	displacement @ failure for present study(m)
0.5	1818.4	304.3	0.0087
1.0	1818.4	1111.6	0.039
1.5	1818.4	1807.5	0.075
2.0	1818.4	1807	0.076
2.5	1818.4	1825.5	0.081
3.0	1818.4	1802.7	0.082
3.5	1818.4	1816	0.099
5.0	1818.4	1812.9	0.086
7.0	1818.4	1818.4	0.097
10.0	1818.4	1808.3	0.09
15.0	1818.4	1807.3	0.085

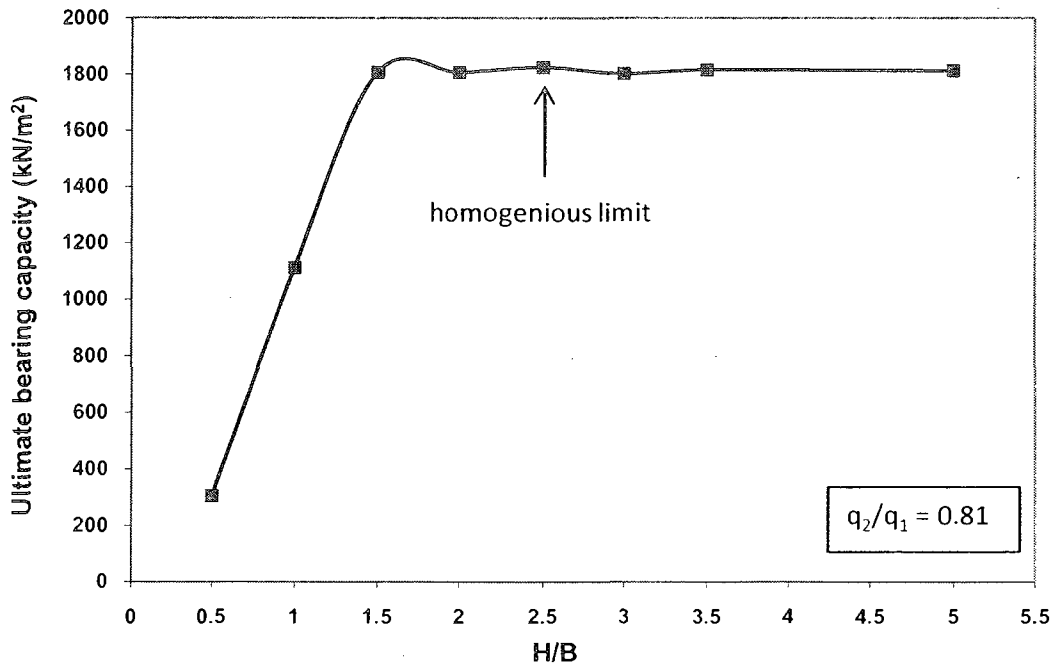


Fig. (4-4) Variation of the bearing capacity with H/B for the present study for  $\phi_1 = 43^\circ$  and  $\phi_2 = 42^\circ$

Table 4.6:  $\phi_1 = 47^\circ$   $\phi_2 = 35^\circ$   $C_u = 1 \text{KN/m}^2$

$H/B$	$q_u$ Hanna1981 ( $\text{KN/m}^2$ )	$q_u$ present study ( $\text{KN/m}^2$ )	displacement @ failure for present study(m)
0.5	782.7	380.02	0.18
1.0	1260.1	1232.02	0.095
1.5	1840.4	1830.3	0.141
2.0	2523.6	2519.2	0.207
2.5	3309.7	3279.6	0.29
3.0	4036.7	3994.7	0.378
3.5	4036.7	4074.0	0.359
5.0	4036.7	4082.6	0.298
7.0	4036.7	4056.1	0.286
10.0	4036.7	4041.2	0.258
15.0	4036.7	4065.9	0.179

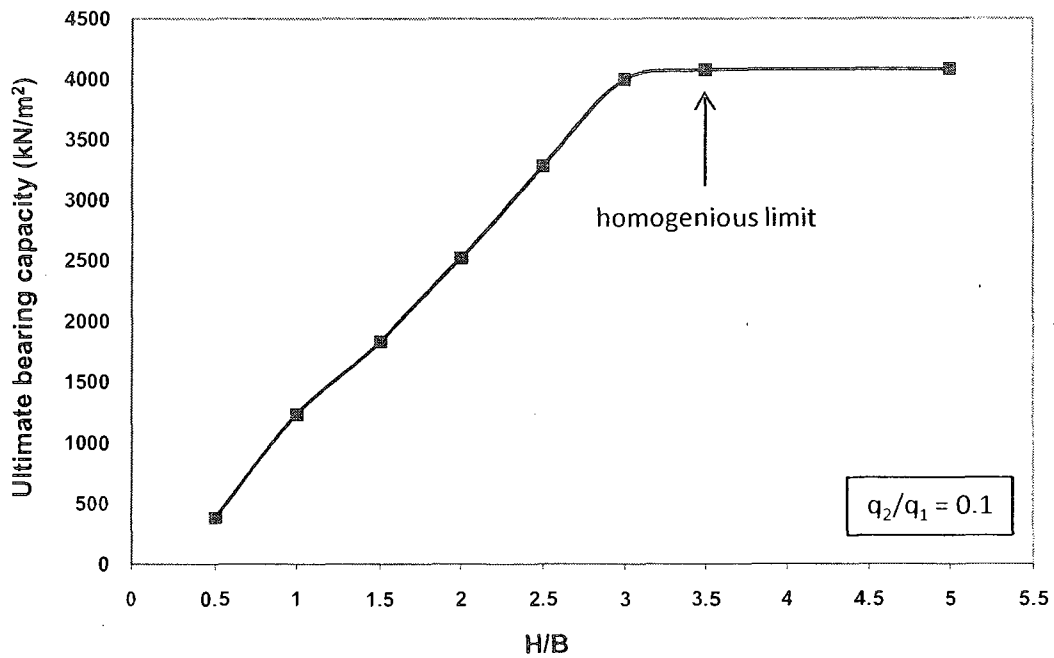


Fig: (4-5) Variation of the bearing capacity with H/B for the present study for  $\phi_1 = 47^\circ$  and  $\phi_2 = 35^\circ$

Table 4.7:  $\varphi_1 = 47^\circ$   $\varphi_2 = 40^\circ$   $C_u = 1 \text{ KN/m}^2$

$H/B$	$q_u$ Hanna <sup>1981</sup> ( $\text{KN/m}^2$ )	$q_u$ present study ( $\text{KN/m}^2$ )	displacement@ failure for present study(m)
0.5	1683.7	486.56	0.017
1.0	2516.7	1879.4	0.103
1.5	3483.7	3256.7	0.198
2.0	4036.7	3975.9	0.235
2.5	4036.7	4001	0.235
3.0	4036.7	3989.6	0.235
3.5	4036.7	4012.3	0.228
5.0	4036.7	4037.8	0.212
7.0	4036.7	4019.2	0.225
10.0	4036.7	4022.6	0.231
15.0	4036.7	4019.7	0.166

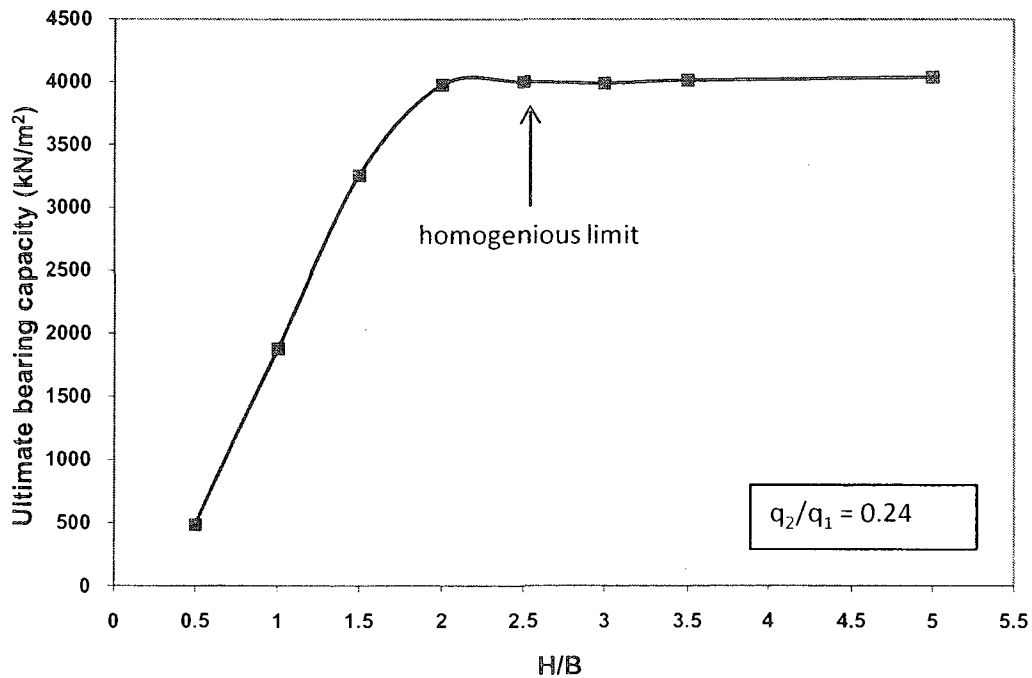


Fig. (4-6); Variation of the bearing capacity with H/B for the present study for  $\varphi_1 = 47^\circ$  and  $\varphi_2 = 40^\circ$

### 4.3 DATA ANALYSIS

In this investigation, the ultimate bearing capacity was determined as the peak point deduced from the load settlement curve. The curves (4-1 to 4-6), show the relation between the ultimate bearing capacity and the H/B ratio for each combination of upper stronger sand and the lower weaker sand. It is essential to point out that the properties of each layer, (like  $E, \gamma, \psi, \nu, C_u$ ) are changing accordingly as it is shown in table (3-2).

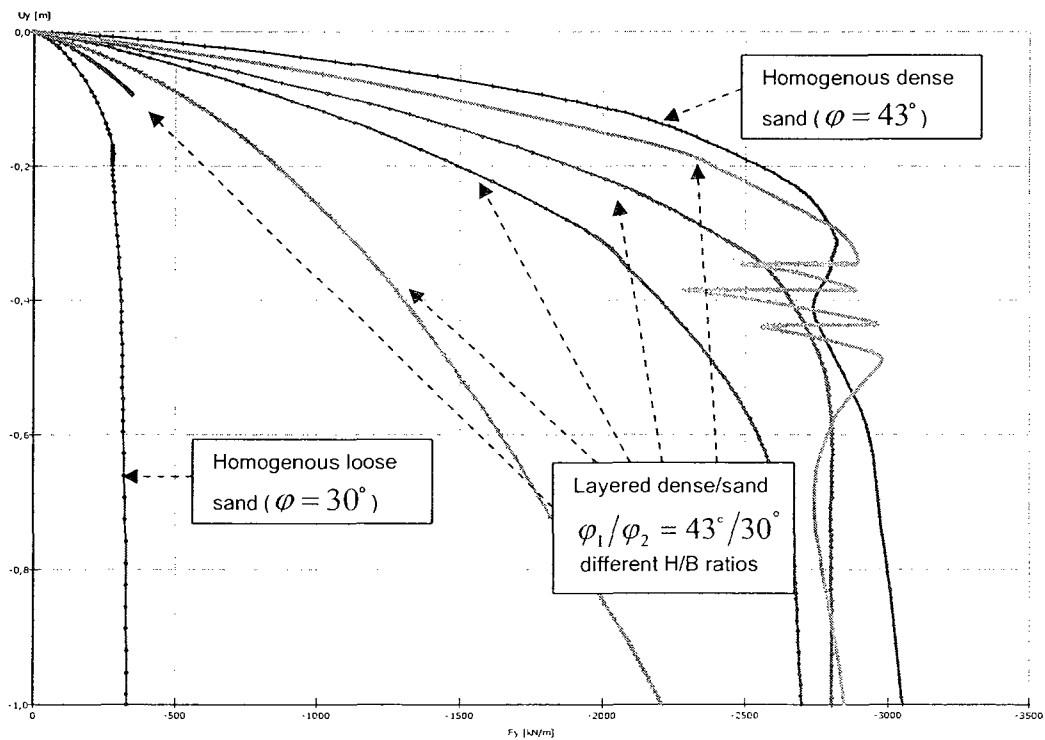


Fig. (4-7) Load-displacement curve.

The bearing capacity of footings on homogenous soil that has the same properties as those of the first layer ( $q_t$ ), and that of a homogenous soil of the lower second layer ( $q_b$ ) act as upper and lower bound for the bearing capacity of a layered system; Figure (4-7).

#### **4.4 PARAMETRIC STUDY**

Observing the results obtained from semi-empirical equations of Hanna (1981), the experimental results of Hanna's (1978) and the presented numerical model, it can be conclude that the most effective parameters upon the bearing capacity in layered soils are:

##### **4.4.1 EFFECT OF THE RATIO H/B**

The load settlement curves of footings on dense sand overlying weak sand possess a peak value at higher H/B ratios, where the mode of failure is general shear. The curvature of the load-settlement curve tends to decrease as the H/B ratio decreases.

On the other hand the effect of the H/B ratio tends to diminish at and beyond a value, at which the bearing capacity reached the value for the homogeneous upper layer (see Figures 4.1 to 4.6)

##### **4.4.2 EFFECT OF THE RELATIVE STRENGTH OF THE LAYERS ( $\phi_1/\phi_2$ )**

The relative strength between the two layers has a big effect on the bearing capacity of the soil system. As shown in table 4.2 to 4.7, that the higher the ratio

$\varphi_1/\varphi_2$  the high the bearing capacity of the system for the same H/B ratio, up to the maximum given above.

#### 4.4.3 EFFECT OF THE STRENGTH OF THE UPPER LAYER ( $\varphi_1$ )

Plotting the relation between H/B and the ultimate bearing capacity for four cases where the strength of the upper layer varies in the range of  $\varphi_1 = 43^\circ$  &  $47^\circ$  while the lower layer strength remained constant, see figure (4-8). It can be noted that  $\varphi_1$  play an important role in determining the bearing capacity of the system.

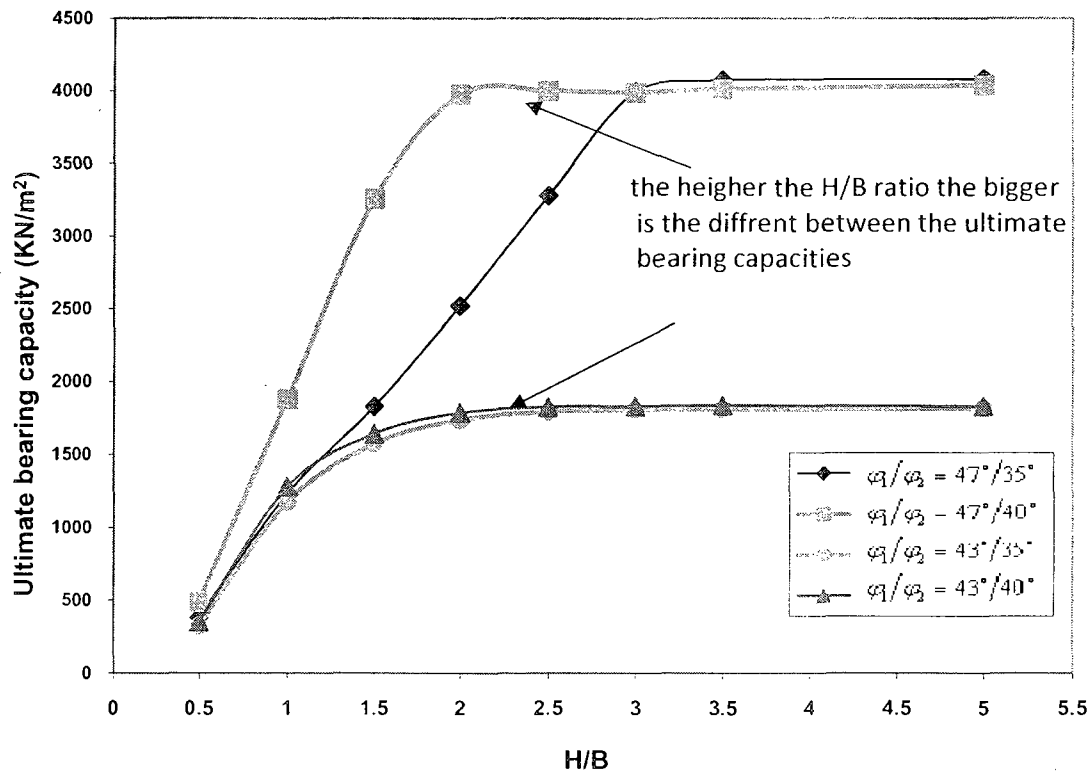


Fig. (4-8), Different stiffness ratios of the two layers, for  $\varphi_1 = 47, 43$  &  $\varphi_2 = 35$  &  $40$

#### 4.4.4 EFFECT OF THE STRENGTH OF THE LOWER LAYER ( $\varphi_2$ )

Figures (4-9) and (4-10) demonstrate the role of the lower layer strength in determining the bearing capacity of the system. It can be noted that the bearing capacity increases due to an increase of the lower layer strength for the same H/B ratio.

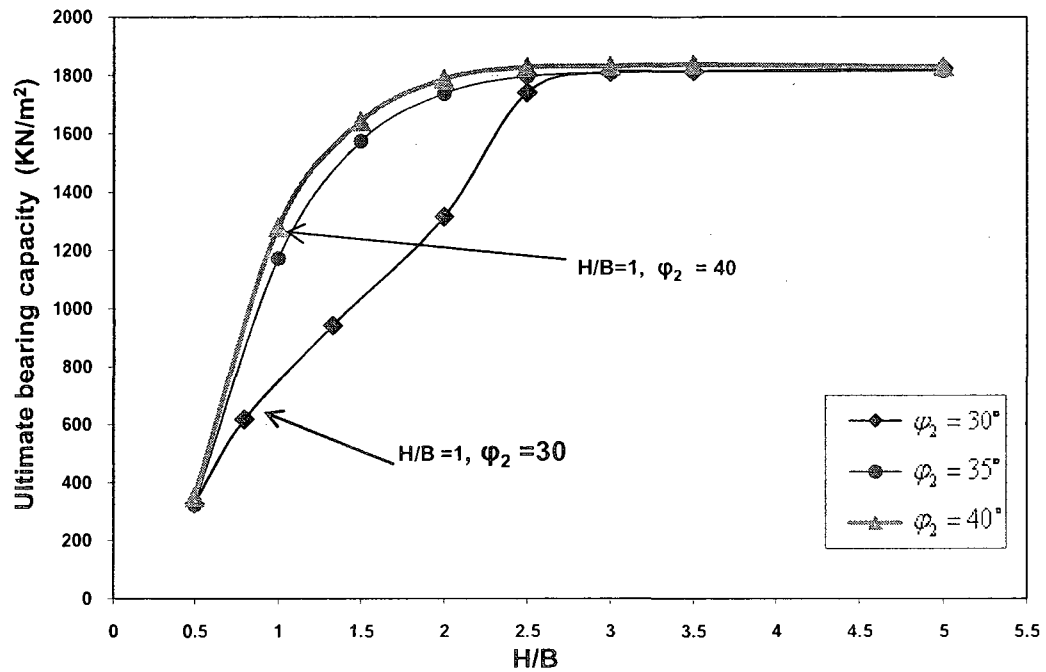


Fig. (4-9), Effect of the strength of the lower layer for different stiffness ratios of the two layers, for  $\varphi_1 = 43$

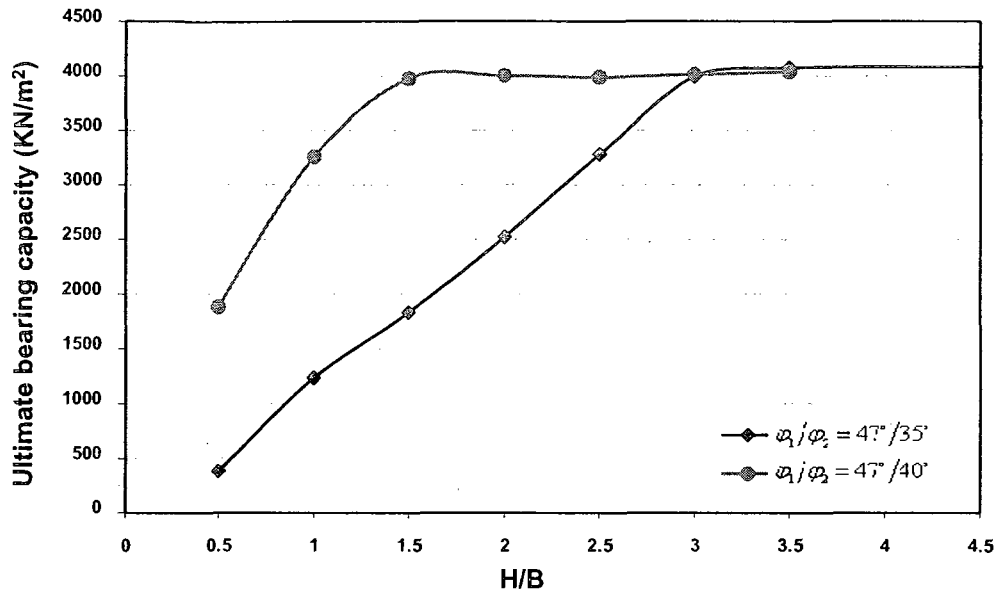


Fig. (4-10), Effect of the strength of the lower layer for different stiffness ratios of the two layers, for  $\phi_1 = 47^\circ$ .

Furthermore, it can be noted that for a thinner upper layer, the strength of the lower layer plays a bigger role in determining the bearing capacity of the layered system.

#### 4.5 DETERMINATION OF THE SHEAR STRENGTH MOBILIZED ON THE PUNCHING COLUMN

The soil layers used in this analysis are the ratio of the relative strength of both layers will be defined as the ration of ( $q_2/q_1$ ), beside the other geotechnical properties of the soil ( $E, \nu, \gamma_{dry}, \gamma_{sat}, and C$ ).

Where:

$$q_1 = 0.5\gamma_1 BN \gamma_1$$

$$q_2 = 0.5\gamma_2 BN \gamma_2$$

The ranges of parameters used in this analysis are given in table (4-8) below:

Table (4-8): Properties for the assumed soils for the generation of the  $\delta$  results model.

Soil Type	$\phi$	$E_s$	$\gamma_{dry}$	$\gamma_{sat.}$	$C_u$	$\nu$	$\psi$
V.D.sand& gravel	47	100	20	23	1	0.38	17
v.d. sand	45	90	19.5	22	1	0.38	15
D. sand	43	80	19.5	22	1	0.38	13
d. sand	40	65.1	18	20	1	0.35	10
L. sand	35	48	17	19	1	0.35	5
v.L. sand	30	11	13	16	1	0.3	0

In this analysis, nine combinations of soil's properties were selected for the upper and lower layers to give wider range for the study. The objective of this study is to evaluate the level of the shear strength mobilized on the punching column in terms of the angle of shearing resistance ( $\delta$ ).

Table (4-9): Bearing capacity of homogenous sand layers  $q_1$  &  $q_2$ , and the ratio  $q_2/q_1$ .

$\Phi_1$	$\Phi_2$	$\gamma_1$ $KN/m^3$	$\gamma_2$ $KN/m^3$	$N_{\gamma_1}$	$N_{\gamma_2}$	$q_1$	$q_2$	$q_2/q_1$
43	30	19.5	13	186.54	22.40	1818.76	145.6	0.08
43	35	19.5	17	186.54	48.03	1818.76	408.255	0.22
43	40	19.5	18	186.54	109.41	1818.76	984.69	0.54
45	30	19.5	13	271.76	22.40	2649.66	145.6	0.05
45	35	19.5	17	271.76	48.03	2649.66	408.255	0.15
45	40	19.5	18	271.76	109.41	2649.66	984.69	0.37
47	30	20	13	403.67	22.40	4036.7	145.6	0.04
47	35	20	17	403.67	48.03	4036.7	408.255	0.10
47	40	20	18	403.67	109.41	4036.7	984.69	0.24

The value of the ultimate bearing capacity of homogenous upper and lower layers ( $q_1, q_2$ ) of the system were calculated using equation (3-12) and the bearing capacity factors  $N_\gamma$  values, which were obtained from Meyerhof (1974).

The results are listed in table (4-9). Those ratios are used later in the presentation of the design charts for the determination of the mobilized angle of shearing resistance on the plane of failure of the upper layer ( $\delta_{avr.}/\phi_1$ ).

## 4.6 RESULTS AND ANALYSIS

The normal and shear stresses along the vertical interfaces' elements obtained from the numerical model were recorded. Using equation (3-7) the values of the angle  $\delta$  mobilized on the punching column were determined for both sides of the column. These results are summarized in tables 4-10 to 4-18.

Table (4-10): the calculated  $\delta$  angle for five selective points for the case of ( $q_2/q_1 = 0.08$ ) and different H/B ratios.

H/B			Y-coordinate.	Left side interface			Right side interface		
				$\tan \delta$	$\delta$	$\delta/\phi_1$	$\tan \delta$	$\delta$	$\delta/\phi_1$
1	43	30	36	-0.721	-35.77	-0.83	0.754	37.028	0.861
			35.75	-0.959	43.786	-1.02	0.954	43.671	1.015
			35.5	-0.838	39.967	-0.93	0.842	40.119	0.933
			35.25	-0.610	31.390	-0.73	0.674	33.98	0.790
			35	-0.977	44.335	-1.03	0.981	44.457	1.033
2	43	30	36	-0.957	43.734	-1.017	0.953	43.634	1.014
			35.5	-0.922	42.677	-0.992	0.943	43.32	1.007
			35	-0.612	31.465	-0.731	0.663	33.577	0.780
			34.5	-0.702	35.074	-0.815	0.690	34.630	0.805
			34	-0.398	21.693	-0.504	0.418	22.704	0.528
3	43	30	36	-0.959	44.268	-1.029	0.959	44.785	1.041
			35.25	-0.948	43.479	-1.011	0.948	43.476	1.011
			34.5	-0.764	37.381	-0.869	0.753	36.98	0.860
			33.75	-0.657	33.319	-0.774	0.683	34.33	0.798
			33	-0.555	29.041	-0.675	0.510	27.032	0.628
4	43	30	36	-0.484	25.861	-0.601	0.486	25.937	0.603
			35	-0.938	43.193	-1.004	0.939	43.201	1.004
			34	-0.425	23.025	-0.535	0.799	38.63	0.89
			33	-0.635	32.429	-0.754	0.614	31.574	0.734
			32	-0.486	25.940	-0.603	0.463	24.874	0.578
5	43	30	36	-0.997	44.934	-1.044	0.916	42.51	0.988
			34.75	-0.865	40.886	-0.950	0.868	40.98	0.953
			33.5	-0.716	35.610	-0.828	0.817	39.281	0.913
			32.25	-0.050	-2.872	-0.066	0.069	3.965	0.09
			31	-0.019	-1.069	-0.024	0.020	1.169	0.027
6	43	30	36	-0.935	43.095	-1.002	0.940	43.241	1.005
			34.5	-0.823	39.466	-0.917	0.857	40.604	0.94
			33	-0.479	25.611	-0.595	0.511	27.069	0.629
			31.5	0.021	1.217	0.028	-0.015	-0.904	-0.021
			30	-0.009	-0.552	-0.013	0.009	0.519	0.012

Table (4-11): the calculated  $\delta$  angle for five selective points for the case of ( $q_2/q_1 = 0.22$ ) and different H/B ratios.

H/B	$\varphi_1$	$\varphi_2$	Y-coordinate	Left side interface			Right side interface		
				$\tan \delta$	$\delta$	$\delta/\varphi_1$	$\tan \delta$	$\delta$	$\delta/\varphi_1$
1	43	35	36	-0.986	44.603	-1.037	1.019	45.529	1.059
			35.75	-0.953	43.629	-1.015	0.960	43.837	1.019
			35.5	-0.944	-43.346	-1.008	0.945	43.369	1.009
			35.25	-0.943	-43.333	-1.008	0.945	43.388	1.009
			35	-0.943	-43.316	-1.007	0.945	42.111	0.979
2	43	35	36	-1.158	-49.198	-1.144	1.026	45.730	1.063
			35.5	-0.938	-43.177	-1.004	0.941	43.258	1.006
			35	-0.847	-40.249	-0.936	0.851	40.397	0.939
			34.5	-0.760	-37.234	-0.866	0.726	35.979	0.837
			34	-0.683	-34.345	-0.799	0.530	27.902	0.649
3	43	35	35.9375	-0.974	-44.244	-1.029	0.977	44.325	1.031
			35.25	-0.746	-36.720	-0.854	0.758	37.178	0.865
			34.5	-0.814	-39.159	-0.911	0.783	38.061	0.885
			33.75	-0.672	-33.916	-0.789	0.726	35.971	0.837
			33	-0.961	-43.870	-1.020	0.942	43.290	1.007
4	43	35	36	-0.966	-43.995	-1.023	0.966	43.995	1.023
			35	-0.809	-38.959	-0.906	0.808	38.954	0.906
			34	-0.436	-23.554	-0.548	0.436	23.559	0.548
			33	-0.193	-10.915	-0.254	0.193	10.917	0.254
			32	-0.070	-3.992	-0.093	0.070	3.989	0.093
5	43	35	36	-0.888	-41.610	-0.968	0.897	41.897	0.974
			34.75	-0.801	-38.678	-0.899	0.794	38.442	0.894
			33.5	-0.825	-39.506	-0.919	0.775	37.767	0.878
			32.25	-0.446	-24.053	-0.559	0.427	23.141	0.538
			31	-0.055	-3.142	-0.073	0.066	3.768	0.088
6	43	35	36	-0.929	-42.888	-0.997	0.950	43.520	1.012
			34.5	-0.772	-37.675	-0.876	0.771	37.649	0.876
			33	-0.836	-39.883	-0.928	0.825	39.511	0.919
			31.5	-0.240	-13.493	-0.314	0.239	2.585	0.060
			30	-0.049	-2.807	-0.065	0.048	2.762	0.064

Table (4-12): the calculated  $\delta$  angle for five selective points for the case of ( $q_2/q_1 = 0.54$ ) and different H/B ratios.

H/B	$\varphi_1$	$\varphi_2$	Y-coordinate	Left side interface			Right side interface		
				$\tan \delta$	$\delta$	$\delta/\varphi_1$	$\tan \delta$	$\delta$	$\delta/\varphi_1$
1	43	40	36	-1.048	-45.060	-1.048	0.991	46.438	1.080
			35.75	-0.948	-43.477	-1.011	0.948	43.474	1.011
			35.5	-0.898	-41.911	-0.975	0.941	43.247	1.006
			35.25	-0.940	-43.224	-1.005	0.924	42.742	0.994
			35	-0.800	-38.653	-0.899	0.772	37.663	0.876
2	43	40	36	-1.012	-45.332	-1.054	1.005	45.129	1.050
			35.5	-0.944	-43.337	-1.008	0.905	42.132	0.980
			35	-0.819	-39.308	-0.914	0.843	40.118	0.933
			34.5	-0.843	-40.133	-0.933	0.875	41.195	0.958
			34	-0.623	-31.936	-0.743	0.541	28.431	0.661
3	43	40	36	-1.005	-45.131	-1.050	1.004	45.126	1.049
			35.25	-0.835	-39.855	-0.927	0.834	39.838	0.926
			34.5	-0.837	-39.921	-0.928	0.845	40.199	0.935
			33.75	-0.923	-42.714	-0.993	0.897	41.895	0.974
			33	-0.680	-34.226	-0.796	0.732	36.212	0.842
4	43	40	35.8	-0.953	-45.465	-1.057	0.953	44.970	1.046
			35	-0.816	-39.229	-0.912	0.799	38.635	0.898
			34	-0.844	-40.167	-0.934	0.842	40.104	0.933
			33	-0.656	-33.263	-0.774	0.642	32.708	0.761
			32	-0.226	-12.739	-0.296	0.229	12.923	0.301
5	43	40	36	-0.951	-45.699	-1.063	0.953	44.383	1.032
			34.75	-0.810	-39.024	-0.908	0.803	38.774	0.902
			33.5	-0.856	-40.557	-0.943	0.821	39.374	0.916
			32.25	-0.464	-24.891	-0.579	0.449	24.196	0.563
			31	-0.055	-3.155	-0.073	0.069	3.963	0.092
6	43	40	36	-1.017	-45.485	-1.058	0.977	44.325	1.031
			34.5	-0.793	-38.421	-0.894	0.785	38.128	0.887
			33	-0.962	-43.902	-1.021	0.955	43.672	1.016
			31.5	-0.221	-12.479	-0.290	0.218	12.282	0.286
			30	-0.055	-3.148	-0.073	0.055	3.159	0.073

Table (4-13): the calculated  $\delta$  angle for five selective points for the case of ( $q_2/q_1 = 0.04$ ) and different H/B ratios.

H/B	$\varphi_1$	$\varphi_2$	Y-coordinate	Left side interface			Right side interface		
				$\tan \delta$	$\delta$	$\delta/\varphi_1$	$\tan \delta$	$\delta$	$\delta/\varphi_1$
1	47	30	40	-0.791	-38.351	-0.816	0.770	37.594	0.800
			39.75	-1.071	-46.973	-0.999	1.091	47.491	1.010
			39.5	-0.719	-35.725	-0.760	0.866	40.884	0.870
			39.25	-0.542	-28.442	-0.605	0.620	31.792	0.676
			39	-0.566	-29.529	-0.628	0.574	29.839	0.635
2	47	30	40	-1.004	-45.116	-0.960	0.910	42.310	0.900
			39.5	-0.826	-39.556	-0.842	0.783	38.048	0.810
			39	-0.810	-38.991	-0.830	0.880	41.340	0.880
			38.5	-0.554	-28.967	-0.616	0.675	34.019	0.724
			38	-0.350	-19.300	-0.411	0.790	38.301	0.815
3	47	30	40	-1.066	-46.833	-0.996	1.017	45.483	0.968
			39.25	-0.756	-37.104	-0.789	0.907	42.214	0.898
			38.5	-0.659	-33.388	-0.710	0.885	41.512	0.883
			37.75	-1.063	-46.754	-0.995	1.017	45.478	0.968
			37	-0.615	-31.585	-0.672	0.775	37.769	0.804
4	47	30	40	-0.987	-44.633	-0.950	1.096	47.618	1.013
			39	-0.822	-39.409	-0.838	0.854	40.487	0.861
			38	-0.741	-36.530	-0.777	0.696	34.827	0.741
			37	-0.993	-44.786	-0.953	1.064	46.778	0.995
			36	-1.122	-48.285	-1.027	0.589	30.497	0.649
5	47	30	40	-0.785	-38.141	-0.812	0.535	28.160	0.599
			38.75	-0.996	-44.891	-0.955	0.888	41.616	0.885
			37.5	-0.650	-33.034	-0.703	0.606	31.232	0.665
			36.25	0.930	42.931	0.913	0.364	20.020	0.426
			35	-0.131	-7.463	-0.159	0.038	2.172	0.046
6	47	30	40	-1.105	-47.864	-1.018	1.104	47.829	1.018
			38.5	-0.994	-44.837	-0.954	0.987	44.637	0.950
			37	-0.705	-35.165	-0.748	0.706	35.213	0.749
			35.5	0.306	17.032	0.362	-0.199	11.245	-0.239
			34	-0.055	-3.168	-0.067	0.042	2.380	0.051

Table (4-14): the calculated  $\delta$  angle for five selective points for the case of ( $q_2/q_1 = 0.1$ ) and different H/B ratios.

H/B	$\varphi_1$	$\varphi_2$	Y-coordinate	Left side interface			Right side interface		
				$\tan \delta$	$\delta$	$\delta/\varphi_1$	$\tan \delta$	$\delta$	$\delta/\varphi_1$
1	47	35	40	-1.151	-49.011	-1.043	1.164	49.344	1.050
			39.75	-1.053	-46.488	-0.989	0.990	44.705	0.951
			39.5	-1.076	-47.109	-1.002	0.934	43.036	0.916
			39.25	-1.086	-47.368	-1.008	1.087	47.383	1.008
			39	-0.665	-33.631	-0.716	0.672	33.883	0.721
2	47	35	40	-0.941	-43.256	-0.920	0.980	44.407	0.945
			39.5	-0.937	-43.130	-0.918	0.933	43.006	0.915
			39	-0.912	-42.359	-0.901	0.918	42.554	0.905
			38.5	-0.946	-43.411	-0.924	0.963	43.918	0.934
			38	-0.579	-30.083	-0.640	0.574	29.872	0.636
3	47	35	40	-1.085	-47.328	-1.007	1.068	46.885	0.998
			39.25	-0.982	-44.476	-0.946	0.972	44.197	0.940
			38.5	-0.934	-43.052	-0.916	0.896	41.860	0.891
			37.75	-0.699	-34.969	-0.744	0.668	33.757	0.718
			37	-0.573	-29.806	-0.634	0.557	29.111	0.619
4	47	35	40	-1.104	-47.820	-1.017	1.104	47.825	1.018
			39	-0.745	-36.704	-0.781	0.745	36.699	0.781
			38	-0.407	-22.151	-0.471	0.407	22.154	0.471
			37	-0.189	-10.706	-0.228	0.189	10.706	0.228
			36	-0.064	-3.669	-0.078	0.064	3.684	0.078
5	47	35	40	-1.105	-47.856	-1.018	1.105	47.859	1.018
			38.75	-0.654	-33.179	-0.706	0.654	33.179	0.706
			37.5	-0.242	-13.615	-0.290	0.242	13.617	0.290
			36.25	-0.093	-5.325	-0.113	0.093	5.325	0.113
			35	-0.030	-1.690	-0.036	0.030	1.700	0.036
6	47	35	40	-1.081	-47.226	-1.005	1.081	47.226	1.005
			38.5	-0.540	-28.371	-0.604	0.540	28.370	0.604
			37	-0.149	-8.475	-0.180	0.149	8.474	0.180
			35.5	-0.052	-2.963	-0.063	0.052	2.963	0.063
			34	-0.016	-0.906	-0.019	0.016	0.912	0.019

Table (4-15): the calculated  $\delta$  angle for five selective points for the case of ( $q_2/q_1 = 0.24$ ) and different H/B ratios.

H/B	$\varphi_1$	$\varphi_2$	Y-coordinate	Left side interface			Right side interface		
				$\tan \delta$	$\delta$	$\delta/\varphi_1$	$\tan \delta$	$\delta$	$\delta/\varphi_1$
1	47	40	40	-0.988	-44.666	-0.950	1.112	48.038	1.022
			39.75	-0.832	-39.752	-0.846	1.029	45.831	0.975
			39.5	-1.075	-47.058	-1.001	0.918	42.559	0.906
			39.25	-1.063	-46.754	-0.995	0.951	43.550	0.927
			39	-1.081	-47.219	-1.005	1.024	45.680	0.972
2	47	40	40	-0.738	-36.410	-0.775	1.127	48.425	1.030
			39.5	-1.048	-46.346	-0.986	0.865	40.861	0.869
			39	-1.080	-47.214	-1.005	1.024	45.690	0.972
			38.5	-0.861	-40.716	-0.866	0.815	39.174	0.833
			38	-0.568	-29.595	-0.630	0.526	27.747	0.590
3	47	40	40	-0.620	-31.785	-0.676	0.701	35.035	0.745
			39.25	-0.986	-44.605	-0.949	0.962	43.897	0.934
			38.5	-0.971	-44.162	-0.940	0.947	43.435	0.924
			37.75	-0.783	-38.052	-0.810	0.737	36.408	0.775
			37	-0.688	-34.545	-0.735	0.719	35.723	0.760
4	47	40	40	-1.016	-45.460	-0.967	1.076	47.100	1.002
			39	-0.919	-42.595	-0.906	0.909	42.262	0.899
			38	-0.879	-41.326	-0.879	0.875	41.186	0.876
			37	-0.887	-41.570	-0.884	0.894	41.806	0.889
			36	-0.713	-35.474	-0.755	0.707	35.254	0.750
5	47	40	40	-1.091	-47.483	-1.010	1.091	47.487	1.010
			38.75	-0.910	-42.316	-0.900	0.908	42.229	0.898
			37.5	-0.835	-39.852	-0.848	0.847	40.274	0.857
			36.25	-0.722	-35.822	-0.762	0.756	37.084	0.789
			35	-0.180	-10.186	-0.217	0.194	10.996	0.234
6	47	40	40	-1.071	-46.968	-0.999	1.071	46.968	0.999
			38.5	-0.569	-29.625	-0.630	0.569	29.624	0.630
			37	-0.147	-8.353	-0.178	0.147	8.353	0.178
			35.5	-0.049	-2.796	-0.059	0.049	2.796	0.059
			34	-0.017	-0.959	-0.020	0.017	0.961	0.020

Table (4-16): the calculated  $\delta$  angle for five selective points for the case of ( $q_2/q_1 = 0.05$ ) and different H/B ratios.

H/B	$\varphi_1$	$\varphi_2$	Y-coordinate	Left side interface			Right side interface		
				$\tan \delta$	$\delta$	$\delta/\varphi_1$	$\tan \delta$	$\delta$	$\delta/\varphi_1$
1	45	30	36	-0.685	-34.420	-0.765	0.860	40.705	0.905
			35.75	-1.023	-45.650	-1.014	1.021	45.584	1.013
			35.5	-0.983	-44.522	-0.989	0.876	41.229	0.916
			35.25	-0.713	-35.484	-0.789	0.720	35.751	0.794
			35	-0.468	-25.061	-0.557	0.431	23.298	0.518
2	45	30	36	-1.019	-45.545	-1.012	0.969	44.105	0.980
			35.5	-0.917	-42.508	-0.945	0.903	42.082	0.935
			35	-0.824	-39.493	-0.878	0.812	39.089	0.869
			34.5	-0.665	-33.627	-0.747	0.617	31.690	0.704
			34	-0.307	-17.067	-0.379	0.450	24.240	0.539
3	45	30	36	-0.752	-36.944	-0.821	0.453	24.352	0.541
			35.25	-0.848	-40.284	-0.895	0.711	35.424	0.787
			34.5	-0.857	-40.603	-0.902	0.924	42.729	0.950
			33.75	-0.623	-31.923	-0.709	0.601	30.996	0.689
			33	-0.513	-27.162	-0.604	0.527	27.810	0.618
4	45	30	36	-0.940	-43.230	-0.961	0.918	42.567	0.946
			35	-0.930	-42.908	-0.954	0.913	42.396	0.942
			43	-1.065	-46.812	-1.040	0.819	39.332	0.874
			33	-0.212	-11.993	-0.267	0.261	14.650	0.326
			32	-0.069	-3.962	-0.088	0.041	2.331	0.052
5	45	30	36	-0.947	-43.447	-0.965	0.838	39.952	0.888
			34.75	-0.861	-40.733	-0.905	0.812	39.093	0.869
			33.5	-0.473	-25.305	-0.562	0.553	28.963	0.644
			32.25	-0.452	-24.324	-0.541	1.021	45.592	1.013
			31	-0.149	-8.474	-0.188	0.264	14.811	0.329
6	45	30	36	-0.592	-30.639	-0.681	0.974	44.241	0.983
			34.5	-0.887	-41.559	-0.924	0.885	41.493	0.922
			33	-0.730	-36.115	-0.803	0.645	32.831	0.730
			31.5	0.195	11.040	0.245	0.309	17.174	0.382
			30	-0.147	-8.355	-0.186	0.141	8.021	0.178

Table (4-17): the calculated  $\delta$  angle for five selective points for the case of ( $q_2/q_1 = 0.15$ ) and different H/B ratios.

H/B	$\varphi_1$	$\varphi_2$	Y-coordinate	Left side interface			Right side interface		
				$\tan \delta$	$\delta$	$\delta/\varphi_1$	$\tan \delta$	$\delta$	$\delta/\varphi_1$
1	45	35	36	-1.045	-46.264	-1.028	1.051	46.425	1.032
			35.75	-0.926	-42.811	-0.951	0.938	43.162	0.959
			35.5	-0.860	-40.683	-0.904	0.857	40.586	0.902
			33.25	-0.933	-43.020	-0.956	0.973	44.218	0.983
			35	-0.998	-44.929	-0.998	1.009	45.255	1.006
2	45	35	36	-1.107	-47.903	-1.065	1.043	46.217	1.027
			35.5	-1.010	-45.288	-1.006	1.009	45.250	1.006
			35	-1.010	-45.273	-1.006	0.845	40.211	0.894
			34.5	-0.868	-40.967	-0.910	0.894	41.783	0.929
			34	-0.423	-22.935	-0.510	0.543	28.497	0.633
3	45	35	36	-1.053	-46.483	-1.033	1.039	46.089	1.024
			35.25	-1.007	-45.187	-1.004	1.007	45.189	1.004
			34.5	-0.869	-40.994	-0.911	0.984	44.530	0.990
			33.75	-0.838	-39.968	-0.888	0.742	36.580	0.813
			33	-0.348	-19.172	-0.426	0.482	25.722	0.572
4	45	35	36	-0.886	-41.543	-0.923	0.948	43.483	0.966
			35	-0.705	-35.165	-0.781	0.688	34.538	0.768
			34	-0.652	-33.120	-0.736	0.552	28.919	0.643
			33	-0.755	-37.069	-0.824	0.703	35.111	0.780
			32	-0.960	-43.821	-0.974	0.876	41.214	0.916
5	45	35	36	-1.031	-45.880	-1.020	1.064	46.779	1.040
			34.75	-0.784	-38.082	-0.846	0.755	37.048	0.823
			33.5	-0.888	-41.600	-0.924	1.005	45.156	1.003
			32.25	-0.725	-35.937	-0.799	0.838	39.958	0.888
			31	0.231	13.004	0.289	-0.219	-12.350	-0.274
6	45	35	36	-1.029	-45.817	-1.018	1.026	45.733	1.016
			34.5	-0.937	-43.123	-0.958	0.881	41.388	0.920
			33	-0.878	-41.288	-0.918	0.897	41.901	0.931
			31.5	-0.402	-21.883	-0.486	0.386	21.099	0.469
			30	-0.017	-0.967	-0.021	0.008	0.471	0.010

Table (4-18): the calculated  $\delta$  angle for five selective points for the case of ( $q_2/q_1 = 0.37$ ) and different H/B ratios.

H/B	$\varphi_1$	$\varphi_2$	Y-coordinate	Left side interface			Right side interface		
				$\tan \delta$	$\delta$	$\delta/\varphi_1$	$\tan \delta$	$\delta$	$\delta/\varphi_1$
1	45	40	36	-0.920	-42.602	-0.947	0.953	43.608	0.969
			35.75	-1.001	-45.027	-1.001	0.950	43.520	0.967
			35.5	-0.981	-44.447	-0.988	0.955	43.670	0.970
			35.25	-0.871	-41.051	-0.912	0.952	43.577	0.968
			35	-0.952	-43.590	-0.969	0.990	44.705	0.993
2	45	40	36	-1.034	-45.962	-1.021	1.039	46.098	1.024
			35.5	-0.872	-41.085	-0.913	1.009	45.248	1.006
			35	-0.967	-44.041	-0.979	0.933	43.012	0.956
			34.5	-0.823	-39.443	-0.877	0.862	40.767	0.906
			34	-0.556	-29.071	-0.646	0.633	32.333	0.719
3	45	40	36	-1.056	-46.550	-1.034	1.188	46.688	1.038
			35.25	-0.967	-44.041	-0.979	0.968	44.057	0.979
			34.5	-0.998	-44.935	-0.999	0.945	43.384	0.964
			33.75	-0.870	-41.015	-0.911	0.738	36.446	0.810
			33	-0.601	-30.997	-0.689	0.572	29.790	0.662
4	45	40	36	-0.533	-28.042	-0.623	0.557	29.137	0.647
			35	-1.007	-45.187	-1.004	0.814	39.146	0.870
			34	-0.952	-43.601	-0.969	0.887	41.568	0.924
			33	-0.916	-42.503	-0.945	0.795	38.488	0.855
			32	-0.640	-32.632	-0.725	0.697	34.857	0.775
5	45	40	36	-1.105	-47.847	-1.063	1.104	47.843	1.063
			34.75	-0.803	-38.771	-0.862	0.803	38.779	0.862
			33.5	-0.300	-16.713	-0.371	0.300	16.708	0.371
			32.25	-0.109	-6.206	-0.138	0.109	6.208	0.138
			31	-0.039	-2.231	-0.050	0.039	2.230	0.050
6	45	40	36	-0.978	-44.376	-0.986	0.977	44.338	0.985
			34.5	-0.737	-36.376	-0.808	0.736	36.360	0.808
			33	-0.210	-11.870	-0.264	0.210	11.871	0.264
			31.5	-0.069	-3.973	-0.088	0.069	3.973	0.088
			30	-0.024	-1.380	-0.031	0.024	1.380	0.031

The values deduced for the ratios  $(\delta/\varphi_1)$  are plotted in graphical form in figures 4-11 to 4-18. On these figures, the best fitting curves were determined for each side for the given H/B ratio was also given.

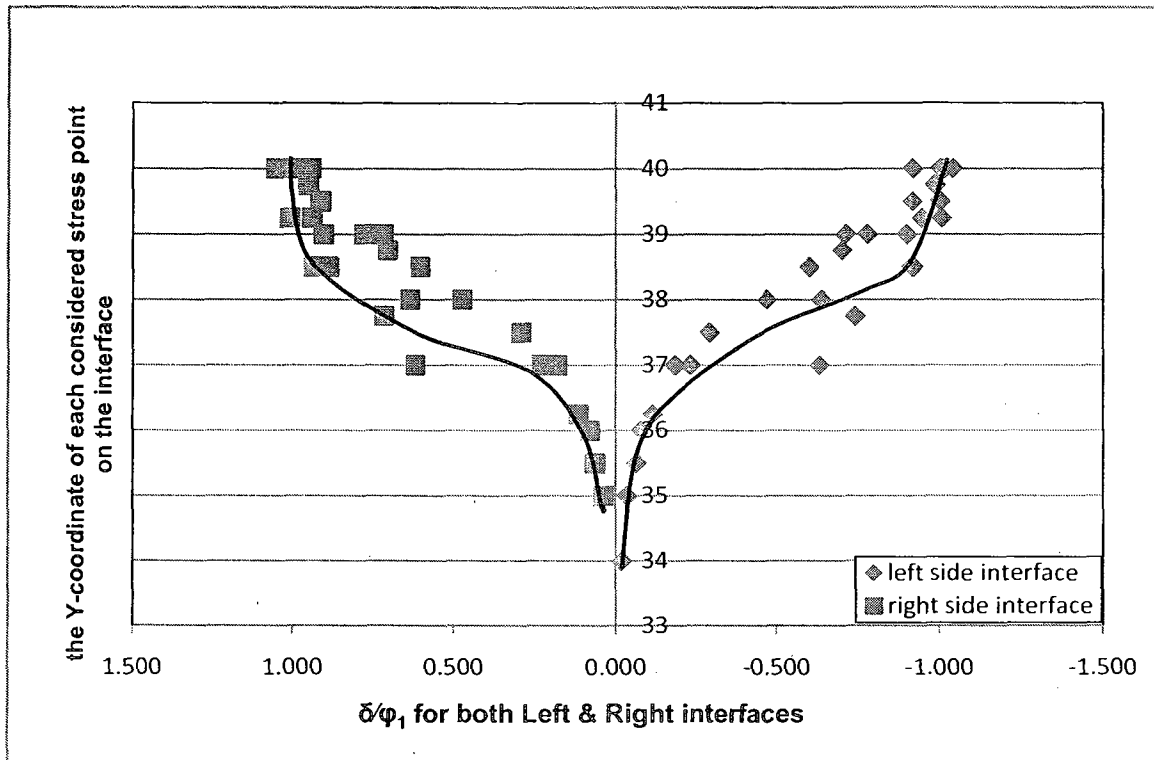


Fig. (4-11) Variation of  $(\delta/\varphi_1)$  with the height of the punching column for  $q_2/q_1=0.1$

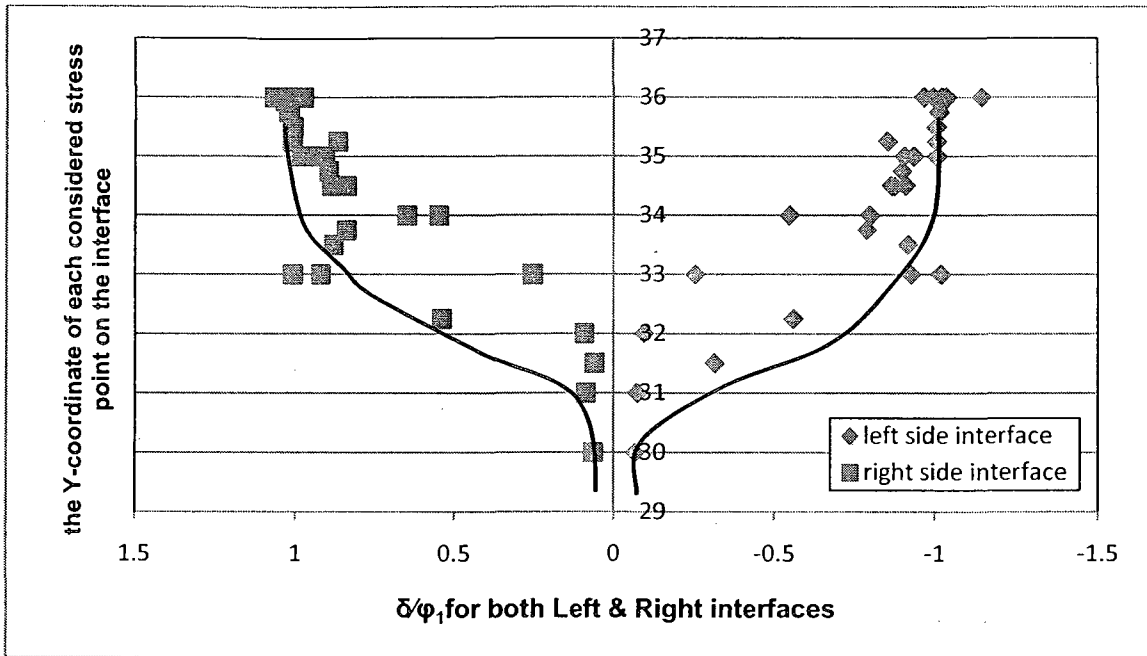


Fig. (4-12) Variation of  $(\delta/\phi_1)$  with the height of the punching column for  $q_2/q_1 = 0.22$

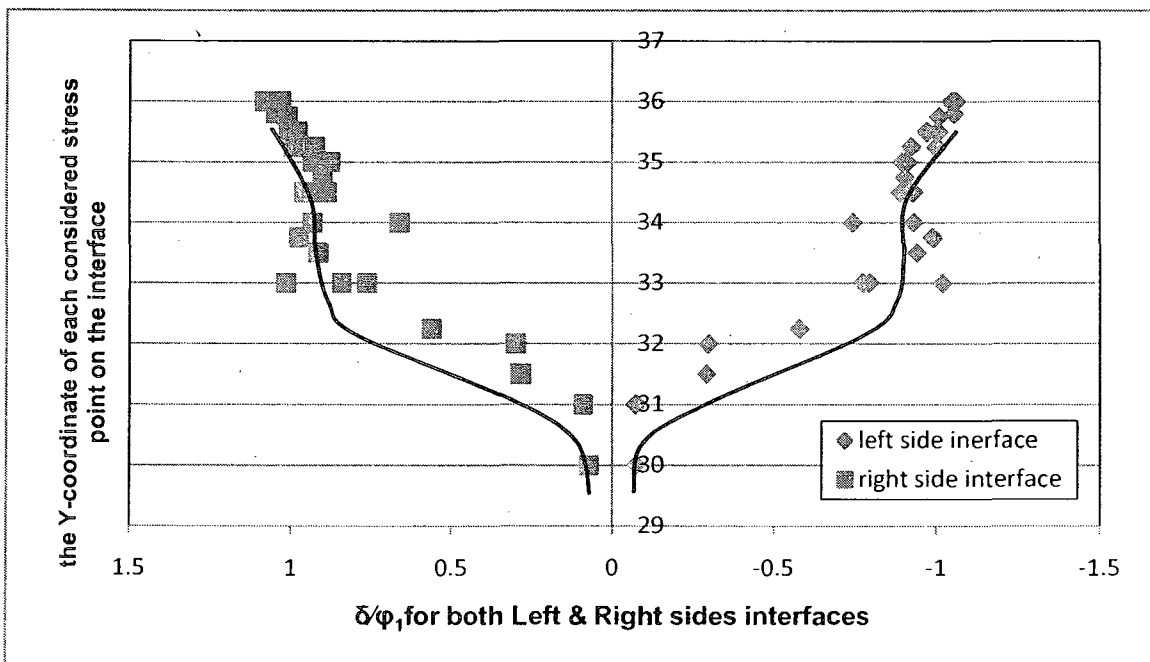


Fig. (4-13) Variation of  $(\delta/\phi_1)$  with the height of the punching column for  $q_2/q_1 = 0.54$

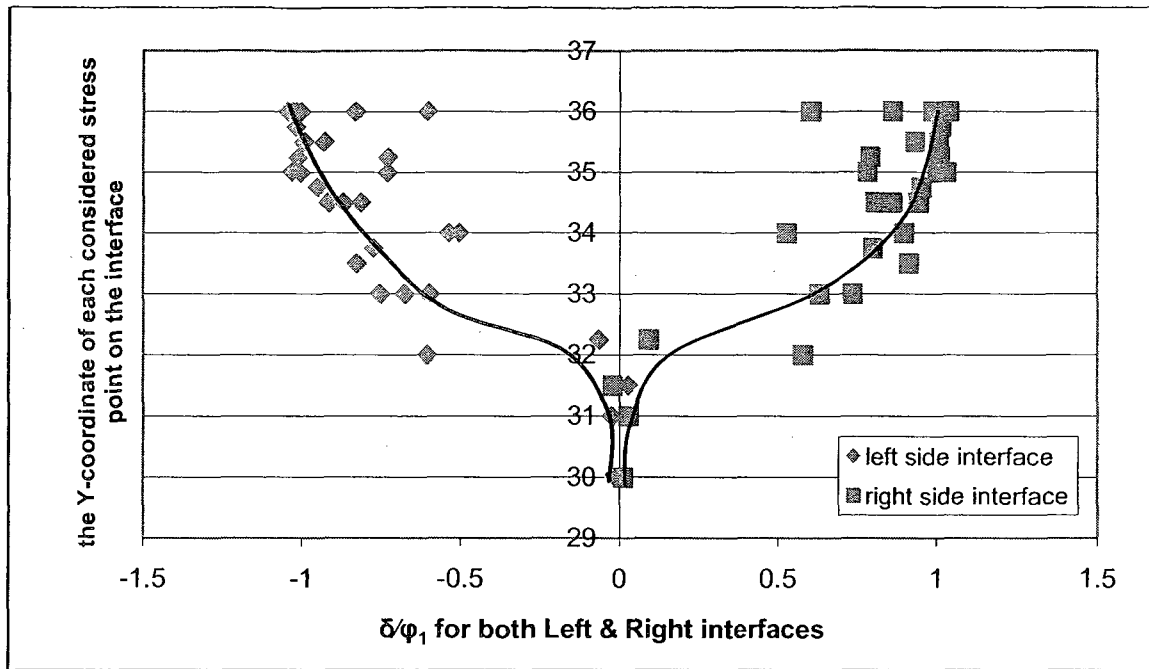


Fig. (4-14) Variation of  $(\delta/\phi_1)$  with the height of the punching column for  $q_2/q_1 = 0.08$

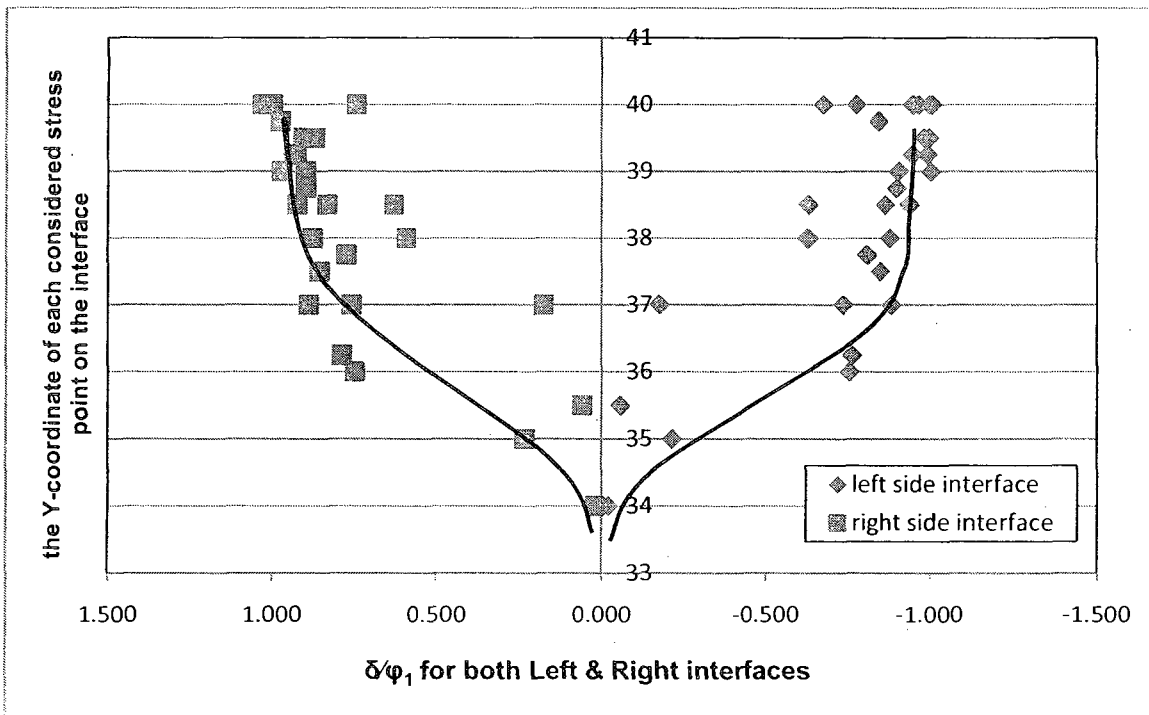


Fig. (4-15) Variation of  $(\delta/\phi_1)$  with the height of the punching column for  $q_2/q_1 = 0.24$

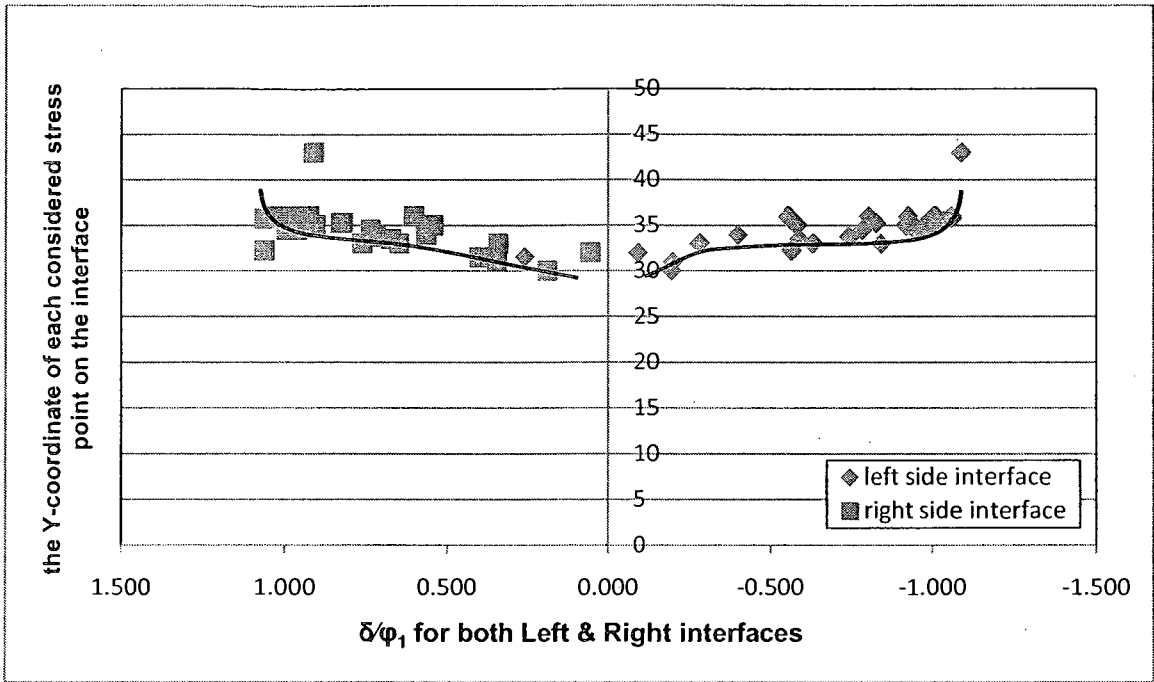


Fig. (4-16) Variation of  $(\delta/\varphi_1)$  with the height of the punching column for  $q_2/q_1 = 0.04$

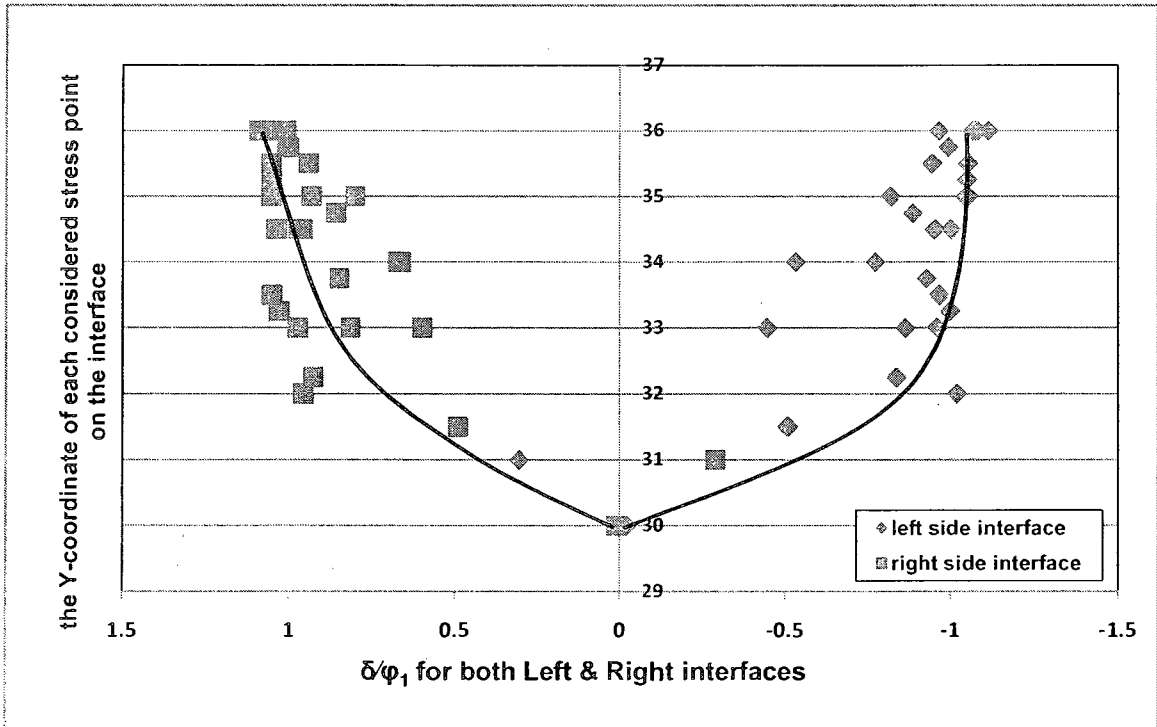


Fig. (4-17) Variation of  $(\delta/\varphi_1)$  with the height of the punching column for  $q_2/q_1 = 0.15$

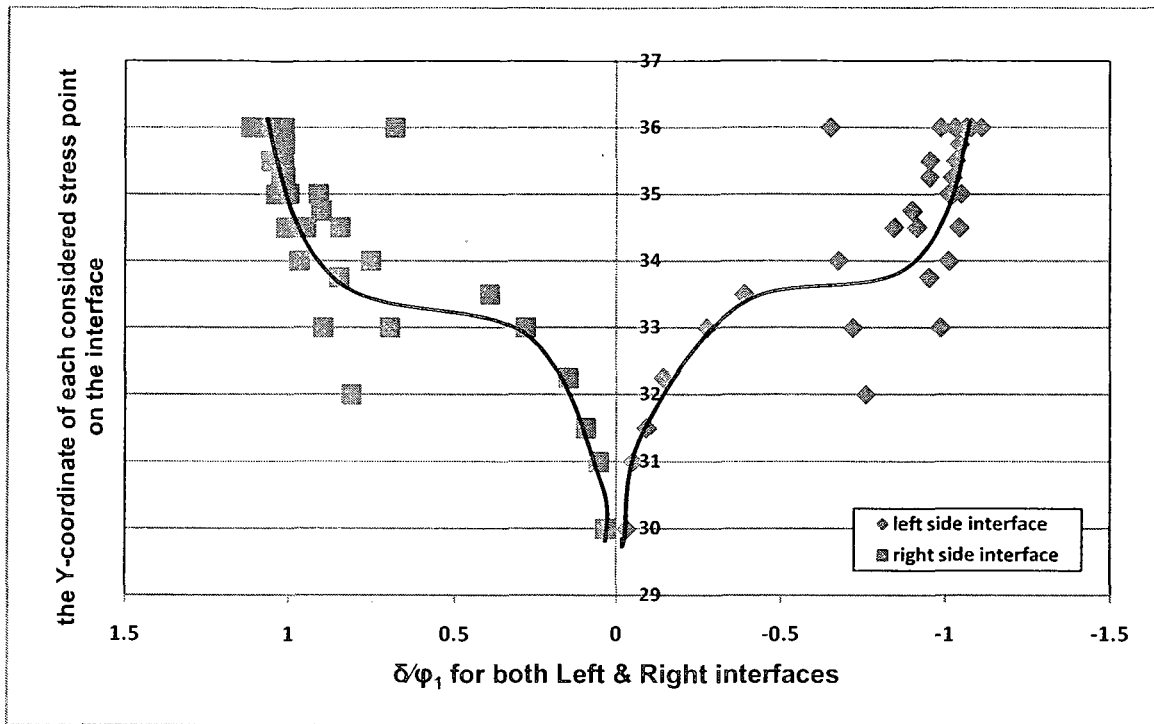


Fig. (4-18) Variation of  $(\delta/\varphi_1)$  with the height of the punching column for  $q_2/q_1=0.37$

From these figures, it can be noted the contribution of the depth of the upper layer on the  $(\delta/\varphi_1)$  ratio. Where's, for the same ratio of  $q_2/q_1$  as the thickness of the upper layer increases (H) the ratio of  $(\delta/\varphi_1)$  decreases, until it reaches a zero value at the interface between the two layers. This effect had been neglected by Hanna (1978) on the average mobilized angle of shearing resistance ( $\delta$ ), as it was assumed that the ratio  $(\delta/\varphi_1)$  constant for all values of the thickness of the upper layer (H).

#### 4.7 RELATIVE STRENGTH OF BOTH LAYERS

The variation of  $\delta/\varphi_1$  ratio with the relative strength of the two layers are given in figures (4-19) and (4-20) for ( $q_2/q_1 = 0.08, 0.22$  and  $0.54$  for  $H/B = 1$  and  $3$ ). It can be noted from these figures that the ratio  $\delta/\varphi_1$  for smaller  $q_2/q_1$  value decreases by  $\pm 10\%$  with the increases of  $H/B$  from one to three. Nevertheless, this percentage decreases due to the increase of the ratio of the relative strength of ( $q_2/q_1$ ).

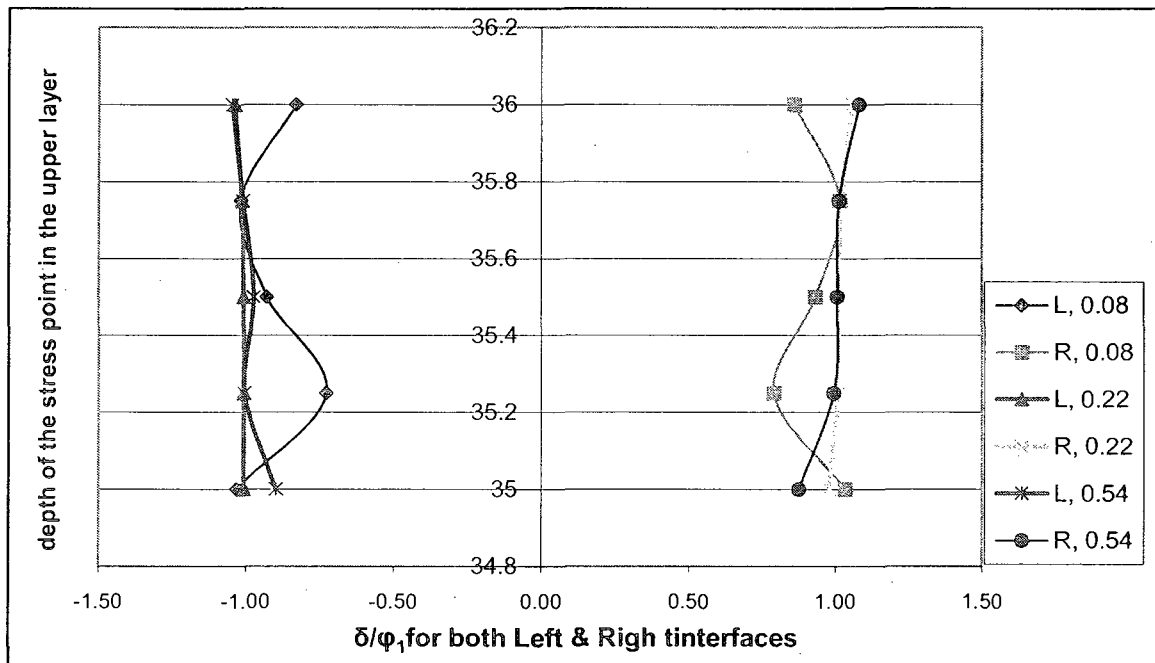


Fig.(4-19); the variation of  $\delta/\varphi_1$  for different ( $q_2/q_1$ ) ratios &  $H/B=1$

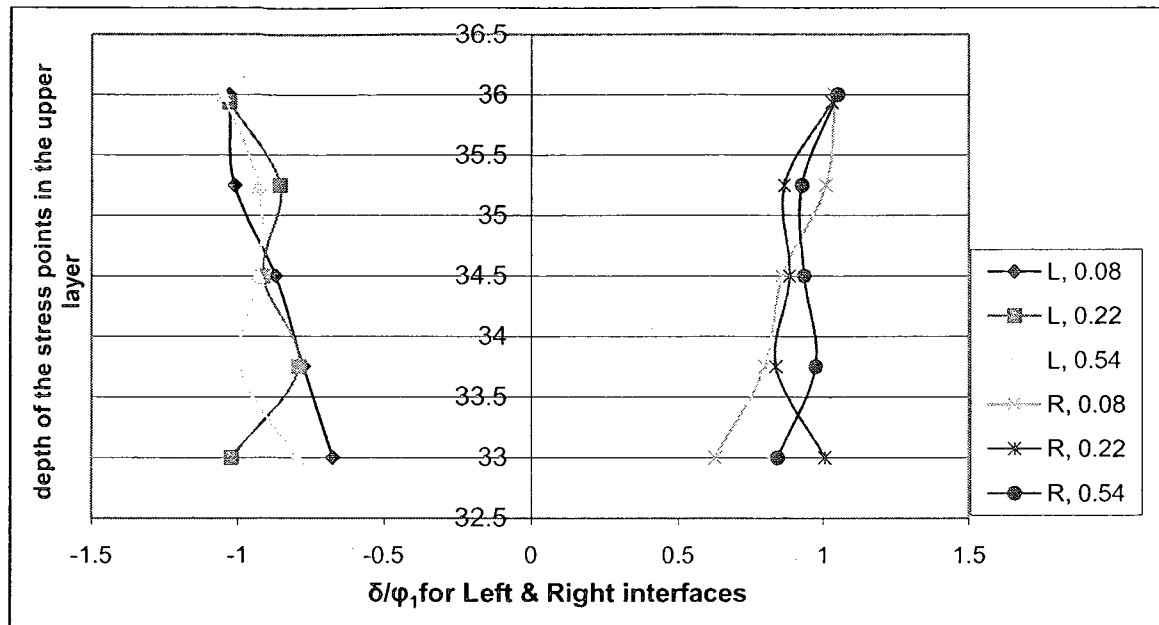


Fig.(4-20); Variation of  $\delta/\varphi_1$  for different ( $q_2/q_1$ ) ratios &  $H/B=3$

#### 4.8 DESIGN CHARTS

The results of the present investigation have demonstrated that the ratio  $\delta_{avr}/\varphi_1$  ratio are not only depends on the relative strength ( $q_2/q_1$ ), but also on the ratio of the height of the upper layer to the width of the footing ( $H/B$ ). As the height of the upper layer increases, the ratio  $\delta_{avr}/\varphi_1$  decreases. This is due to the fact that with the increase in the depth  $H$ , the actual failure deviate further from the assumed failure plain causing the decrease is the value of  $\delta_{avr}$ . Furthermore, The amount and the direction of the slope of the curve are governed by the  $q_2$  and  $q_1$  values individually. The slop is (-ve) for weaker lower layers and (+ve) for stronger ones, for all the  $H/B \leq 2$ , after which the slop direction is governed by the effect of the strength of the upper layer. To impliment this new

finding in the design theory for predicting the bearing capacity of strip footings, design charts were developed and presented in figures 4-21 to 4-29 for predicting the ratio of  $\delta_{avr}/\phi_1$  as function of the ratios of  $q_2/q_1$  and  $H/B$ .

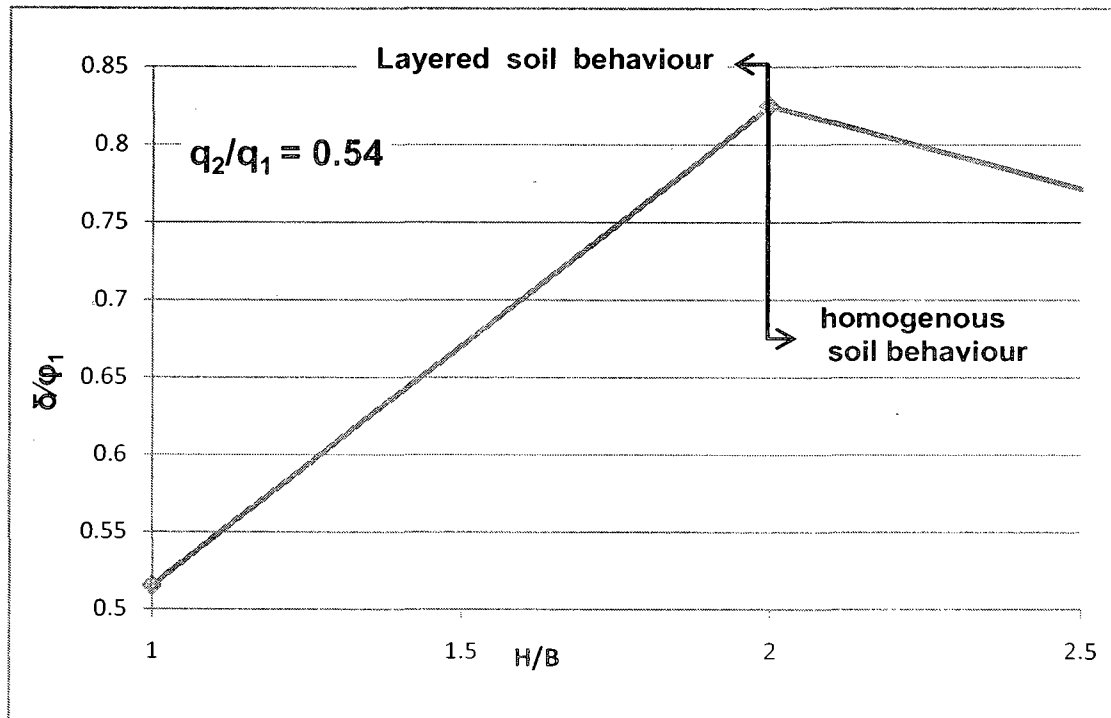


Fig.(4-21);  $\delta/\phi_1$  for different  $H/B$  ratios and ( $q_2/q_1 = 0.54$ ).

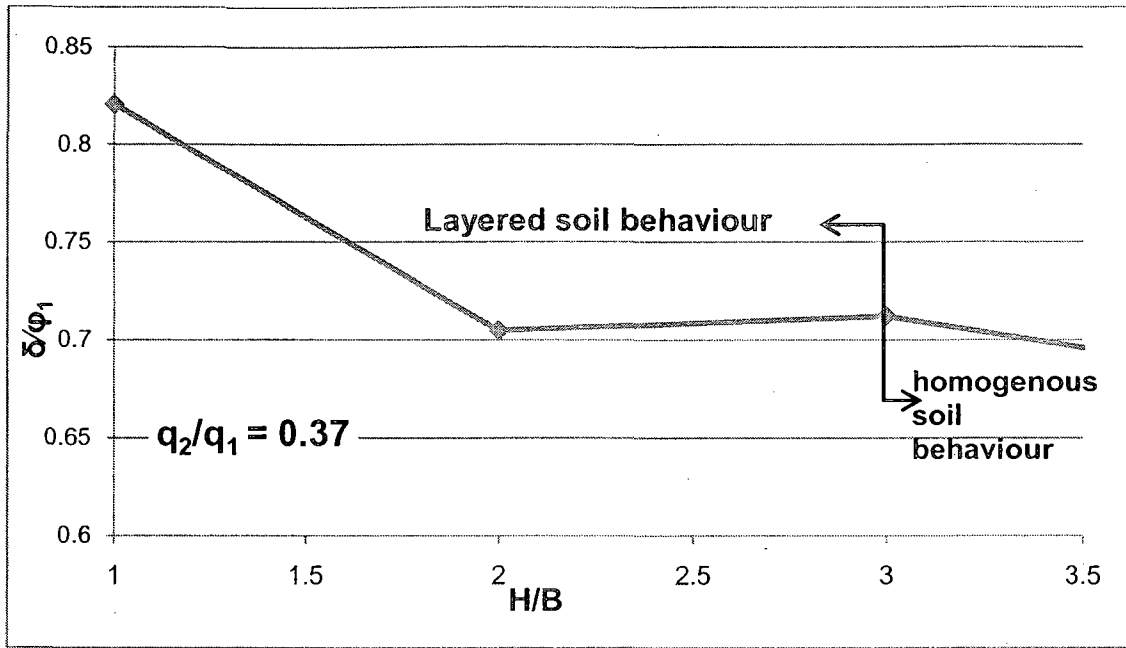


Fig.(4-22);  $\delta/\phi_1$  for different  $H/B$  ratios and ( $q_2/q_1 = 0.37$ ).

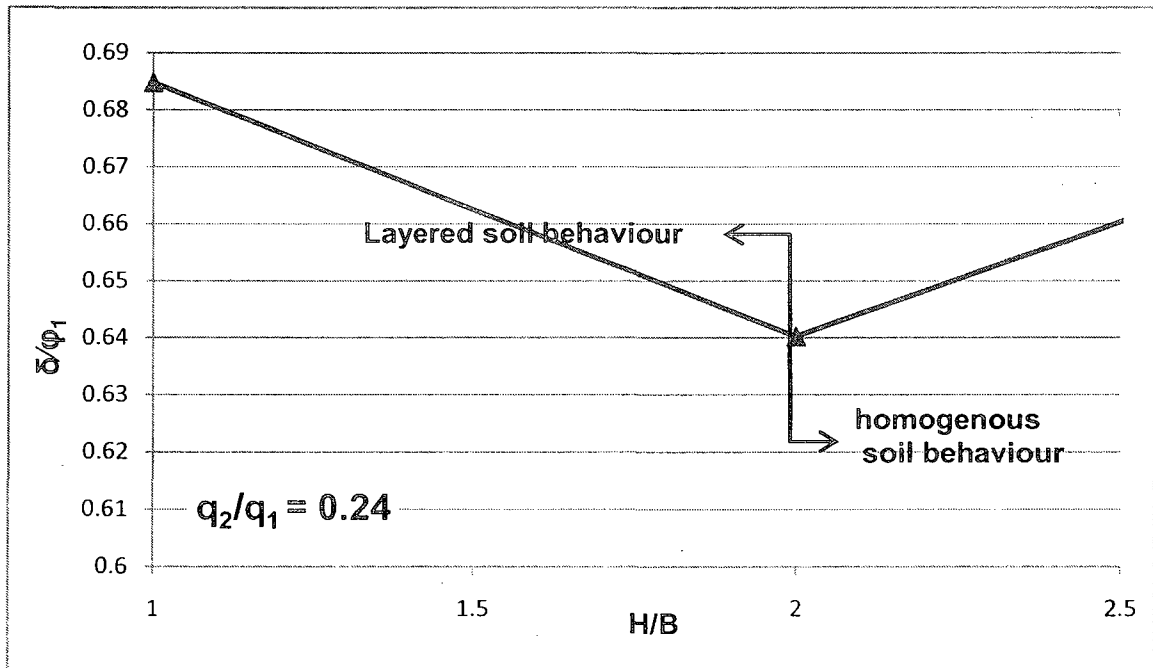


Fig.(4-23);  $\delta/\phi_1$  for different  $H/B$  ratios and ( $q_2/q_1 = 0.24$ ).

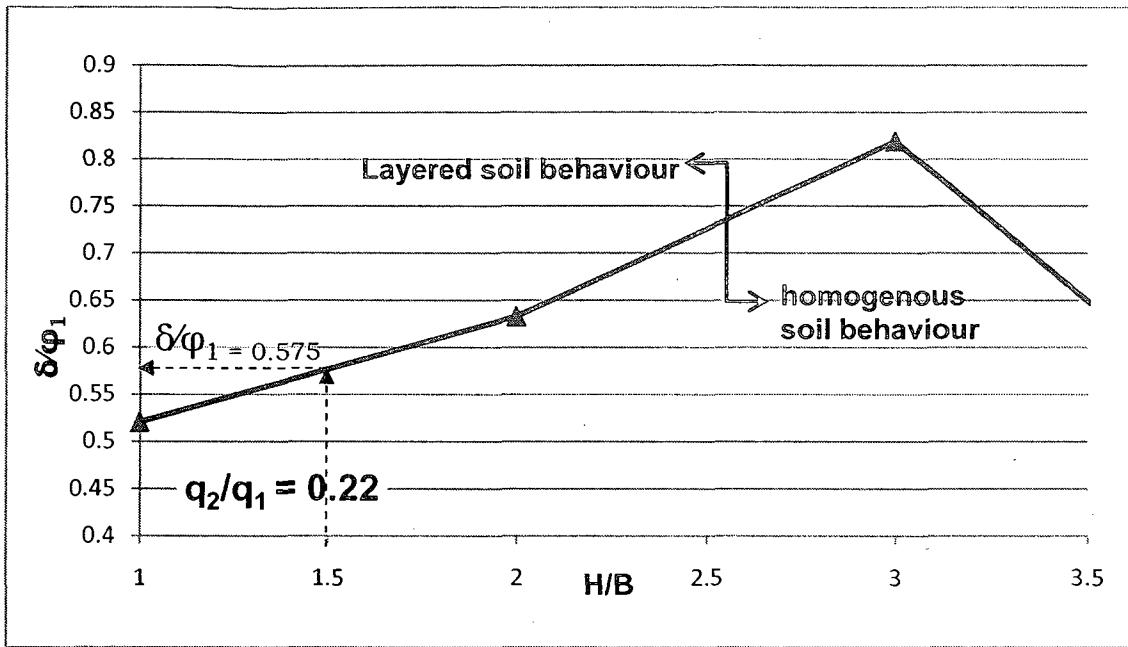


Fig.(4-24);  $\delta/\phi_1$  for different  $H/B$  ratios and ( $q_2/q_1=0.22$ ).

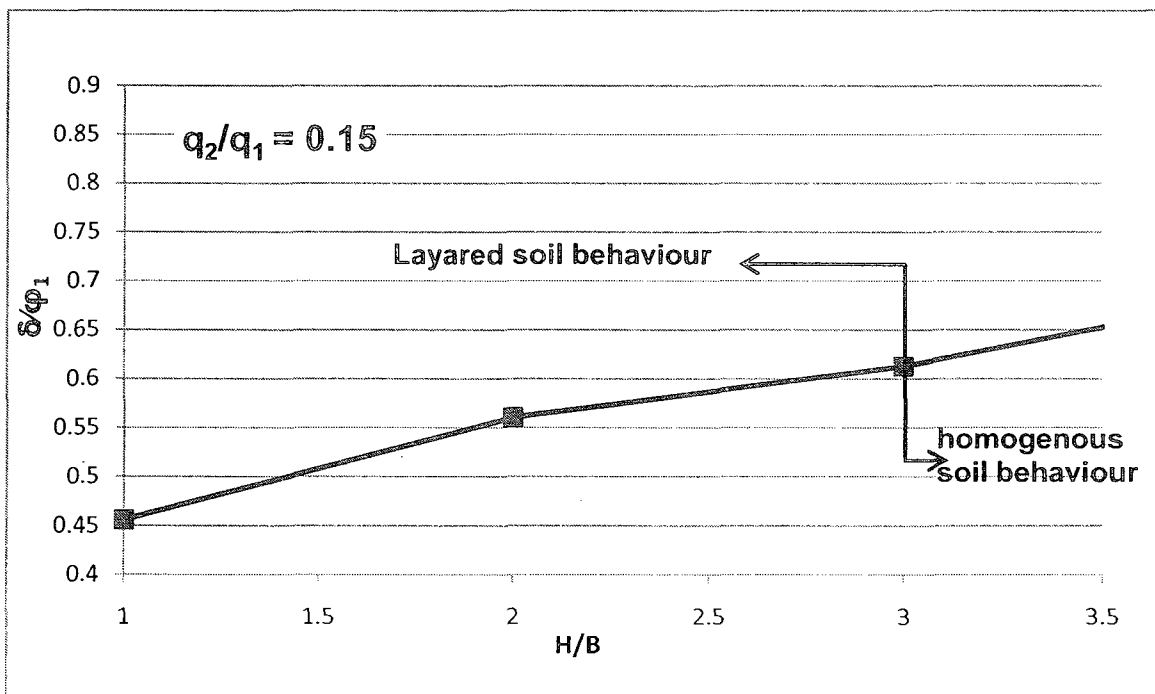


Fig.(4-25);  $\delta/\phi_1$  for different  $H/B$  ratios and ( $q_2/q_1=0.15$ ).

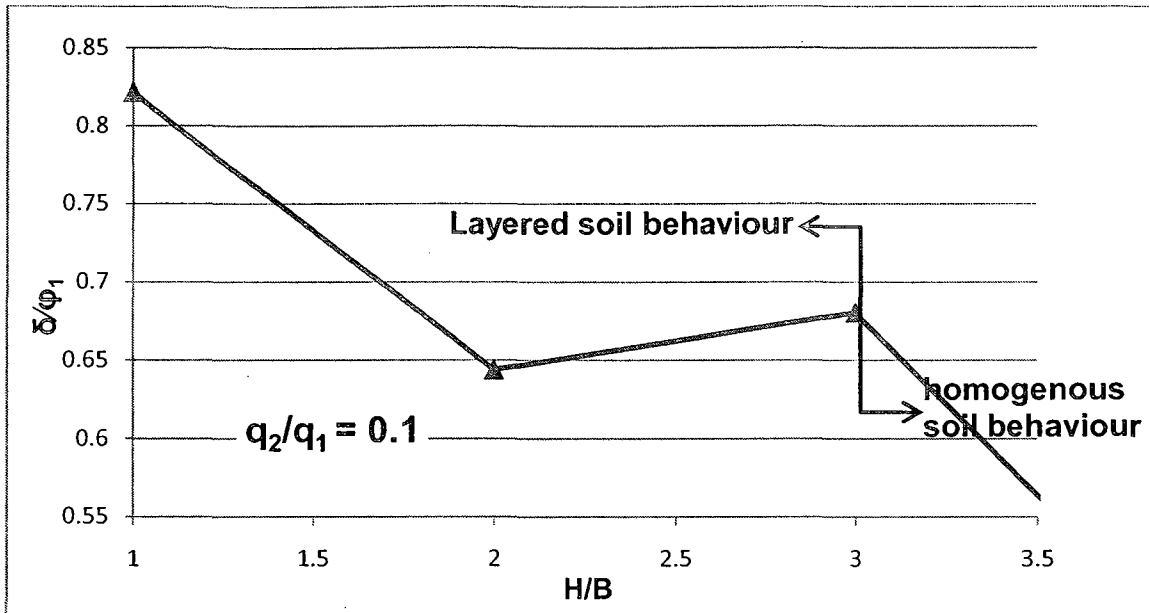


Fig.(4-26);  $\delta/\phi_1$  for different H/B ratios and ( $q_2/q_1=0.1$ ).

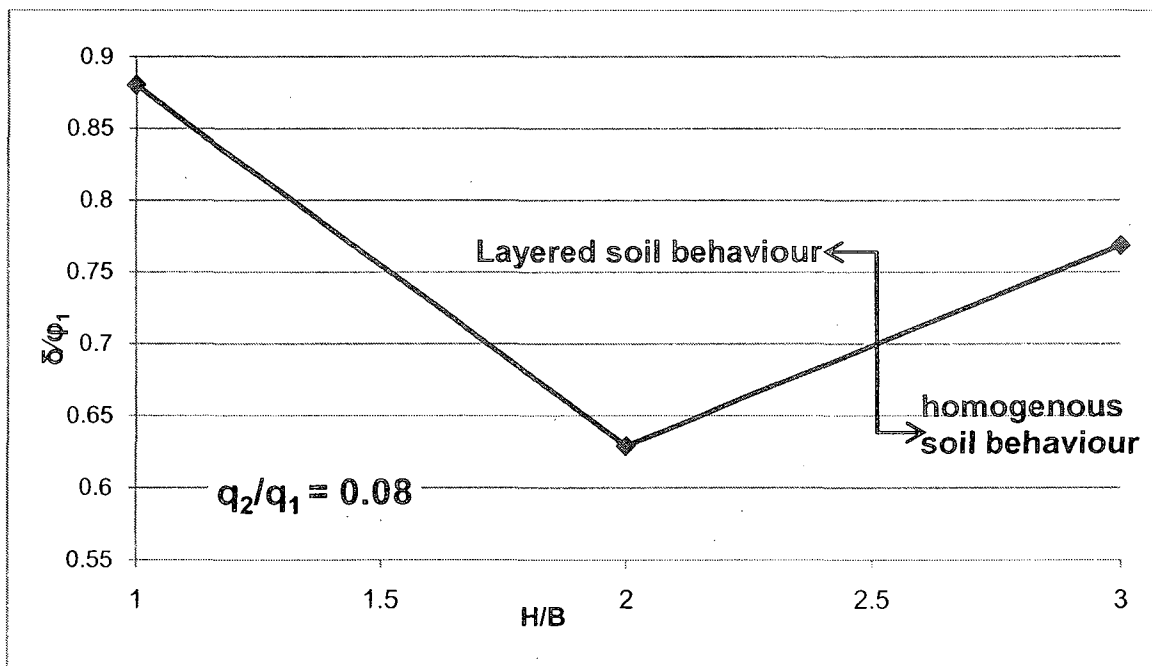


Fig.(4-27);  $\delta/\phi_1$  for different H/B ratios and ( $q_2/q_1=0.08$ ).

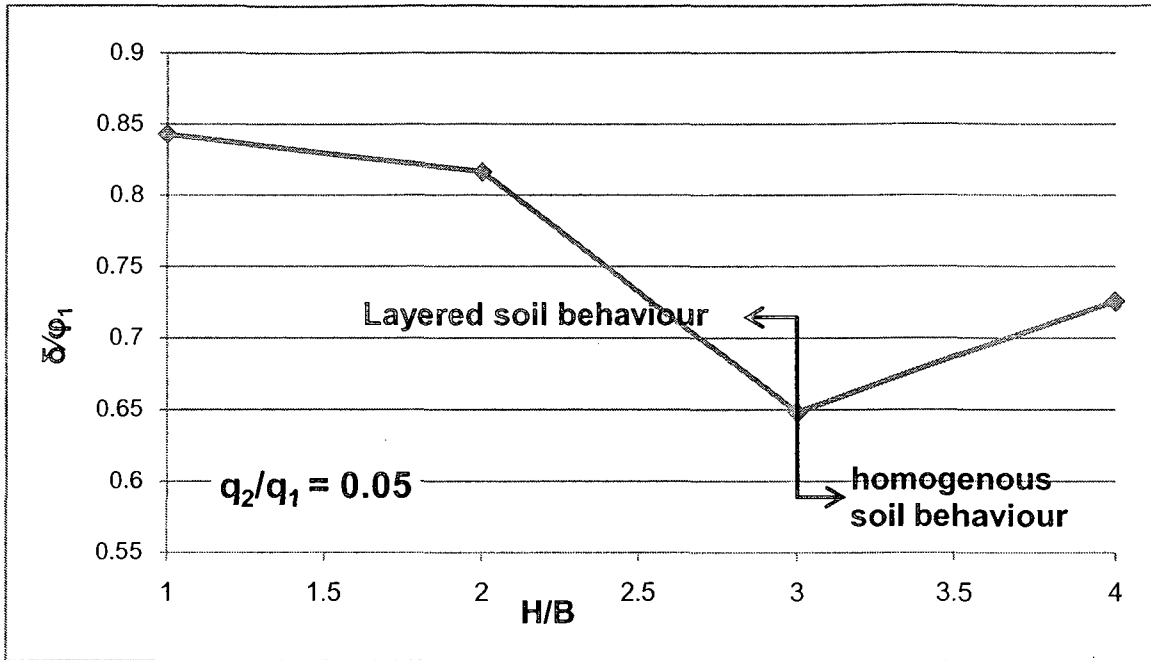


Fig.(4-28);  $\delta/\phi_1$  for different H/B ratios and ( $q_2/q_1 = 0.05$ ).

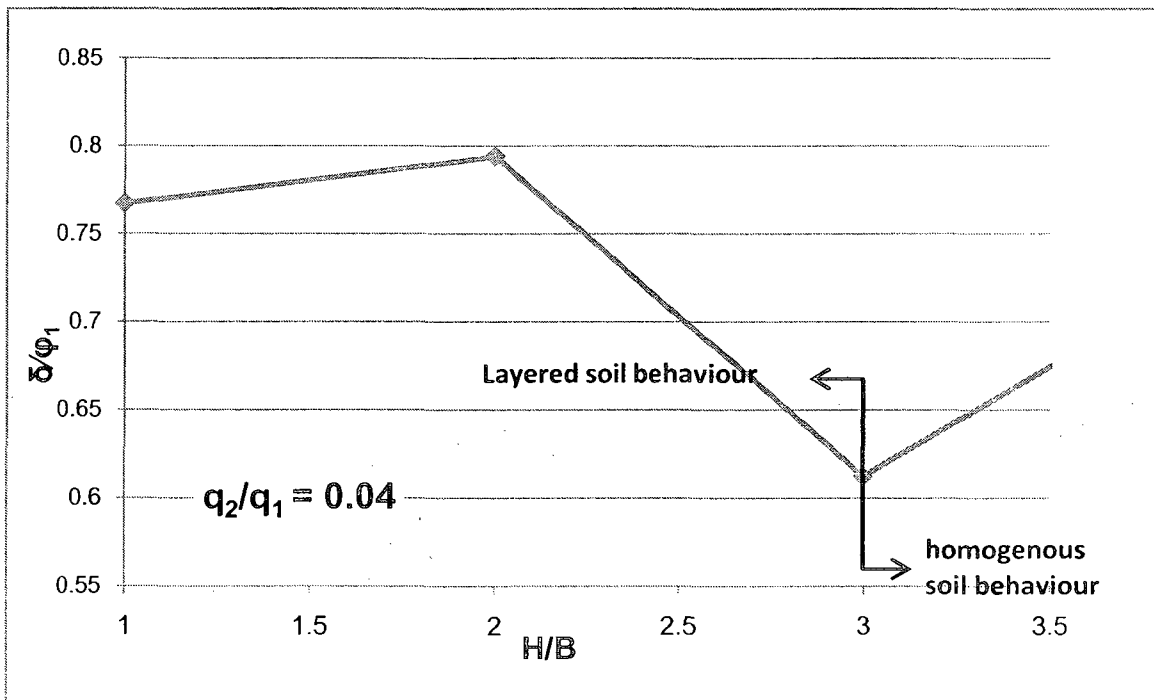


Fig.(4-29);  $\delta/\phi_1$  for different H/B ratios and ( $q_2/q_1 = 0.04$ ).

#### 4.9 SUGESTED DESIGN PROCEDURE

For a given values of footings width (B), upper layer height (H) and the angles of shearing resistance of both layers ( $\phi_1, \phi_2$ ), the following is a step-by-step to estimate the ultimate bearing capacity for these footings:

- 1- From  $\phi_1$  and  $\phi_2$  determine the bearing capacity factors ( $N_{\gamma_1}, N_{\gamma_2}$ ) for the upper and the lower soil layers respectively from the tables presented by Meyerhof (1974). Then calculate the bearing capacity of each layer ( $q_1$  and  $q_2$ ) from the following relation

$$q_1 = 0.5\gamma_1 BN\gamma_1 \quad \text{for the upper layer}$$

$$q_2 = 0.5\gamma_2 BN\gamma_2 \quad \text{for the lower layer}$$

- 2- For the calculated value of ( $q_2/q_1$ ) and for a given H/B ratio, use the charts given in figures (4-21 to 4-29) to estimate the ratio  $\delta/\phi_1$
- 3- Use the chart developed by Hanna (1981), the  $\phi_1$  and  $\phi_2$  values to find the coefficient of punching shear resistance ( $K_s$ ).
- 4- Use the following equation to find the coefficient of passive earth pressure  $K_p$ .

$$K_s \tan \phi_1 = K_p \tan \delta$$

- 5- Use the found  $\delta$  and  $K_p$  in the following equation to calculate  $P_p$

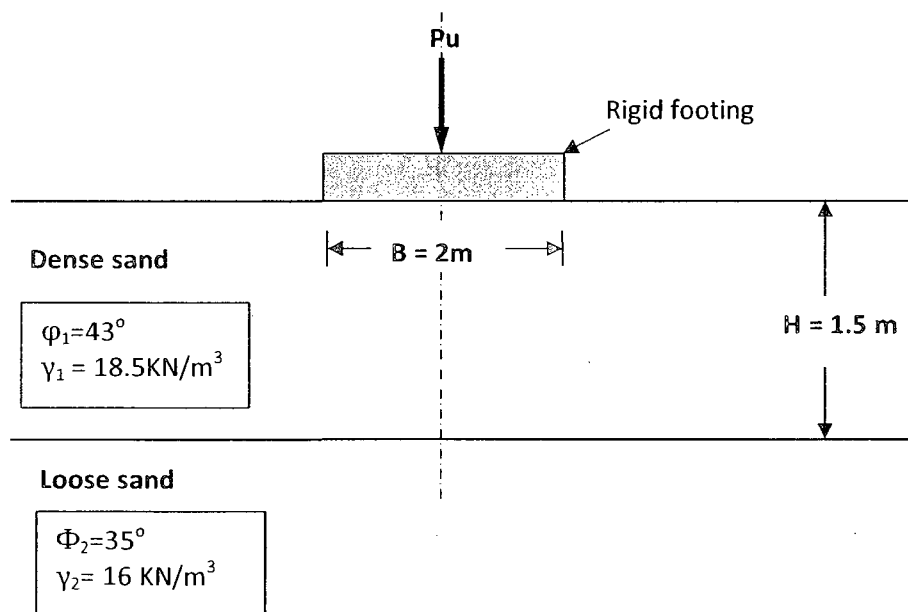
$$P_p = 0.5\gamma_1 H^2 \frac{K_p}{\cos \delta} \quad \dots\dots\dots \text{Hanna (1981- a)}$$

6- The ultimate bearing capacity is then can be calculated using the following equation:

$$q_u = q_2 + \frac{2}{B} (P_p \sin \delta) - \gamma_1 H \leq q_1$$

#### 4.10 DESIGN EXAMPLE

Calculate the bearing capacity for a continuous footing of width  $B=2\text{m}$ , resting on the surface of two layers sandy subsoil, for the setoff properties assigned for each layer, as shown in the figure below.



From  $\phi_1$  &  $\phi_2$  get the bearing capacity factors ( $N_{\gamma_1}, N_{\gamma_2}$ ) from the tables of Meyerhof (1974):

$$N_{\gamma_1} = 186.54, \text{ and } N_{\gamma_2} = 48.03$$

So;  $q_1 = 0.5\gamma_1 BN\gamma_1 = 0.5 * 18.5 * 2 * 189.54 = 3506.49$

$$q_2 = 0.5\gamma_2 BN\gamma_2 = 0.5 * 16 * 2 * 48.03 = 768.48$$

And,  $q_2/q_1 = 0.22$

From this value, get to fig. (4-24), for  $H/B=1.5$ ; get  $\delta/\phi_1 = 0.575$

So,  $\delta = 24.73^\circ$

From Hanna (1981) get  $K_s \approx 0.7$ , find  $K_p$  from

$$K_s \tan \phi_1 = K_p \tan \delta$$

$$K_p = 1.42$$

$$P_p = 0.5\gamma_1 H^2 \frac{K_p}{\cos \delta} = 32.475 \text{ KN/m}$$

And finally;  $q_u = q_2 + \frac{2}{B}(P_p \sin \delta) - \gamma_1 H \leq q_1$

$$= 768.48 + (32.475 * \sin(24.73)) - 18.5 * 1.5 \leq 3506.49$$

$$= 754.32 \text{ KN/m}$$

## CHAPTER FIVE

### CONCLUSIONS AND RECOMENDATIONS

#### 5.1 CONCLUSION

A numerical model was developed to simulate the case of footing on dense sand overlying loose cohesionless material. The objective of this research was to evaluate the level and distribution of mobilization of the shearing strength along the punching column. The following can be concluded:

1. The model has been validated with the experimental results of Hanna (1978) and Hanna (1981).
2. To the contrary to what has been published in the literature, the mobilized shearing strength on the punching column is a function of not only the relative strength of the layered system, but also the H/B ratio.
3. The ratio of  $\delta/\varphi_1$  is a function of the H/B ratio, the  $q_2/q_1$  ratio as well as the individual strength of the lower layer or the upper layer;  $q_2$ , and  $q_1$  respectively.
4. The strengths of both the lower and upper layers have major effects on the produced bearing capacity as well as the level of mobilization of the shear strength on the punching column.

5. The effect of the upper layer thickness diminishes at a depth at which the ultimate bearing capacity of the system is equal to the homogenous case.
6. The ultimate bearing capacity of the homogenous upper or lower layers constitute the upper and lower bounds for the bearing capacity of the layered system

## 5.2 RECOMMENDATIONS

1. This work should be continued to model the cases of sand over clay and a clay layer sandwich between two sand layers.
2. As for the calculations of the mobilized angle of shearing resistance  $\delta$  more work is needed to establish a mathematical relationship between  $\delta$  and  $\varphi_1$  (angle of internal shearing resistance of the upper layer).
3. Full scale testing and field data are needed to validate further the theories developed.

## REFERENCE:

1. **Abou Farah Carlos (2004)**, "*Ultimate bearing capacity of shallow foundations on layered soils*," Thesis for the degree of Master of Applied Science in the Department of Building, Civil and Environmental Engineering at Concordia University.
2. **Brown J.D. & Meyerhof G.G. (1969)**, "*Experimental study of bearing capacity in layered clays*," 7<sup>th</sup> International Conference on Soil Mechanics and Foundation Engineering. Mexico. Vol. 2. Pp.45-51.
3. **Button, S.J. (1953)**, "*The bearing capacity of footings on tow-layer cohesive subsoil*," Proceedings of the 3<sup>rd</sup> International Conference on Soil Mechanics and Foundation Engineering. Switzerland.
4. **Carter, J. P. and Balaam, N. (1995)**, *AFENA users manual*, Geotechnical Research Center, the University of Sydney.
5. **Casagrande, A., and Carrillo, N. (1954)**, "Shear failure of anisotropic materials," Journal of the Boston Society of Civil Engineers, contributions to soil mechanics 1941-1953
6. **Das Braja M. & Puri Vi jay K. (1989)**, "*Bearing capacity of shallow strip foundation on strong clay underlain by weak clay*," Foundation Engineering. Pp.1199- 1210.
7. **Florkiewicz Antoni (1989)**, "*Upper bound to bearing capacity of layered soils*," Canadian Geotechnical Journal. Vol.26.No.4. Pp.730-736.
8. **Frydmen S. & Burd H.J. (1997)**, "*Bearing capacity of plane-strain footings on layered soils*," Canadian Geotechnical Journal. Vol.34. Pp.241-253.
9. **Georgiadis Michael & Michalopoulos Alex P. (1984)**, "*Bearing capacity bases on layered soil*," Journal of Geotechnical Engineering, ASCE, Vol.111. No. 6. Pp.712-729.
10. **Hanna A.M. (1978)**, "*Bearing capacity of footings under vertical and inclined loads on layered soils*," Thesis submitted to the Nova Scotia technical

college for the faculty of graduate studies for degree of doctor of philosophy in civil engineering.

11. **Hanna A.M. and Meyerhof G.G. (1978)**, "*Ultimate bearing capacity of foundations on layered soils under inclined load*," Canadian Geotechnical Journal Vol.15. Pp.565-572.
12. **Hanna A.M. & Meyerhof G.G. (1979)**, "*Ultimate bearing capacity of foundations on a three-layer soil, with special reference to layered sand*," Canadian Geotechnical Journal. Vol.16. No. 2. Pp.412-414.
13. **Hanna A.M. & Meyerhof G.G. (1980)**, "*Design charts for ultimate bearing capacity of foundations on sand overlying soft clay*," Canadian Geotechnical Journal, Vol.17. No. 2. Pp.300-303.
14. **Hanna A.M. (1981- a)**, "*Foundations on strong sand overlying weak sand*," Journal of the Geotechnical Engineering Division, ASCE, Vol.107. No. GT7. Pp.915- 927.
15. **Hanna A.M. (1981- b)**, "*Experimental study on footings in layered soil*," Journal of the Geotechnical Engineering Division, ASCE, Vol.107. No.GT8. Pp.1113-1127.
16. **Hanna A. M. (1982)**, "*Bearing capacity of foundations on a weak sand layer overlying a strong deposit*," Canadian Geotechnical Journal. Vol.19. No. 3. Pp.392-396.
17. **Hanna A.M. (1987)**, "*Finite element analysis of footings on layered soils*," Department of Civil Engineering, Concordia University. Mathematical Modeling Journal. Vol.9. No.11. Pp. 813-819.
18. **Kenny M.J., Andrawes K.Z. (1996)**, "*The bearing capacity of footings on a sand layer overlying soft clay*," Geotechnique 47, No.2. Pp.339-345.
19. **Lyamin A. V. and Sloan S.W. (2001)**, "*Upper bound limit analysis using Linear finite elements and non-linear programming*," International Journal for Numerical and Analytical Methods in Geomechanics. Vol.26. Pp.181-216.
20. **Lyamin A. V. and Sloan S.W. (2002)**, "*Lower bound limit analysis using non-linear programming*," International Journal for Numerical and Analytical Methods in Geomechanics. Vol.55. Pp.573-611.

21. **Lyamin A. V., Shiau J. S. and Sloan S.W. (2003)**, "*Bearing capacity of sand layer on clay by finite element analysis*," Canadian Geotechnical Journal. Vol.40. Pp.900-915.
22. **Madhira R. Madhav and J.S.N.Sharma (1991)**, "*Bearing capacity of clay overlain by stiff soil*," Journal of Geotechnical Engineering, ASCE, Vol.117. No. 12. Pp.1941-1948.
23. **Michalowski Radoslaw L. and Shi Lei (1995)**, "*Bearing capacity of footings over two-layer foundation soils*," Journal of Geotechnical Engineering, ASCE, Vol.121. No. 5. Pp.420- 427.
24. **Meyerhof G. G. (1974)**, "*Ultimate bearing capacity of footings on sand layer overlying clay*," Canadian Geotechnical Journal. Vol.11. No. 2. Pp.223-229.
25. **Oda Masanobu and Win Soe (1990)**, "*Ultimate bearing capacity tests on sand with clay layer*," Journal of Geotechnical Engineering, ASCE, Vol.116. No. 12, pp.1903-1907.
26. **Reddy A. Siva and Srinivasan R. J. (1967)**, "*Bearing capacity of footings on layered clays*," Journal of Soil Mechanics and Foundations Division Proceedings of the American Society of Civil Engineers. Vol.93. No.SM2. Pp.83-100.
27. **Satyanarayana B. and Garg R.K. (1980)**, "*Bearing capacity of footings on layered C- $\phi$  soils*," Journal of the Geotechnical Engineering Division, ASCE, Vol.106. No. GT7 Pp.819- 823.
28. **Sloan S.W. (1989)**, "*Upper bound limit analysis using finite elements and liner programming*," International Journal for Numerical and Analytical Methods in Geomechanics. Vol.13. Pp.263-282.
29. **Sloan S.W. and Kleeman P.W. (1995)**, "*Upper bound limit analysis using discontinuous velocity fields*," Computer Methods Applied Mechanics and Engineering. Vol.127. Pp.293-314.
30. **Sloan S.W., Merifield R.S. and Yu H.S. (1999)**, "*Rigorous plasticity solutions for the bearing capacity of tow-layered clays*," Geotechnique 49, No.4. Pp.471-490.

31. **Tamura T. (1989)**, "*Rigid-plastic limit analysis of discontinuous media by a finite element method*," Canadian Geotechnical Journal. Vol.26. Pp.369-374.
32. **Terzaghi, K. (1943)**, "*Theoretical soil mechanics*" Wiley, J. and sons, New York, N.Y., 1943.
33. **Vesic, A. S. (1973)**, "*Analysis of ultimate loads of shallow foundations*" Journal of Soil Mechanics, *Fdn Engng Div.*, ASCE 99, No. SM1, 45-75.
34. **Wang Changxin and Carter John P. (2001)**, "*Deep penetration of strip and circular footings into layered clays*," Research Report No R807. FIEAust and MASCE. University of Sydney, Department of Civil Engineering.